Carbon Finance: Equilibrium Modeling and Empirical Analysis

Zur Erlangung des akademischen Grades eines
Doktors der Wirtschaftswissenschaften

(Dr. rer. pol.)

von der Fakultät für
Wirtschaftswissenschaften
des Karlsruher Instituts für Technologie (KIT)

genehmigte

DISSERTATION

von

Dipl.-Math. Steffen Hitzemann

Tag der mündlichen Prüfung: 24.10.2013
Referentin: Prof. Dr. Marliese Uhrig-Homburg
Korreferent: Prof. Dr. Karl-Martin Ehrhart
Karlsruhe 2013

Acknowledgements

I would like to express my gratitude to Professor Marliese Uhrig-Homburg, who has been an excellent advisor and mentor throughout my doctoral studies. I also owe many thanks to Professor Karl-Martin Ehrhart and Professor Christof Weinhardt for many valuable discussions and inspirations for my research. Further, I thank Professor Ute Werner for serving on my thesis committee.

I am grateful to all my colleagues at the Institute of Finance, Banking, and Insurance. In particular I would like to thank Jasmin Berdel, Stefan Fiesel, Martin Hain, Michael Hofmann, Annika Jung, Sorana Sarbu, Timo Schläfer, Claus Schmitt, Philipp Schuster, and Nils Unger for making the past years a very productive and enjoyable time. Thanks also to all professors and colleagues at the Graduate School "Information Management and Market Engineering" (IME) for many interesting interdisciplinary conversations.

I thank Professor René Carmona for inviting me to Princeton University, where I had an excellent time in all respects.

I gratefully acknowledge financial support by the IME Graduate School at the Karlsruhe Institute of Technology (KIT) funded by Deutsche Forschungsgemeinschaft (DFG) and financial support by the Karlsruhe House of Young Scientists (KHYS) for the research stay at Princeton University.

Finally, I would like to thank my family, my friends, and everyone else who has supported me.

Contents

List of Figures

List of Tables

Acronyms

AAU . . . . Assigned Amount Unit
AIC . . . . Akaike information criterion

CA ETS . . . . California Emissions Trading Scheme
CCA . . . . California Carbon Allowance
CDM . . . . Clean Development Mechanism
CER . . . . Certified Emission Reduction
CITL . . . . Community Independent Transaction Log
CPM . . . . Carbon Pricing Mechanism
CPRS . . . . Carbon Pollution Reduction Scheme
CU . . . . Carbon Unit

ECX . . . . European Climate Exchange
EEA . . . . European Environment Agency
ERU . . . . Emission Reduction Unit
EU ETS . . . . EU Emissions Trading System
EUA . . . . European Union Allowance
EUTL . . . . European Union Transaction Log

GARCH . . . . generalized autoregressive conditional heteroscedasticity
GBM . . . . geometric Brownian motion
GGAS . . . . Greenhouse Gas Abatement Scheme

IET . . . . International Emissions Trading
ITM . . . . in-the-money

JI . . . . Joint Implementation

LULUCF . . . . land use, land-use change and forestry

NAP . . . . National Allocation Plan
NIG . . . . normal-inverse Gaussian
NIM . . . . National Implementation Measure
NZ ETS . . . . New Zealand Emissions Trading Scheme
NZU . . . . New Zealand Unit

OTM . . . . out-of-the-money

PDE . . . . partial differential equation

RGGI . . . . Regional Greenhouse Gas Initiative
RMU . . . . Removal Unit
RRMSE . . . . relative root-mean-squared error

SDE . . . . stochastic differential equation

UNFCCC . . . . United Nations Framework Convention on Climate Change

WCI . . . . Western Climate Initiative

1. Introduction

1.1. Motivation

The attention given to market-based policy instruments to reduce greenhouse gas emissions has materially increased in the recent years. The idea is to require polluters to acquire a right for each ton of greenhouse gas they emit, and to cap the overall number of available rights. Starting from an initial allocation, these rights, called *emission permits*, can be traded among the polluters and other investors. Under perfect market conditions, an efficient allocation of the emission permits is attained, such that emissions are realized where it is most costly to abate them, and the emission reductions that are necessary to comply with the cap are achieved at lowest cost for the economy.[1] The public perception of such *cap-and-trade systems*[2] is controversial. Supporters emphasize that these instruments promote economic efficiency — to achieve environmental objectives at lowest possible cost — combined with a sufficient amount of flexibility to be compatible to intergovernmental political processes,[3] and consider emissions trading as the key instrument to combat climate change (Stavins 2011). Opponents doubt the ability of emission trading systems to generate permanent incentives for abatement and environment-friendly investments through their price signals and feel vindicated by the problems that some established emission trading systems are currently facing.[4] The

[1] The concept of emissions trading was developed by the seminal works of Coase (1960), Crocker (1966), Dales (1968), and Montgomery (1972), among many others. Taschini (2009) provides an overview of the related literature.

[2] This thesis focuses on cap-and-trade systems as the most prominent form of emission trading systems. There are also alternative designs of emission trading schemes, for example baseline-and-credit systems. See Boom and Dijkstra (2009) for an overview and comparison of both types of systems.

[3] Both, theoretical and empirical work shows that market-based approaches achieve environmental objectives at lower cost than conventional command-and-control systems (see Montgomery 1972; Cronshaw and Kruse 1996; Rubin 1996 as well as Carlson et al. 2000; Burtraw et al. 2005). Paterson (2012) elaborates on the advantageous properties of emission trading systems from a political perspective.

[4] We discuss challenges that existing emission trading systems are currently facing in the conclusion and outlook of this thesis in Section 6.

general skepticism against market mechanisms has been fueled further by the recent financial crisis and its economic consequences.

Notwithstanding these objections, mandatory emission trading schemes have recently been introduced on international, national, or domestic levels all over the world: in the European Union, for several states of the US, in New Zealand and Australia, for the metropolitan area of Tokyo, and the list will grow in the coming years. With them, the financial market for emission permits has experienced tremendous growth, with a global transaction volume of USD 176 billion in 2011.[5] The emission permit market is of great relevance for various agents and brings along a number of financial and economic issues related to this new asset class. According to the nature of an emission trading system, polluting companies trade in the market to satisfy their demand for emission permits, and are exposed to related price risk. Managing this risk requires detailed knowledge of the fine structure of permit prices and also involves the use of derivatives written on emission permits, such as futures and options. Trading in derivatives markets, however, gives rise to the need for suitable valuation approaches. Furthermore, the existence of an emission trading system fosters investments into environment-friendly technologies and projects. Polluters have to assess their investment opportunities based on the price signals given by the market, and make decisions on which projects to realize and on their timing strategy. On the other side, it is of great interest for the regulator to design the emission trading system in such way that it creates a permanent incentive for sustainable investments. Besides these original objectives, emission permits and related derivatives also provide a promising option for diversification to institutional and private investors. It stands to reason that emission permit prices are driven by different factors than stocks, bonds, or classical commodities. Sound investment strategies, however, require a good understanding of the risk profile of these instruments.

Although these issues appear very diverse, they all depend critically on the *stochastic behavior* of the underlying asset prices, as is widely recognized in the classical finance and commodity literature.[6] More precisely, important questions are:

- What kind of permit price behavior is induced by the design of today's cap-and-trade systems?

[5] See Kossoy and Guigon (2012).

[6] In the finance literature on commodities, important studies dealing with these issues are Brennan and Schwartz (1985), Schwartz (1997), Routledge et al. (2000), Schwartz and Smith (2000), Casassus and Collin-Dufresne (2005), and Trolle and Schwartz (2009).

- How does the futures price curve look like?
- How should market models be specified to capture the characteristics of permit prices appropriately?
- How are derivatives priced in this market?
- What is the short-term impact of news?

This thesis contributes to these questions both from a theoretical and an empirical perspective. In the existing theoretical literature, equilibrium models for emissions markets are developed either under certainty (e.g., Cronshaw and Kruse 1996; Rubin 1996; Schennach 2000), or under uncertainty but for a set of regulatory rules that do not completely match the actual rules of state-of-the-art cap-and-trade systems (Seifert et al. 2008; Cetin and Verschuere 2009; Carmona et al. 2009, 2010; Kijima et al. 2010; Chesney and Taschini 2012). Consequently, these approaches explain basic effects in this market within a simplified setting, but are not entirely suitable to investigate the specific stochastic properties of permit prices induced by the design of today's emission trading systems. We study the characteristics of emission permit prices as well as futures and related derivatives within an equilibrium model for emissions markets that captures all important design features of current emission trading systems.

On the empirical side, several existing studies investigate the properties of emission permit spot, futures, and option prices by calibrating standard models like geometric Brownian motion, jump-diffusion, mean-reverting, regime-switching, or stochastic volatility models to market data (Wagner 2007; Paolella and Taschini 2008; Benz and Trück 2009; Daskalakis et al. 2009; Frey 2010). In contrast, Grüll and Taschini (2009) and Carmona and Hinz (2011) propose reduced-form market models that account for the specific properties of emission permits and are still feasible for calibration to futures or option prices. We provide a generic extension of these approaches to a reduced-form model framework, calibrate a battery of model variants to futures and option price data, and evaluate the performance of different specifications with respect to historical model fit and option pricing performance.

Furthermore, we are the first to study the general impact of the yearly emissions announcement, an outstanding news event in the European emissions market. Related effects are considered up to now only for one or two selected events (Chevallier et al. 2009; Mansanet-Bataller and Pardo 2009; Grüll and Kiesel 2012). We consider the emissions announcements from 2007 to 2012 to investigate the impact of this event on prices, volumes, intraday volatilities, and option-implied volatilities of European permit futures.

1.2. Structure of the Thesis

This thesis is structured as follows.

Chapter 2 gives a concise overview of existing and proposed emission trading schemes worldwide and introduces the regulatory features of today's cap-and-trade systems. We describe the EU Emissions Trading System (EU ETS) as the world's largest emission trading system in more detail, with a special focus on the financial instruments that are traded within this system.

In Chapter 3, we propose a stochastic equilibrium model for emissions markets that accounts for all important design features of today's emission trading systems.[7] Regulated companies reduce their emissions by implementing abatement measures and trade emission permits in the market. We characterize an emission permit as a strip of European binary options written on economy-wide cumulative emissions. Exploiting this option analogy, we derive several general properties of the spot and futures price dynamics of emission permits. We calibrate the model to a setting in accordance with the EU ETS and investigate the specific properties of permit prices, volatilities, and their dependency on abatement costs and future compliance periods. Based on a simulation study, we further shed light on the characteristic properties of the volatility smile in this market.

Chapter 4 simplifies the permit price dynamics derived in Chapter 3 by specifying the dynamics of economy-wide cumulative emissions exogenously, following the reduced-form approach by Carmona and Hinz (2011).[8] We obtain a framework of reduced-form models for the permit price dynamics that accounts for the specific properties of emission permits and is still feasible for calibration to futures or option prices. For historical calibration to spot or futures prices, we develop a general estimation approach based on the unscented Kalman filter. Option pricing formulae are derived in our framework

[7] Chapter 3 is based on the working paper Hitzemann and Uhrig-Homburg (2013b).
[8] Chapter 4 builds on the working paper Hitzemann and Uhrig-Homburg (2013a).

along the lines of Carmona and Hinz (2011). We calibrate a battery of model variants to historical futures prices to evaluate their empirical performance. Furthermore, we analyze the in- and out-of-sample option pricing performance based on implicit calibration.

Chapter 5 focusses on the short-term dynamics of emission permit prices related to the annual announcement of emissions realized in the previous year.[9] We investigate the impact of this event on the European carbon market with respect to abnormal returns, trading volumes, intraday volatilities, and option-implied volatilities.

Chapter 6 summarizes the thesis and gives an outlook to possible future research.

[9]Chapter 5 is based on the working paper Hitzemann et al. (2013).

2. Emissions Trading: Current State

2.1. Emissions Trading Around the World

The foundation of global emissions trading is the Kyoto Protocol,[10] which was adopted in December 1997 to supplement the United Nations Framework Convention on Climate Change (UNFCCC). It defines limits on the amount of greenhouse gases to be emitted in the years from 2008 to 2012 for several countries listed in Annex I of the UNFCCC.[11] The Kyoto Protocol does not require, however, that all Annex I countries comply with their limits on an individual basis as long as the aggregate emissions do not exceed the overall cap. Countries are allowed to transfer parts of their assigned amount to other countries if they over-achieve their emission reduction goal, and the other countries are consequently allowed to emit more according to the increased amount.[12] These rules establish International Emissions Trading (IET) in the form of a cap-and-trade system. The amount of emissions allowed to the countries is represented by a number of tradable Assigned Amount Units (AAUs), which are emission permits for one ton of carbon dioxide equivalent each.[13] Besides AAUs, the Kyoto Protocol introduces three other kinds of emission permits: Emission Reduction Units (ERUs), Certified Emission Reductions (CERs), and Removal Units (RMUs). ERUs arise from Joint Implementation (JI) projects in which an Annex I party invests into an emission reduction project that is hosted by another Annex I country. For compensation, AAUs from the host country are converted into ERUs and credited to the investing party. Similarly, CERs can

[10] See United Nations (1998).
[11] The limits are defined in Annex B of the Kyoto Protocol.
[12] See Article 3 and Article 17 of the Kyoto Protocol.
[13] Greenhouse gas emissions are usually expressed in carbon dioxide equivalent, i.e., the amount of all greenhouse gases measured by their accelerating effect on global warming is translated to the amount of carbon dioxide that would cause the same effect when no other greenhouse gases are emitted to the atmosphere.

be awarded to an investing Annex I party for participating in projects in Non-Annex I countries under the Clean Development Mechanism (CDM). Finally, forestation activities are considered separately from other measures to emission reduction and are compensated by RMUs.[14] While ERUs do not change the overall amount of emissions allowed to Annex I parties, RMUs and CERs add to this amount. The differentiation between AAUs and the other *Kyoto units* is necessary with regard to the supplementarity principle of the Kyoto protocol, which says that countries are supposed to achieve their emission reduction goals predominantly by domestic emission reductions, while other measures are only supplemental.[15] In consequence, the use of ERUs, CERs, and RMUs for compliance in the current and following commitment periods of the Kyoto Protocol is restricted, while AAUs are generally usable.[16]

The idea of greenhouse gas emissions trading has been adapted in the recent years to introduce international, national, or domestic emission trading systems all over the world.[17] Some of these systems are directly linked to the Kyoto framework and pass on emission limits to the countries' industry sectors, while others are independent and pursue individual emission reduction goals. As highlighted by Figure 2.1, the EU ETS is the most significant emission trading system both in terms of the amount of emission permits allocated per year and the transaction volume. It was launched in 2005 and covers about 40% of the overall greenhouse gas emissions of the 27 EU member states, plus Croatia, Iceland, Liechtenstein, and Norway.[18] Starting with the power sector and energy-intensive industries, the scheme is steadily extended and includes the aviation sector since 2012 and several further industries by 2013. The domestic emission permits traded within the EU ETS are called European Union Allowances (EUAs) and stand for one ton of carbon dioxide equivalent emissions each. Furthermore, the EU ETS is

[14] The JI mechanism is defined in Article 6 of the Kyoto Protocol, the CDM in Article 12. Article 3.3 states the rules for land use, land-use change and forestry (LULUCF) measures.

[15] The supplementarity principle is introduced by Article 6.1 (d), Article 12.3 (b), and Article 17 of the Kyoto Protocol.

[16] We refer to Betz et al. (2005) for further details on the eligibility of different Kyoto units for compliance. For an excellent overview of the legal framework of international and regional emissions trading see Freestone and Streck (2009).

[17] The overview of different emission trading systems given in this section incorporates related information from the reports by Hood (2010), Perdan and Azapagic (2011), Kossoy and Guigon (2012), and the International Emissions Trading Association (2012).

[18] Important regulations are Directive 2003/87/EC (see European Parliament and Council 2003) as well as the amending Directive 2009/29/EC (see European Parliament and Council 2009) and the *Linking Directive* 2004/101/EC (see European Parliament and Council 2004). A comprehensive outline of the system is given in the brochure of the European Commission (2008b). Further information is provided on the official website `http://ec.europa.eu/clima/policies/ets/`.

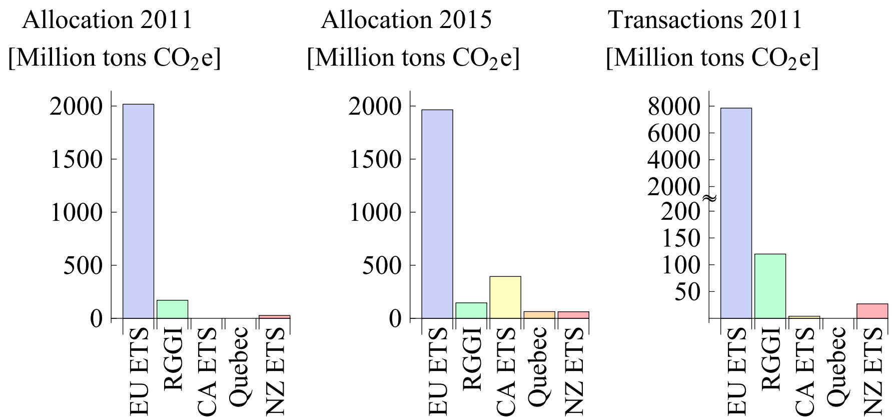

Figure 2.1.: Size of the most significant emission trading systems with respect to the amount of allocated permits in 2011, the proposed allocation for 2015, and the transaction volume in 2011, denoted in terms of the corresponding amount of carbon dioxide equivalent (CO_2e) emissions. Transaction volumes include spot and forward transactions and are provided by Kossoy and Guigon (2012). EU ETS is the EU Emissions Trading System, RGGI stands for the Regional Greenhouse Gas Initiative, CA ETS is the California Emissions Trading Scheme, Quebec stands for the emission trading system in Quebec, and NZ ETS is the New Zealand Emissions Trading Scheme.

linked to the Kyoto mechanisms by allowing to use ERUs and CERs to a certain extent equivalently to European Union Allowances (EUAs) for compliance. We refer to the EU ETS as an example of application for our theoretical model in Chapter 3, and for our empirical analysis in Chapter 4 and Chapter 5. Therefore, we consider the specific design features and regulations of the EU ETS in detail in Section 2.3.

In North America there are two significant emission trading initiatives, the Regional Greenhouse Gas Initiative (RGGI) and the Western Climate Initiative (WCI). Both are inter-regional initiatives — an attempt to establish mandatory US-wide emissions trading failed when the American Clean Energy and Security Act of 2009[19] was approved by the House of Representatives, but not by the Senate. The RGGI launched an emission trading system in 2009 that covers emissions from the electricity sector of nine US

[19]See 111th United States Congress (2009).

states along the East Coast.[20] From its introduction, the scheme had to deal with severe over-allocation problems, and trading had broken down consequently. A comprehensive review of the RGGI was conducted in 2012 with the result that the member states agreed on a reduction of the cap by 45%, which has revitalized the market again.[21] The WCI is a coalition of the state of California and the four Canadian provinces British Columbia, Manitoba, Ontario, and Quebec. It was initiated in 2007 with the intention to collaborate on the reduction of greenhouse gas emissions in the member states.[22] Both California and Quebec are operating a mandatory cap-and-trade system since the beginning of 2013. The California Emissions Trading Scheme (CA ETS) includes emissions from the power sector and large industries from the beginning and is extended in 2015, especially to the transport sector.[23] It thereby covers 85% of California's greenhouse gas emissions, which makes it to the second largest emission trading scheme in the world (see Figure 2.1). In anticipation of the first compliance period starting in 2013, first forward contracts on California Carbon Allowances (CCAs) were traded as early as in August 2011. Quebec's emission trading scheme is designed very similarly to the CA ETS, and Quebec and California will link their schemes by the beginning of 2014.[24] Due to the withdrawal of the United States and Canada from the Kyoto Protocol, the Northern American emission trading systems are not linked to the Kyoto mechanisms.

A number of developments related to carbon emissions trading are also observable in Australia and New Zealand. Already on January 1, 2003, the Australian State of New South Wales introduced the Greenhouse Gas Abatement Scheme (GGAS), a baseline-and-credit system to reduce carbon emissions of the electricity sector.[25] It was closed at the end of June 2012[26] and is superseded by the Australia-wide Carbon Pricing Mecha-

[20] These states are Connecticut, Delaware, Maine, Maryland, Massachusetts, New Hampshire, New York, Rhode Island, and Vermont. Further information is provided on `http://www.rggi.org`.

[21] This review was scheduled already in 2005, see Article 6.D of the Memorandum of Understanding for the Regional Greenhouse Gas Initiative (2005). The results were published in February 2013 by the Regional Greenhouse Gas Initiative (2013).

[22] See Western Regional Climate Action Initiative (2007).

[23] See Table II-1 of the cap-and-trade regulation of the California Environmental Protection Agency (2010). Further information is provided on the official website `http://www.arb.ca.gov/cc/capandtrade/capandtrade.htm`.

[24] See the related regulations adopted by the California Environmental Protection Agency (2013).

[25] Related information is available on `http://www.greenhousegas.nsw.gov.au`.

[26] See New South Wales Government (2012).

nism (CPM) since July 2012. The CPM is established by the Clean Energy Act 2011[27] that was adopted in view of the goal to reduce Australia's emissions by at least 80% until 2050, compared to the year 2000. It introduces a cap-and-trade system that covers about 60% of Australia's carbon dioxide emissions.[28] The CPM, however, starts with a 3-year period during which Australian Carbon Units (CUs) — the domestic emission permits needed for compliance under the CPM — can be acquired at a fixed price of AUD 23 per ton.[29] After that, price flexibility is increased in two steps: From July 2015 to July 2018, prices are flexible and determined by the market, but the fluctuation is bounded by a predefined price floor and ceiling. The price floor is set to AUD 15, while the ceiling is linked to international carbon prices, defined to be AUD 20 above the prevailing CER price. From July 2018 on, prices can fluctuate freely.[30] Like the EU ETS, the CPM is linked to the Kyoto mechanisms and allows the use of Kyoto units for compliance for up to 50% of a company's emissions as of 2015.[31] In New Zealand, the New Zealand Emissions Trading Scheme (NZ ETS) is in operation already since 2008, but was subject to a major revision enacted in December 2009.[32] In particular, a transition phase for the scheme was set from July 2010 to December 2012, during which regulated companies were able to buy New Zealand Units (NZUs) for a fixed price of NZD 25 and use each NZU for two tons of emissions, while an NZU usually only covers one ton. Alternatively, compliance can be achieved by using Kyoto units without any limit, which strongly links the NZ ETS to international carbon prices.

More or less concrete plans to establish carbon emissions trading exist in many other parts of the world. Most notably, the Republic of Korea has passed a bill that establishes a nation-wide emissions trading scheme by 2015. Countries like China, Japan, and Brazil underpin their ambitions to establish emissions trading by setting up domestic

[27] The Clean Energy Act 2011 (see Australian Government 2011) is part of the Clean Energy Legislative Package, see `http://www.cleanenergyfuture.gov.au`. A previously proposed emission trading scheme, the Carbon Pollution Reduction Scheme (CPRS), was rejected by the Senate.

[28] See Australian Government (2012).

[29] In this sense, the CPM effectively implements a *carbon tax* for the first three years. The comparison of such price-based mechanisms to quantity-based mechanisms like emissions trading is in the focus of the seminal work by Weitzman (1974).

[30] Related rules are defined in Section 100 of the Clean Energy Act 2011, the price floor is specified in Section 111. It starts at AUD 15 and increases to AUD 16 and AUD 17.05 in the following years.

[31] See Section 121 of the Clean Energy Act 2011.

[32] Corresponding regulations are the Climate Change Response (Emissions Trading) Amendment Act 2008 (see New Zealand Government 2008) and the Climate Change Response (Moderated Emissions Trading) Amendment Bill (see New Zealand Government 2009). Further information is available on the website `http://www.climatechange.govt.nz/emissions-trading-scheme/`.

schemes on a mandatory or voluntary basis. Japan has launched mandatory emissions trading in the metropolitan area of Tokyo in 2010, and Brazil starts a scheme in the state of Rio de Janeiro in 2013 and plans another one in São Paulo. China is working on the introduction of voluntary pilot emissions trading systems in several cities and regions. The success of such pilot projects and the developments of the global emissions market will decide about the permanent establishment of emissions trading in these and many other countries.

2.2. Design of Cap-and-Trade Systems

The design of sensible, cost-effective cap-and-trade systems involves a number of decisions on different dimensions.[33] Once the scope of the system is defined, in particular the geographical coverage, the regulated industries, and the greenhouse gases that are included,[34] the regulator has to decide on the design of the *temporal dimension* as well as the allocation and enforcement mechanism of the system. Currently established or proposed cap-and-trade systems are designed in a very similar fashion with respect to these aspects, as we point out in the following.

On the temporal dimension, the regulator defines compliance periods and sets a cap on the emission volume within these periods based on predefined reduction goals. An important design issue is the choice between few longer compliance periods and many short ones. While a system with many short periods provides more flexibility to the regulator to align caps on a short-term basis, it constrains the timing flexibility of regulated companies for emission reductions. Moreover, short compliance periods generally lead to a higher volatility of emission permit prices, which delays and reduces irreversible investments into carbon-friendly technologies.[35] It is, however, possible to increase price stability in a system with multiple short compliance periods by allowing to transfer emission permits between different periods. As Fankhauser and Hepburn (2010a) note, one long compliance period is obviously equivalent to multiple short compliance peri-

[33] A very detailed discussion of the different design options can be found in Tietenberg (2006).

[34] This thesis focusses on the design of emission trading systems on the *temporal dimension* and its implications for the stochastic behavior of emission permit prices. Nevertheless, the definition of the scope of an emission trading scheme is a complex decision involving a number of different criteria. We refer to Chapter 4 of Tietenberg (2006) and Fankhauser and Hepburn (2010b) for an overview of design issues on the *spatial dimension*.

[35] This follows from standard results of real options theory, see Pindyck (1988).

ods between which permits are transferable unlimitedly. Current cap-and-trade systems allow to carry over current emission permits to following compliance periods (*banking*). To the contrary, it is usually prohibited to use permits from future allocations in earlier compliance periods (*borrowing*) due to adverse incentives that come along with it.[36] On the one hand, companies might tend to postpone the implementation of abatement measures and borrow permits instead, especially when it is likely that emission reduction targets are relaxed for future compliance periods. On the other hand, firms effectively become debtors when borrowing emission permits, which increases their incentive to campaign for abandoning emissions trading such that their debt gets waived. It also imposes additional complexity to the regulator to evaluate if a company will be able to pay borrowed permits back. Especially in emission trading systems that are intended to have an infinite horizon, unlimited borrowing is not sensible because "repayments" could always be deferred to the future.

For each of the compliance periods, the regulator allocates emission permits to the participants of the system according to the predefined cap. Permits are either distributed for free or through an auction mechanism.[37] In case of free allocation, it is most conventional to distribute permits by *grandfathering*, which means that future allocations to a polluter are based on his historical emissions. Under idealized conditions, the initial allocation is of minor importance since any possible allocation leads to an efficient outcome of the system.[38] This does not hold, however, under imperfect (and more realistic) conditions as shown by Stavins (1995) and Goulder et al. (1997), for example. Especially grandfathering can create incentives for higher emissions in order to get more permits for free in the future.[39] On the other hand, the introduction of emission trading systems in the past has shown that a free allocation of permits is politically more feasible.[40] To connect the strengths of both approaches, current emission trading systems usually start with a small proportion of auctioned permits for the first periods, before increasing the amount auctioned step by step for future allocations.[41]

[36] See Fankhauser and Hepburn (2010a).
[37] A more detailed overview of different allocation procedures is given by Tietenberg (2006), Chapter 6. Different auction mechanisms in particular are considered by Cramton and Kerr (2002).
[38] See Montgomery (1972), Theorem 3.3.
[39] This issue is raised by Hepburn et al. (2006) and Zapfel (2007) in the context of the EU ETS. Harstad and Eskeland (2010) model this aspect as a signaling game.
[40] See Schmalensee et al. (1998).
[41] Exact figures on the auctioning amount in current emission trading systems are given by Perdan and Azapagic (2011), Table 1.

By the end of a compliance period, companies are obliged to cover their emissions with a sufficient number of permits, either originating from their initial allocation or acquired from other participants. To enforce compliance, it is usual to impose a monetary penalty on companies whose emissions exceed the amount of permits. Current emission trading systems penalize each ton of exceeding emissions with a constant amount.[42] In addition, lacking permits have to be delivered in the next compliance period.

Given these basic components of a cap-and-trade system, participants trade emission permits among each other, and prices result from their demand for permits needed to avoid penalties. Although the aspect of price stability is taken into account when designing these basic components, prices can in principal fluctuate freely, so that high volatilities or particularly low or high prices cannot be completely inhibited. Therefore, approaches are developed that restrict price flexibility by adding a price floor, price cap, or both of them (i.e., a price collar) to a cap-and-trade system. Grüll and Taschini (2011) give an overview of such design options and show that all these hybrid approaches can be decomposed into an ordinary cap-and-trade scheme (without these features) and a number of different financial options written on emission permits that are allocated to the participants. Studying emission trading systems with restricted price flexibility thus naturally involves the analysis of ordinary cap-and-trade systems, enhanced by the financial options standing for the particular price restriction.

Finally, an aspect that gains importance with the increasing number of emission trading systems around the world is the linkage of different schemes. By linking different emission trading systems, the flexibility for abatements is increased, making it possible to achieve the aggregate reduction goals at lower overall cost. Moreover, it increases liquidity on related markets. These potentials can obviously be exploited in the most complete way if schemes are integrated by a bilateral link that allows to transfer permits in both directions (see Mehling and Haites 2009). However, this requires the coordination of policy-makers in order to ensure the compatibility of the linked systems. For example, if a scheme that prohibits banking of permits is bilaterally linked to a system with unlimited banking, then banking becomes effectively allowed in the former scheme by transferring permits forwards and backwards. A much more flexible solution is to link systems unilaterally, so that permits can be transferred between the systems only in one direction. As an example, the link of the EU ETS to the Kyoto mechanisms

[42] The properties of a constant penalty compared to different penalty structures are investigated by Stranlund (2007).

is unilateral, since Kyoto units can be used for compliance within the EU ETS, but EUAs are not usable under the Kyoto Protocol.

2.3. EU Emissions Trading System

2.3.1. Specific Design Features

As the world's largest emission trading system, the EU ETS is the main example of application in this thesis when it comes to model calibration and empirical analysis. It was launched in 2005 and started with a trial period from 2005 to 2007 (Phase I) under relaxed conditions. Particularly, the penalty was set to 40 Euros for each ton of exceeding emissions instead of 100 Euros, and the amount of emission permits allocated to the regulated companies was fairly generous. As a consequence, there were a lot of leftover EUAs not needed for compliance, leading to a price collapse because banking into the next compliance period was prohibited at the end of Phase I. That effectively meant a restart of the scheme with the beginning of the compliance period from 2008 to 2012 (Phase II). This period coincides with the first commitment period of the Kyoto Protocol and is followed by compliance periods from 2013 to 2020 (Phase III), 2021 to 2028 (Phase IV), and further eight year periods.[43] It is explicitly allowed to bank permits within and, as of Phase II, also between compliance periods. Borrowing is prohibited between different compliance periods, but it is possible within a period due to the system's yearly schedule: Permits have to be surrendered by April 30 of the following year,[44] while the annual allocation process is completed by February 28 at the latest.[45] Since EUAs of the same compliance period are not distinguishable, this makes it possible to borrow up to the amount allocated in the following year. At realistic emission levels, this allows to cover potentially exceeding emissions within a compliance period by borrowing, such that penalties only accrue at the very end of a period.[46]

The allocation of emission permits in Phase I and Phase II is carried out by the individual member states based on National Allocation Plans (NAPs). A NAP specifies the

[43] See MEMO/08/796 of the European Commission (2008c).
[44] See Article 12 of Directive 2003/87/EC.
[45] See Article 11 of Directive 2009/29/EC.
[46] This simplification cannot be made if there is a significant probability that permits allocated for the current and the following year are completely needed to cover emissions of the current year because borrowing from later years is not allowed.

amount of EUAs to be allocated and to which extent the permits are auctioned to the participants of the system. Permits that are not auctioned are distributed for free, at least 95% (90%) of the permits in Phase I (II).[47] Further, member states have to ensure that their plans are in line with the targets of the Kyoto Protocol and other relevant agreements.[48] NAPs are submitted to the European Commission and can be rejected if they are not in line with these terms. As of Phase III, NAPs are replaced by an EU-wide cap defining the overall amount of allocated EUAs[49] and a "harmonised" allocation procedure for all member states.[50] The cap amounts to about 2.04 billion permits for 2013 and declines annually by 37.4 million EUAs.[51] According to the "harmonised" allocation procedure, the proportion of this cap that is allocated for free is determined based on National Implementation Measures (NIMs).[52] For that, each member state compiles a list of regulated installations and submits it to the European Commission. An amount of EUAs is assigned to each installation based on the emissions of a corresponding benchmark installation, set at the "average performance of the 10% most efficient installations."[53] Of this benchmark amount, 80% are allocated for free in 2013, and this proportion decreases to 30% by 2020. From 2027 on, no further EUAs will be allocated for free.[54] The part of the cap that is not allocated for free is auctioned by the member states.[55]

After allocation, EUA holdings are managed within electronic databases called *registries*. Transferring an emission permit from one account to another is a simple electronic procedure which involves to change the corresponding entries in the registry. All transactions are monitored by an independent transaction log.[56] Until 2012, each member state hosted a national registry, and transfers between accounts from different countries were coordinated by the Community Independent Transaction Log (CITL).

[47] See Article 10 of Directive 2003/87/EC.
[48] See Article 9 and Annex III of Directive 2003/87/EC.
[49] See Article 9 of Directive 2009/29/EC.
[50] See Article 10a of Directive 2009/29/EC.
[51] This amount is equivalent to 1.74% of the average yearly allocation in Phase II, as stated by Decision 2010/634/EU of the European Commission (2010a).
[52] See Article 11 of Directive 2009/29/EC.
[53] See Article 10a(2) of Directive 2009/29/EC.
[54] Exceptions are installations from the power generation sector which do generally not get any free allocation, and industries that are likely to be affected by carbon leakage, getting all permits for free. These rules are specified in the amendments to Article 10a, especially numbers 1, 11, and 12, in Directive 2009/29/EC, together with MEMO/10/338 of the European Commission (2010c).
[55] See Article 10 of Directive 2009/29/EC.
[56] See Article 19 and 20 of Directive 2003/87/EC.

Several national registries were under attack by cyber-criminals in 2011 who stole EUAs of about 50 million Euros by transferring allowances from hacked accounts.[57] In response to that, the EU Commission revised the existing registry infrastructure by replacing the national registries with a single Union Registry which works under enhanced security standards.[58] The Union Registry is in operation since June 20, 2012. The CITL is superseded by the European Union Transaction Log (EUTL), which fills the same role for the Union Registry.

The registry also handles the compliance procedure, to balance the companies' emissions with a sufficient number of EUAs. For that, companies are obliged to monitor their emissions over the year, and to report them by March 31 of the following year.[59] After verification, a corresponding amount of EUAs is surrendered and deleted from the account in the registry. If too few permits are surrendered, a penalty of 100 Euros is incurred for each ton of exceeding emissions in Phase II, and the penalty increases "in accordance with the European index of consumer prices"[60] for subsequent compliance periods. Additionally, companies are required to deliver the lacking permits in the following year.[61] Aggregated information on the realized emissions of regulated companies is released to the public every year since 2006, with an announcement date in early April since 2007.[62] The effects of this news event on the European carbon market are in the focus of our analysis in Chapter 5.

2.3.2. Markets and Products

European Union Allowances and related derivatives are traded on several exchanges across Europe as well as over-the-counter. In 2011, 49% of all trades related to the European carbon market were processed through exchanges, and 51% through brokers or bilaterally.[63] Interestingly, the spot market accounts for only 2% of the overall EUA transaction volume,[64] and most of the trading (around 88% in 2011) takes place in EUA

[57] See Kossoy and Guigon (2012).
[58] See Regulation 1193/2011 of the European Commission (2011a).
[59] See Article 15 of Directive 2003/87/EC.
[60] See Article 16(4) of Directive 2009/29/EC.
[61] See Article 16 of Directive 2003/87/EC.
[62] The data is published on the website of the CITL/EUTL, see `http://ec.europa.eu/environment/ets/`.
[63] See Kossoy and Guigon (2012).
[64] The largest spot exchange in 2011 was BlueNext, accounting for 62% of the spot trading volume according to their own statements.

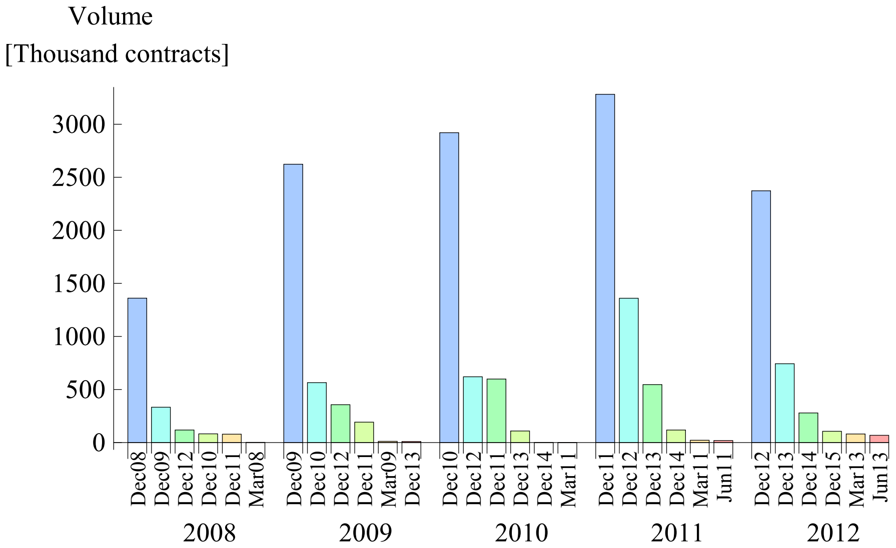

Figure 2.2.: Yearly trading volumes of the six most liquid EUA futures contracts on the European Climate Exchange (ECX). Volumes are denoted in thousands of futures contracts traded, with a contract size of 1,000 EUAs per contract.

futures.[65] While a predominant role of the futures market is typical for markets in which physical delivery or storage of the spot asset is particularly complicated or costly, the delivery of an EUA only involves an electronic transfer in the registry.[66] A possible explanation for the low spot trading volumes is that futures trading ties up less capital and polluting companies do not need to own EUAs at any other time than right before the compliance date at the end of April. Thus, they can adjust their permit holdings for compliance through futures contracts and do not have to engage in spot market trading (see Daskalakis et al. 2011). On top of that, the cyber-theft incidents have damaged the reputation of the spot market. On the one hand, it was unclear if holders of spot EUAs would be held liable for possessing stolen permits. On the other hand, registries were closed after these incidents for some time, so that spot markets had to be suspended. Finally, with the migration to the Union Registry a delay of 26 hours was introduced between the initiation of a trade and its final completion. This delay is abolished again with the introduction of trusted account lists.[67]

[65] See Kossoy and Guigon (2012).
[66] BlueNext used to carry out the delivery of an EUA within 15 minutes, see Daskalakis et al. (2011).
[67] See Article 24 and 36(3) of Regulation 1193/2011.

Figure 2.3.: Daily EUA futures prices from January 2008 to June 2012 provided by the ECX. The futures price series is constructed by taking the December contract next to maturity and rolling over to the next contract on the last day of October.

The most important trading venue for EUA futures is the European Climate Exchange (ECX) with a market share of more than 92%, which makes it also to the world's largest carbon futures exchange.[68] EUA futures are available with quarterly expiries on the last Monday of March, June, September, and December for the first years, and with yearly expiry in December up to 2020. Considering the trading volumes of the different futures in Figure 2.2 clearly reveals that the December contract next to maturity is always traded with highest liquidity. It is generally followed by the December contracts with longer maturities in corresponding order. As an exception, the December 2012 contract has a special role because its maturity date almost coincides with the end of Phase II, and it is traded more liquidly than some of the shorter maturities. Futures not maturing in December account only for small parts of the overall trading volume.

In line with these observations, the empirical parts of this thesis (Chapter 4 and Chapter 5) build on a time series constructed by taking the EUA December futures next to

[68]The ECX is operated by IntercontinentalExchange (ICE), see `http://www.theice.com`.

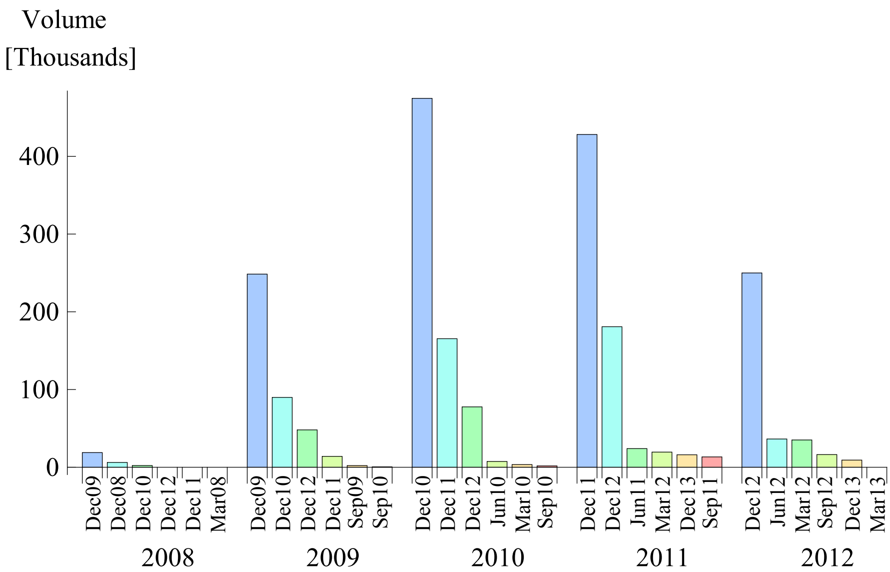

Figure 2.4.: Yearly trading volumes of the six most liquidly traded maturities of EUA futures options on the European Climate Exchange (ECX). Volumes are denoted in thousands of options traded. One EUA futures option allows to enter one EUA futures contract at expiry.

maturity and rolling over to the next contract on the last day of October. Although futures maturing within the same compliance period are completely linked by the standard cost-of-carry relationship,[69] price information from the most liquid contract should be least affected by equilibrium errors caused by market microstructure effects. Figure 2.3 illustrates EUA futures prices from 2008 to June 2012. Prices first rose up to a high of 29.33 Euros in July 2008, before they plummeted in consequence of the financial crisis and the subsequent economic downturn. Since then prices are less volatile, but still cover a range from 6 to 17.50 Euros.

Besides EUA futures, the most important derivatives in the European carbon market are European options written on these futures. Options on all futures contracts are available and expire three trading days before the futures' maturity. The trading volumes of options with different maturities on the ECX (see Figure 2.4) basically follow the same pattern as the futures contracts, i.e., options expiring in the next December are most

[69]This can be shown theoretically (see Section 3.3.2) and is confirmed by empirical studies (Uhrig-Homburg and Wagner 2009; Rittler 2012).

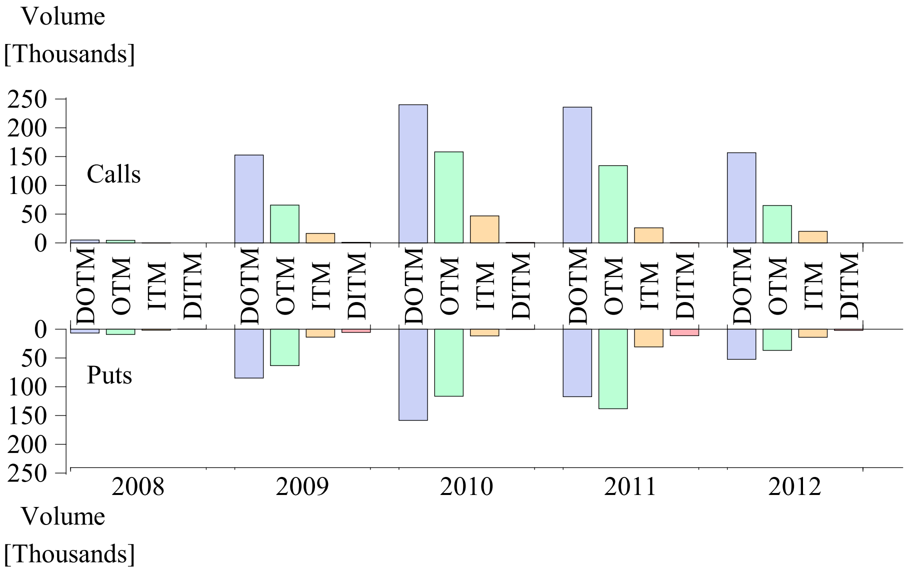

Figure 2.5.: Yearly trading volumes of EUA futures options on the European Climate Exchange (ECX) classified by option type and moneyness category. We call a call (put) option OTM if its moneyness, i.e., the strike price divided by the underlying futures price, is between 1 and 1.15 (0.85 and 1), deep OTM if its moneyness is larger (smaller) than 1.15 (0.85), ITM if the moneyness is between 0.85 and 1 (1 and 1.15), and deep ITM if the moneyness is smaller (larger) than 0.85 (1.15). Volumes are denoted in thousands of options traded. One EUA futures option allows to enter one EUA futures contract at expiry.

frequently traded, followed by the later December expiries and other quarterly maturities. In contrast to futures contracts, options expiring in the following compliance period (2013 or later) are only traded to a very minor degree. Subdividing the option data into different moneyness categories reveals further insights into the structure of the option market. As Figure 2.5 shows, (deep) out-of-the-money (OTM) options are traded much more actively than (deep) in-the-money (ITM) options, which is typical for option markets in general (see, e.g., Barone-Adesi et al. 2008 for the case of equity options). Further, we observe that call options are traded more extensively than put options in the European emissions market.

3. Equilibrium Price Dynamics of Emission Permits

3.1. Introduction

In this chapter, we propose a stochastic equilibrium model for emissions markets to analyze the specific properties of emission permit prices and derive implications for the most important related derivatives. Our model accounts for all important design features of current emission trading systems as described in Section 2.2: a sequence of consecutive compliance periods, allowance of banking and prohibition of borrowing, penalties for non-compliance, and later delivery of lacking permits. Companies have stochastic greenhouse gas emissions and choose an optimal trade-off between implementing abatement measures, taking the risk of penalty payments, and trading permits at equilibrium prices.

Equilibrium models for permit markets are considered under certainty in the environmental economics literature, among others by Cronshaw and Kruse (1996), Rubin (1996), and Schennach (2000). More recently, Seifert et al. (2008) and Carmona et al. (2009, 2010) develop stochastic models for emission trading schemes of one finite compliance period to characterize equilibrium outcomes and analyze the behavior of permit prices. Chesney and Taschini (2012) investigate the effects of asymmetric information in a similar setting. Different to those models, Kijima et al. (2010) and Cetin and Verschuere (2009) construct markets with two compliance periods. The general equilibrium framework of Kijima et al. (2010) allows either both inter-period banking and borrowing or neither of them, while Cetin and Verschuere (2009) focus on a setting without inter-period banking. Carmona and Fehr (2011) consider a system of multiple compliance periods in the context of linking different emission permit markets.

The next section introduces our model framework. In Section 3.3, we derive equilibrium outcomes and discuss the price properties of emission permits induced by the design of the emission trading scheme. Most importantly, we characterize an emission permit as a strip of European binary options written on economy-wide emissions. In contrast to classical financial options, the dynamics of this non-tradable underlying is no longer exogenously given, but derived endogenously through abatement measures. We exploit this option analogy to derive several general characteristics of emission permit spot and futures prices. Section 3.4 calibrates the model to a setting in accordance with Phase II of the EU ETS. In this setting, we investigate permit prices, volatilities, and their dependency on abatement measures and future compliance periods. We further analyze the futures price curve for different emissions scenarios. Finally, a simulation study based on our model allows us to deduce characteristic properties of the option-implied volatility smile in emission permit markets.

3.2. Theoretical Model

We consider an economy given by a set of companies I whose greenhouse gas emissions are regulated under a cap-and-trade system with n consecutive compliance periods $[0, T_1], [T_1, T_2], \ldots, [T_{n-1}, T_n]$. At time 0, each company $i \in I$ receives an endowment $(e_1^i, \ldots, e_n^i)$ of emission permits for the different periods of the system, i.e., e_k^i is the initial amount of *period-k permits* that are valid for compliance in period $[T_{k-1}, T_k]$, with $T_0 = 0$. Companies are obliged to cover the emissions realized during period k by a sufficient number of period-k permits by the end of the period, T_k. For enforcement, a penalty of p_k is imposed for each ton of exceeding emissions. In addition, lacking permits have to be delivered in the following compliance period, effectively reducing the number of period-$k + 1$ permits. In a similar way, leftover permits not needed for compliance in period k are banked into the next period, adding to the amount of period-$k + 1$ permits. It is not allowed, however, to borrow permits that are allocated for a future compliance period and use them in the ongoing period. After $[T_{n-1}, T_n]$, the last period of the system, left-over permits as well as obligations to later delivery are forfeited.

Let us consider these rules for a company i whose emissions during the n different compliance periods are specified by random variables $x_{0,T_1}^i, x_{T_1,T_2}^i, \ldots, x_{T_{n-1},T_n}^i$. For ease of illustration we first ignore the company's abatement and trading activities. If i's overall emissions during period 1 are larger than e_1^i, the exceeding $(x_{0,T_1}^i - e_1^i)$ tons of emissions are penalized, and i has to deliver the lacking permits in period 2, decreasing the number of period-2 permits by the same amount. If, to the contrary, $x_{0,T_1}^i < e_1^i$, then i banks the leftover period-1 permits into period 2, adding $(e_1^i - x_{0,T_1}^i)$ to the amount of period-2 permits. In summary, i pays a penalty of $p_1(x_{0,T_1}^i - e_1^i)^+$ and the number of period-2 permits is altered to $e_2^i + (e_1^i - x_{0,T_1}^i)$.[70] Analyzing the same for period 2, we see that penalties are incurred if $x_{T_1,T_2}^i - (e_2^i + e_1^i - x_{0,T_1}^i) > 0$. This can be reinterpreted in the sense that the amount of exceeding emissions at the end of period 2 is the difference between i's cumulative emissions from 0 up to T_2, $x_{0,T_2}^i = x_{0,T_1}^i + x_{T_1,T_2}^i$, and the cumulative amount of permits $q_2^i = e_1^i + e_2^i$ that is allocated for periods 1 and 2. In general terms, the amount of lacking or leftover permits in period k results as the difference between i's cumulative emissions up to T_k and the cumulative allocation $q_k^i = \sum_{j=1}^{k} e_j^i$ for all compliance periods up to k, that is $x_{0,T_k}^i - q_k^i$. For convenience we simply write x_{T_k} for x_{0,T_k} throughout the rest of the thesis. Overall, the present value of the expected penalty imposed on i by the cap-and-trade system is

$$\mathbb{E}_0\left\{\sum_{j=1}^{n} e^{-rT_j} p_j (x_{T_j}^i - q_j^i)^+\right\}, \tag{3.1}$$

where r is the constant risk-free interest rate and $\mathbb{E}_t\{.\}$ denotes the expectation based on time-t information.

Companies actively manage their risk of paying penalties by trading permits in the market and reducing their emissions through emission abatement measures. At each point in time, a company chooses the amount $\theta_{k,t}^i$ of period-k permits it buys or sells in the market at equilibrium price $S_k(t)$, adjusting its time-t holdings to $e_k^i + \int_0^t \theta_{k,s}^i ds$. Incorporating the trading strategy alters the expected penalty payment (3.1) by replacing q_k^i with $Q_k^i = \sum_{j=1}^{k} \left(e_j^i + \int_0^{T_j} \theta_{j,s}^i ds\right)$.

In the same way, the company decides about the operative abatement measures ξ_t^i it implements at t to reduce its instantaneous emissions. Without abatement, i's emissions are driven by two components: A persistent business-as-usual emission rate y^i

[70] Throughout this thesis, we write z^+ for $\max\{0, z\}$.

following the Itô process

$$y_t^i = y_0^i + \int_0^t \mu_y^i(s)ds + \int_0^t \sigma_y^i(s)dZ_s^i \tag{3.2}$$

with time-dependent drift $\mu_y^i(t)$ and volatility $\sigma_y^i(t) > 0$, and short-term emission shocks n^i given by

$$n_t^i = \sigma_\varepsilon^i \varepsilon_t^i \tag{3.3}$$

with $\sigma_\varepsilon^i > 0$. Z^i is a standard Wiener process and ε^i is a standard Gaussian white noise process, and we assume that the increments of $W_t^i = \int_0^t \varepsilon_s^i ds$ and Z_t^i are uncorrelated.[71] While y^i captures deterministic patterns of the emission rate like seasonalities as well as fluctuations that are permanent in nature, n^i represents temporary shocks like the outage of a carbon-friendly production unit that is instantaneously replaced by a more polluting one. Reduced by operative abatement ξ_t^i, i's instantaneous emission rate is $y_t^i + n_t^i - \xi_t^i$, and its cumulative emissions up to time t result as

$$x_t^i = \int_0^t (y_s^i + n_s^i - \xi_s^i)ds. \tag{3.4}$$

Abating at an instantaneous rate of ξ_t^i costs $C^i(\xi_t^i)$, where C^i is a differentiable and convex abatement cost function, as motivated by detailed bottom-up studies (e.g., Klepper and Peterson 2006; Nauclér and Enkvist 2009) which point out that marginal abatement costs increase at least linearly.[72]

Given these ingredients, each company maximizes its utility by finding an optimal trade-off between implementing abatement measures, trading permits in the market, and taking the risk of penalty payments. Under risk-neutrality,[73] the company mini-

[71] We also assume that the increments of W_t^i and Z_t^j are uncorrelated across companies, i.e., for all $i, j \in I$.

[72] Note that C^i stands for the costs of operative abatement ξ^i, not for investments into carbon-friendly technologies. Carbon-related investments do not change the instantaneous emission rate, but lead to a flatter operative abatement cost function C^i in the future, similar to general technological progress. Simple models for technological progress resulting in deterministically time-dependent abatement cost functions do not change our results. For optimal investment policies in the context of emission trading systems we refer to Taschini (2008) and the references therein.

[73] The effects of risk aversion on the price dynamics of emission permits are analyzed by Seifert et al. (2008) within a framework of one single compliance period.

mizes overall costs by solving the optimization problem

$$\min_{(\theta^i,\xi^i)} \mathbb{E}_0\left\{ \int_0^{T_n} e^{-rt} C^i(\xi_t^i)dt + \sum_{j=1}^{n} \int_0^{T_j} e^{-rt} S_j(t)\theta_{j,t}^i dt + \sum_{j=1}^{n} e^{-rT_j} p_j (x_{T_j}^i - Q_j^i)^+ \right\} \tag{3.5}$$

with optimal trading strategy $\theta^i = (\theta_1^i, \ldots, \theta_n^i)$, $\theta_k^i = (\theta_{k,t}^i)_{t\in[0,T_k]}$ and abatement strategy $\xi^i = (\xi_t^i)_{t\in[0,T_n]}$. The first term of (3.5) represents the costs for implementing abatement measures and the second term describes the costs of i's trading strategy. The last term incorporates possible penalties at the end of each compliance period in accordance with (3.1).

3.3. Emissions Market Equilibrium

We solve the model for equilibrium permit prices that clear the market when all companies $i \in I$ choose optimal trading and abatement strategies according to (3.5). To begin with, we apply the stochastic maximum principle in conjunction with dynamic programming (see Appendix A.1) to characterize the optimal trading and abatement strategy of a company for given permit prices $S_1, \ldots, S_n$.

Proposition 1 (Optimality Conditions) *For an optimal trading and abatement strategy (θ^i, ξ^i), a company's instantaneous marginal abatement costs are equal to the permit price of the ongoing compliance period,*

$$\frac{\partial C^i}{\partial \xi^i}(\xi_t^i) = S_k(t), \quad t \in [T_{k-1}, T_k]. \tag{3.6}$$

Further, the present value of a company's expected overall penalty for an additional ton of emissions in period k is equal to the price of period-k emission permits, $k = 1, \ldots, n$, that is[74]

$$\sum_{j=k}^{n} e^{-r(T_j-t)} \mathbb{P}_t \left\{ x_{T_j}^i > Q_j^i \right\} p_j = S_k(t), \quad t \in [0, T_k]. \tag{3.7}$$

[74] $\mathbb{P}_t\{.\}$ denotes the probability conditional on time-t information.

The first condition arises due to the fact that companies can achieve compliance equally by abating emissions or by buying additional permits in the market. Both actions reduce the number of uncovered emissions at the end of the ongoing compliance period. Consequently, the marginal cost of both actions is equal for an optimal strategy, since otherwise a company could improve by abating more emissions and buying less permits, or vice versa. This result is central to deterministic models for cap-and-trade systems developed in the environmental economics literature (e.g., Cronshaw and Kruse 1996; Rubin 1996).[75]

The second condition characterizes the marginal value of an emission permit for an individual company, which is induced by the system's penalty mechanism and the rules on banking, borrowing, and later delivery. If a company is short of permits for a particular compliance period k, then an additional permit saves a penalty payment and additionally also reduces the number of permits to be delivered later, which effectively increases the amount of permits in the next compliance period. In case of a permit surplus, an additional permit does not avoid any penalty payment, but it can be banked and adds to the available amount of permits in the following compliance period as well. The same logic applies for the following compliance periods again. Overall, the marginal value of a period-k emission permit equals the sum of penalties for period k and all following compliance periods weighted by the probability that penalties arise. For an optimal strategy, this marginal value is equal to the permit price S_k.[76]

3.3.1. Permit Prices

Proposition 1 implies that in equilibrium, marginal abatement costs as well as the probability of penalties to accrue are equalized over all companies in the economy, in line with the emissions market mechanism first formalized by Montgomery (1972). In a situation where marginal abatement costs differ across companies, companies with lower marginal abatement costs extend their abatement activities and sell emission permits to companies with higher abatement costs, enabling them to cut back their abatement

[75] This result is also shown within stochastic equilibrium models for one compliance period in the literature, see for example Seifert et al. (2008) and Carmona et al. (2009, 2010). In the context of multiple compliance periods, it is important to note that marginal abatement costs are equal to the permit price for the period in which the abatement is actually realized, which is the ongoing period in our case.

[76] For the special case of one single compliance period ($n = 1$), this result and the following Proposition 2 are shown by Carmona et al. (2009, 2010) in a discrete-time model.

actions. If they agree on a permit price between their respective marginal abatement costs, both companies are able to profit from these actions, implying that such situation cannot persist in equilibrium. In the same way, the market is not in equilibrium if some companies have uncovered emissions at the end of a compliance period T_k while others have remaining permits. Taking a global point of view, this condition implies that one and thus every company's emissions exceed their permit holdings exactly when economy-wide cumulative emissions $x_{T_k} = \sum_{i \in I} x^i_{T_k}$ exceed economy-wide permit holdings $Q_k = \sum_{i \in I} Q^i_k$. Since the market clearing condition holds in equilibrium, individual trading strategies cancel out in Q_k and we have $Q_k = q_k = \sum_{i \in I} q^i_k$. Altogether, the following result arises from condition (3.7).

Proposition 2 (Equilibrium Permit Prices) *In equilibrium, the price of a period-k emission permit is given by*

$$S_k(t) = \sum_{j=k}^{n} e^{-r(T_j - t)} \mathbb{P}_t \left\{ x_{T_j} > q_j \right\} p_j \tag{3.8}$$

for $t \in [0, T_k]$*. That is, an emission permit is a strip of European binary call options written on cumulative economy-wide emissions.*

This proposition characterizes emission permits created in the context of environmental trading schemes as a financial derivative. The price of an emission permit consists of one value component for each compliance period of the system representing the probability that penalties accrue for that period because the economy is short of emission permits. At the end of the period, T_k, this value is equal to the penalty for exceeding emissions in that period if cumulative emissions x_{T_k} exceed the cumulative allocation q_k, and zero otherwise. Thus it has a payoff function that is identical to a European binary call option with maturity T_k and strike q_k, written on the cumulative emissions $x_t = \sum_{i \in I} x^i_t$ of the whole economy. The dynamics of this non-tradable underlying is given by

$$dx_t = (y_t - \xi_t)dt + \sigma_\varepsilon dW_t \tag{3.9}$$

in our framework, where $y_t = \sum_{i \in I} y^i_t$ is the economy-wide business-as-usual emission rate following

$$dy_t = \mu_y(t)dt + \sigma_y(t)dZ_t \tag{3.10}$$

and $\xi_t = \sum_{i \in I} \xi_t^i$ is economy-wide abatement. The parameter σ_ε as well as the functions $\mu_y(t)$ and $\sigma_y(t)$ result from aggregating the individual emissions processes (3.2), (3.3), and (3.4) such that W_t and Z_t are standard Wiener processes with uncorrelated increments. A distinctive feature of economy-wide emissions x_t as a non-tradable underlying is that market participants can and obviously do influence its state through their abatement actions ξ_t. Since abatement reduces the companies' greenhouse gas emissions, an emission permit is worth less than the corresponding strip of binary options in a scenario where no abatement is possible.

The specific form of permit prices revealed by Proposition 2 obviously affects their precise distributional properties,[77] but finds also expression in major structural features. First, there is a time-dependent upper bound for emission permit prices,

$$S_k(t) \leq \sum_{j=k}^{n} e^{-r(T_j - t)} p_j, \tag{3.11}$$

corresponding to a scenario of permit shortage for all compliance periods. In such a situation, one permit less means an additional penalty in the current and also in all following compliance periods due to the later delivery rule. This upper bound of emission permit prices obviously depends on the number of compliance periods in the system. Furthermore, the single value components of an emission permit are pulled to one of the two values — zero or the penalty — by the end of the corresponding compliance period. This effect is weak as long as the period end is far and the uncertainty about penalties to accrue is high, such that medium values are attained with significant probabilities. As uncertainty decreases, the convergence to one of the two possible values becomes stronger. As a direct consequence, the prices of period-k and period-$k+1$ permits are either identical at the end of period k, or differ by the amount of the penalty, that is

$$S_k(T_k) - S_{k+1}(T_k) = 1_{\{x_{T_k} > q_k\}} p_k. \tag{3.12}$$

This means that there is a smooth transition when period-k permits are converted into period-$k+1$ permits by banking if the economy is in permit surplus. In contrast, if the

[77] In Chapter 4, we show that reduced-form model variants derived from our equilibrium model are indeed better suited to capture the empirical properties of emission permit prices and related derivatives than standard models for asset price dynamics.

economy is short of permits, prices decrease by the penalty similar to the drop in value of a coupon bond after a coupon payment date.

Understanding an emission permit as a strip of binary options also sheds light on the volatility structure of permit prices. Given the dynamics (3.9) and (3.10) of cumulative emissions and the prevailing emission rate, we obtain local volatilities by applying Itô's Lemma.

Proposition 3 (Local Volatility) *Relative local volatility of emission permit prices, as given by*

$$\sigma_{S_k} = \frac{\sqrt{\left(\frac{\partial S_k}{\partial x}\sigma_\varepsilon\right)^2 + \left(\frac{\partial S_k}{\partial y}\sigma_y\right)^2}}{S_k}, \tag{3.13}$$

is state- and time-dependent.

Due to the binary options characteristics of emission permits, the volatility of the single value components $S_k - S_{k+1}$ clearly depends on the time to the end of the compliance period, T_k, and is almost surely zero at the end of the period.[78] The state-dependency becomes most evident when comparing scenarios of extremely high and medium emissions. In the first case, prices are close to the upper bound (3.11) and absolute volatility (that is, the numerator of (3.13)) is almost zero, since a marginal change in cumulative emissions or the prevailing emission rate hardly changes the probability of penalties. On the other hand, relative volatility is clearly higher in a scenario of medium emissions, since absolute volatility is positive and prices are far away from the upper bound. For very low emissions, however, we do not get a clear indication for the volatility behavior, since absolute volatilities go to zero, but prices approach zero as well. We shed light on this aspect by considering the detailed volatility structure for a calibrated setting in Section 3.4.1.

3.3.2. Futures

It is market convention to consider the emission permits of the actual ongoing compliance period as *spot permits*, such that spot permits are period-1 permits until the end of

[78] Since $\sigma_\varepsilon > 0$, Section 3.3 of Carmona et al. (2013) applies to our model, which implies that the cumulative emissions exactly hit the cap with zero probability, $\mathbb{P}_t \left\{x_{T_k} = q_k\right\} = 0$.

compliance period 1, then period-2 permits until T_2, and so on. This view makes practical sense because only period-1 permits are usable for compliance in period 1, and are converted into period-2 permits by banking at the end of the period. In accordance with that, *permit futures* deliver spot permits at maturity. While a futures contract with maturity $\bar{t} \in [0, T_1)$ delivers a period-1 permit, futures maturing at $\bar{t} \in (T_1, T_2)$ deliver period-2 permits. Based on this convention, we characterize the futures price curve in emission permit markets and discuss the applicability of classical convenience yield models.

Consider an *intra-period* futures contract at $t \in [0, T_1)$ with maturity $\bar{t} \in [t, T_1)$. Since period-1 permits cannot be used for compliance before T_1, they are pure investment assets before that date, and the storability of permits directly implies the standard cost-of-carry relation

$$F(t, \bar{t}) = e^{r(\bar{t}-t)} S_1(t), \tag{3.14}$$

where $F(t, \bar{t})$ is the futures price.

To the contrary, this does not apply to *inter-period* futures, i.e., the case $t \in [0, T_1)$, $\bar{t} \in (T_1, T_2)$. The futures contract delivers a period-2 permit, which can obviously not be used for compliance in period 1, while holding the spot (period-1) permits provides the option to use them at the end of period 1. This additional benefit can be quantified by the difference between period-1 and period-2 permit prices according to (3.8) together with (3.14):

$$F(t, \bar{t}) = e^{r(\bar{t}-t)} S_1(t) - e^{r(\bar{t}-T_1)} \mathbb{P}_t \{x_{T_1} > q_1\} p_1. \tag{3.15}$$

Consequently, the backwardation of inter-period futures defined as the difference between the current spot price and the discounted futures price, $B(t, \bar{t}) = S_1(t) - e^{-r(\bar{t}-t)} F(t, \bar{t})$, is determined by the probability of permit shortage at the end of the ongoing compliance period. We summarize the implications of (3.14) and (3.15).[79]

Proposition 4 (Futures Price Curve) *The futures price curve has the following properties for all $t \in [0, T_1)$:*

a) Futures are in contango within the compliance period, i.e., for $\bar{t} \in [t, T_1)$.

[79] In line with Litzenberger and Rabinowitz (1995), futures with maturity $\bar{t}$ are in contango if $B(t, \bar{t}) \leq 0$ and in (weak) backwardation if the futures price is lower than the compounded spot price, i.e., $B(t, \bar{t}) > 0$. Strong backwardation means that the futures price is lower than the current spot price.

b) *The backwardation of futures with maturity in the following compliance period, i.e., $\bar{t} \in (T_1, T_2)$, is given by*

$$B(t, \bar{t}) = e^{-r(T_1 - t)} \mathbb{P}_t \left\{ x_{T_1} > q_1 \right\} p_1. \tag{3.16}$$

In particular, inter-period futures are in contango if the probability of permit shortage at the end of the ongoing compliance period is 0, in weak backwardation if it is positive, and in strong backwardation if it is above $\left(e^{r(T_1-t)} - e^{-r(\bar{t}-T_1)}\right) \frac{S_1(t)}{p_1}$.

This proposition provides a direct link to the classical commodity literature. Holding the spot asset endows the owner with an embedded usage and timing option as elaborated by Routledge et al. (2000) and Jarrow (2010), among others. However, while for classical commodities any point in time comes into question for exercising this usage option, emission permits can only be consumed at the end of a compliance period. Thus, this option is worthless within a compliance period and holding the spot permit has no advantage compared to futures maturing in the same period. To the contrary, the usage option becomes relevant if the futures' maturity is in the next compliance period. If the economy is short of permits, the option is exercised to save penalty payments. Otherwise, it is not exercised for a number of leftover permits which are banked into the next period. Consequently, inter-period futures are in weak backwardation if the probability of permit shortage at the end of the compliance period is not exactly zero.

Since the seminal work of Brennan (1958), it is common to express the benefit of holding the spot asset rather than a futures contract as a convenience yield. In general, a time-dependent stochastic instantaneous convenience yield δ_t changes the standard cost-of-carry relation to

$$F(t, \bar{t}) = \mathbb{E}_t \left\{ e^{r(\bar{t}-t) - \int_t^{\bar{t}} \delta_s ds} \right\} S_1(t). \tag{3.17}$$

For given $t \in [0, T_1)$ we define $D_t(\bar{t}) := \int_t^{\bar{t}} \delta_s ds$ as the convenience yield from t to $\bar{t}$. From (3.14) and (3.15) we can easily derive necessary properties of D_t.

Proposition 5 (Convenience Yields) *The cumulative convenience yield D_t fulfills*

a) $D_t(\bar{t}) = 0$ *for intra-period futures, i.e.,* $\bar{t} \in [t, T_1)$*, and*

b) $\mathbb{E}_t\left\{e^{-D_t(\bar{t})}\right\} = 1 - \frac{e^{-r(T_1-t)}\mathbb{P}_t\{x_{T_1} > q_1\}p_1}{S_1(t)}$ *for inter-period futures, i.e.,* $\bar{t} \in (T_1, T_2)$.

It is obvious that D_t has to "jump" in T_1 in order to fulfill the conditions of Proposition 5. Therefore it is not possible to define an instantaneous convenience yield δ_t in such way that D_t has these properties. In particular, standard models like a mean-reverting stochastic convenience yield or a simple AR(4) process as used by Daskalakis et al. (2009) and Chevallier (2009) for inter-period futures do not satisfy Proposition 5. These models inevitably lead to relative mispricing when futures of two or more different maturities are considered.

3.3.3. Calculating Equilibrium Prices

We provide a strategy to calculate equilibrium permit prices as the solution of a system of partial differential equations (PDEs). Permit prices are determined by cumulative economy-wide emissions according to (3.8), but it is not simply possible to evaluate the expectation since this non-tradable underlying is influenced through endogenously derived abatement measures. More specifically, economy-wide abatement ξ_t results as the sum of the companies' abatement strategies that solve the individual optimization problems (3.5). Appendix A.2 shows that we can simplify the problem by optimizing economy-wide abatement directly with respect to an aggregate problem.

Proposition 6 (Global Problem) *Assume that economy-wide emissions x_t still follow the dynamics* (3.9)*, but let aggregate abatement ξ_t be the solution of the global problem*

$$\min_{\xi} \mathbb{E}_0\left\{\int_0^{T_n} e^{-rt}C(\xi_t)dt + \sum_{j=1}^{n} e^{-rT_j}p_j(x_{T_j} - q_j)^+\right\}, \tag{3.18}$$

where C is the aggregate abatement cost function of the economy. Then, $S_1, \ldots, S_n$ defined by equation (3.8) *are equilibrium permit price processes. Further, the permit price of the ongoing compliance period is equal to the instantaneous marginal abate-*

ment costs of the economy,

$$S_k(t) = \frac{\partial C}{\partial \xi}(\xi_t), \quad t \in [T_{k-1}, T_k]. \tag{3.19}$$

In light of this result, we determine the optimal abatement strategy of the aggregate problem (3.18). We follow a backward induction approach, starting at the last compliance period $[T_{n-1}, T_n]$ and proceeding to the periods $[T_{n-2}, T_{n-1}], \ldots, [0, T_1]$. For each compliance period k, we include the period $k+1$ solution into the terminal condition and settle the problem by dynamic programming. We state the resulting system of PDEs in here for a quadratic abatement cost function

$$C(\xi_t) = \frac{1}{2}\gamma \xi_t^2 \tag{3.20}$$

with cost coefficient γ, and economy-wide business-as-usual emissions following an arithmetic Brownian motion

$$dy_t = \mu_y dt + \sigma_y dZ_t, \tag{3.21}$$

and refer to Appendix A.3 for the derivation in the general case.

Proposition 7 (PDEs) *For the global problem* (3.18)*, optimal abatement* ξ_t *at time* $t \in [T_{k-1}, T_k]$ *is given by*

$$\xi_t = \frac{1}{\gamma} e^{r(t-T_{k-1})} \frac{\partial V_k}{\partial x}(t, x_t, y_t), \tag{3.22}$$

where V_k *is the time-*T_{k-1} *expected value of an optimal strategy starting at* T_{k-1}*.* V_k *solves the characteristic PDE*

$$\frac{\partial V_k}{\partial t} = -y_t \frac{\partial V_k}{\partial x} + \frac{1}{2\gamma} e^{r(t-T_{k-1})} \left(\frac{\partial V_k}{\partial x}\right)^2 - \frac{\partial V_k}{\partial y}\mu_y - \frac{1}{2}\frac{\partial^2 V_k}{\partial x^2}\sigma_\varepsilon^2 - \frac{1}{2}\frac{\partial^2 V_k}{\partial y^2}\sigma_y^2 \tag{3.23}$$

with boundary condition

$$V_k(T_k, x_{T_k}, y_{T_k}) = e^{-r(T_k - T_{k-1})}(p_k(x_{T_k} - q_k)^+ + V_{k+1}(T_k, x_{T_k}, y_{T_k})) \tag{3.24}$$

and $V_{n+1} = 0$*.*

As shown by Proposition 6, the solution for optimal economy-wide abatement at time t directly implies the equilibrium permit price of the ongoing compliance period through (3.19). Thus, permit prices can be computed by numerically solving the system of PDEs (3.23), (3.24), starting from period n and proceeding backwards.

3.4. Calibration

We calibrate our model to a setting in line with Phase II of the EU ETS as outlined in Section 2.3. Phase II from 2008 to 2012 is followed by periods of eight years length from 2013 onwards. Figures for permit allocations are reported by MEMO/08/796 of the European Commission, with the total number of permits declining in a linear manner.[80] Penalties are 100 Euros per ton of exceeding emissions in Phase II and increase "in accordance with the European index of consumer prices" (see Directive 2009/29/EC), which we assume to be 2.5% per year. The estimation of parameters describing the business-as-usual emissions of the economy is not straightforward. The European Commission officially reports data on emissions within the EU ETS since 2005, but these figures may potentially be biased by the introduction of the scheme itself. On the other hand, the European Environment Agency (EEA) reports data on the total amount of greenhouse gas emissions of the 27 EU member states including all industry sectors except LULUCF activities also before 2005.[81] Apart from the fact that the scope is much larger, this data is considered as a good proxy for emissions within the EU ETS (Ellerman and Buchner 2008). We adjust for the different scope by scaling the EEA data according to the ratio of emissions within the EU ETS and within the EEA data obtained for the years after 2005. We then calculate the mean and standard deviation of the absolute yearly emission changes of the scaled EEA data from 1995 to 2004. The mean of 0.8 is the drift of the business-as-usual emission rate (3.21), and we assume that the standard deviation of 30 is largely due to permanent shocks of the business-as-usual emission rate, while temporary shocks only cause a small fraction of it. Therefore we set σ_y to 28 and σ_ε to 2. Further, linear interpolation of Europe's marginal abatement cost curve reported by Nauclér and Enkvist (2009) and

[80]The amount of permits to be allocated in Phase III was updated by Decision 2010/634/EU of the European Commission. Since Decision 2010/634/EU does not specify updated figures for the other compliance periods, however, we still base our calibration on the information provided by MEMO/08/796.

[81]The EEA aggregates emissions data reported by the countries, publishes it on their website `http://www.eea.europa.eu`, and forwards it to the UNFCCC.

Table 3.1.: Summary of parameter values for a setting in accordance with Phase II of the EU ETS. The allocation and penalties for four compliance periods from 2008 to 2012, 2013 to 2020, 2021 to 2028, and 2029 to 2036 are chosen as outlined by MEMO/08/796 of the European Commission. Parameters for the emissions processes (3.9) and (3.21) are inferred from data provided by the EEA. We consider a scenario of low abatement costs (with coefficient γ_1) compared to the case of higher costs (γ_2). r is the constant risk-free interest rate.

Parameter		Compliance Period k			
		1	2	3	4
End of compliance period	T_k	5	13	21	29
Allocation (Million permits)	e_k	10,400	14,800	12,500	10,100
Penalty (Euro)	p_k	100	122	149	182
Drift of emission rate	μ_y	0.8			
Volatility of emission rate	σ_y	28			
Volatility of emission shocks	σ_ε	2			
Abatement cost coefficient (low)	γ_1	0.1			
Abatement cost coefficient (high)	γ_2	0.2			
Interest rate (p.a.)	r	0.04			

Cline (2011) suggests the abatement cost coefficient of (3.20) to be in the region of 0.1 to 0.2. We consider two different scenarios, $\gamma_1 = 0.1$ and $\gamma_2 = 0.2$, to analyze the impact of abatement measures. Finally, we set the constant risk-free interest rate r to 4%. All parameters are summarized in Table 3.1.

3.4.1. Prices and Volatilities

For the specified EU ETS setting, we investigate the behavior of permit prices and volatilities over time as well as the role of abatement actions and subsequent compliance periods. Figure 3.1 illustrates permit prices S_1 dependent on economy-wide cumulative realized emissions x_t and the prevailing business-as-usual emission rate y_t, calculated according to Proposition 7. We consider three different points in time within the compliance period $[0, T_1]$, and compare on the one hand the two abatement scenarios with cost coefficients $\gamma_1 = 0.1$ and $\gamma_2 = 0.2$, and on the other hand a setting that takes only the first two compliance periods into account to a full four-period setting.

Two Periods

$t = 1.5$

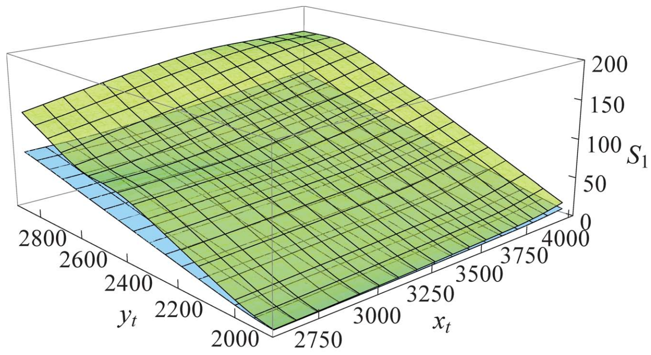

$t = 3$

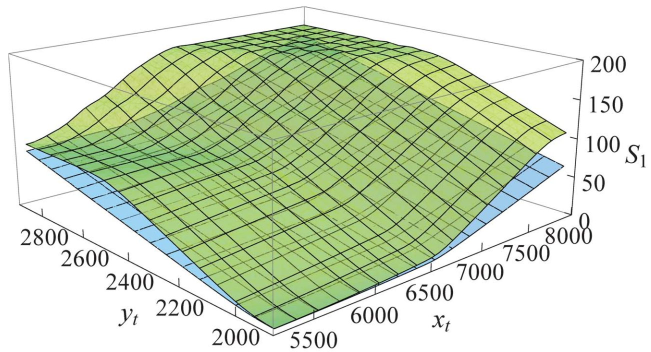

$t = 4.9$

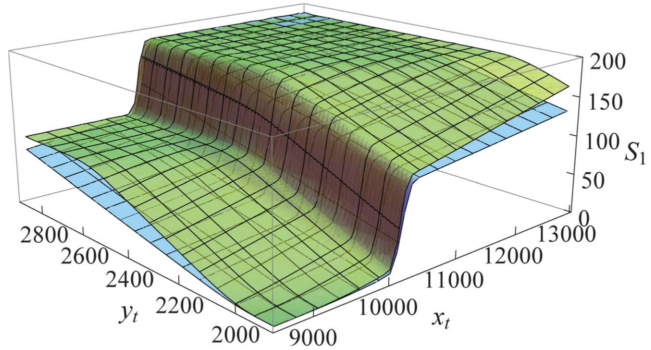

Figure 3.1.: Permit price S_1 dependent on cumulative realized emissions x_t and the prevailing business-as-usual emission rate y_t. We consider a two-period and a four-period setting in line with the EU ETS and consider in each case three different time points within the first compliance period: one and a half ($t = 1.5$) and three years ($t = 3$) after the compliance period's start and shortly before the period's end ($t = 4.9$). The green plots represent the high abatement cost scenario, the blue plots the case of low abatement costs. Parameter values are chosen according to Table 3.1.

Four Periods

$t = 1.5$

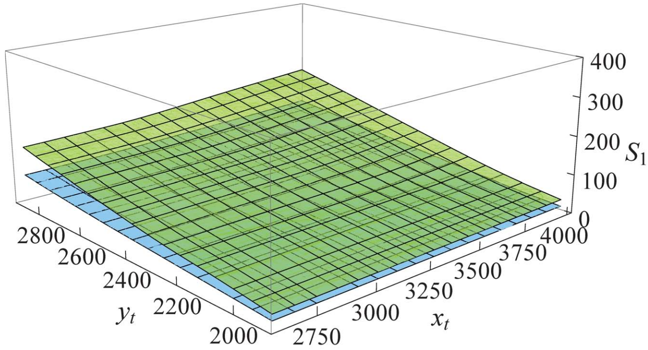

$t = 3$

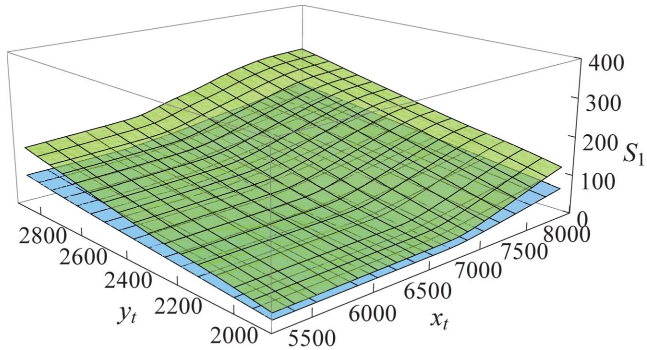

$t = 4.9$

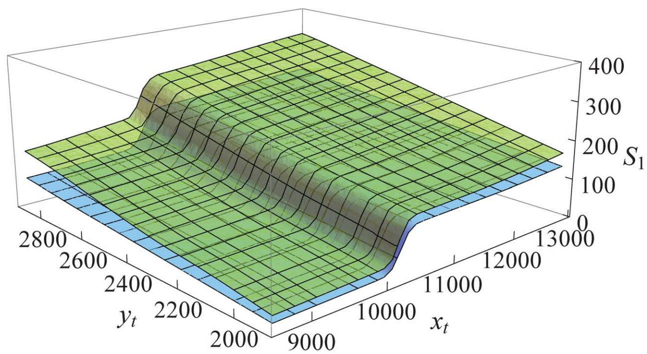

Figure 3.1 (continued).

It is eye-catching how the binary character of emission permit prices becomes visible when approaching the end of the compliance period. While at the beginning of the period, the permit price has a rather unremarkable shape and increases almost linearly in the level of emissions, the picture is dominated by the two states of permit shortage or surplus right before the end of the period. The part of the permit price beyond this binary component is attributable to the following compliance periods and thus naturally larger for the four-period setting. Comparing the two different abatement scenarios, we see that lower abatement costs lead to lower permit prices. This reflects the equilibrium mechanism in this market: Since discounted expected penalties, marginal abatement costs, and permit prices are equal in equilibrium, lower abatement costs lead to lower permit prices and an increased amount of abatement actions, which reduces the probability of penalties. The impact of abatement measures becomes smaller, however, for very low or very high emissions, when the amount of abatement is less crucial for penalties to accrue or not.

Figure 3.2 shows volatilities σ_{S_1} for the two- and four-period setting for the case of low abatement costs. Since the level and shape of the volatility surface for high abatement costs is very similar, we refrain from displaying it. The plots clearly reveal the state- and time-dependent nature of local volatilities pointed out by Proposition 3. As established before, volatility goes to zero for very high levels of cumulative emissions or the prevailing business-as-usual emission rate. To the contrary, volatility is highest for very low emissions. Low prices that are still sensitive towards changes in emission levels lead to high relative volatilities. It follows that volatilities are overall negatively related to emission permit prices. The binary component of permit prices is also reflected by the volatility surface. At the period end, relative volatility is much higher for non-penalty states, for which permit prices are low.

A comparison of the setting with two compliance periods to the four-period setting shows that the volatility is considerably lower in the latter case, especially for low emission levels. The main reason is that the price components attributable to the compliance periods in the remote future react less sensitively to changes in today's cumulative realized emissions or the prevailing emission rate. Furthermore, the tightening allocation in later compliance periods leads to higher values, and thus lower volatilities, for these value components. Accordingly, the value components coming from additional compliance periods weaken the high relative volatility from the current period and cause

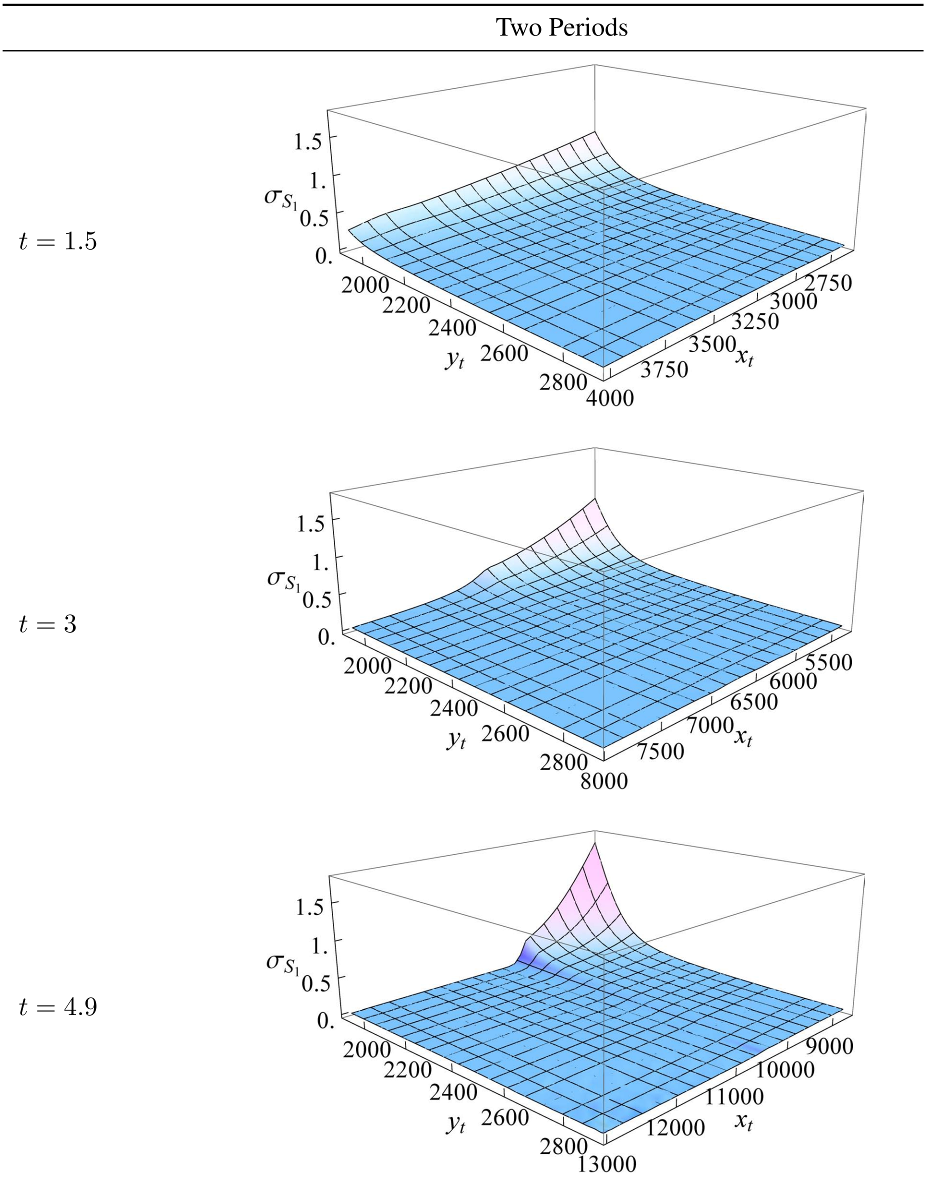

Figure 3.2.: Relative local volatility σ_{S_1} according to (3.13), dependent on cumulative realized emissions x_t and the prevailing business-as-usual emission rate y_t. We consider a two-period and a four-period setting in line with the EU ETS and consider in each case three different time points within the first compliance period: one and a half ($t = 1.5$) and three years ($t = 3$) after the compliance period's start and shortly before the period's end ($t = 4.9$). Parameter values are chosen according to Table 3.1.

	Four Periods
$t = 1.5$	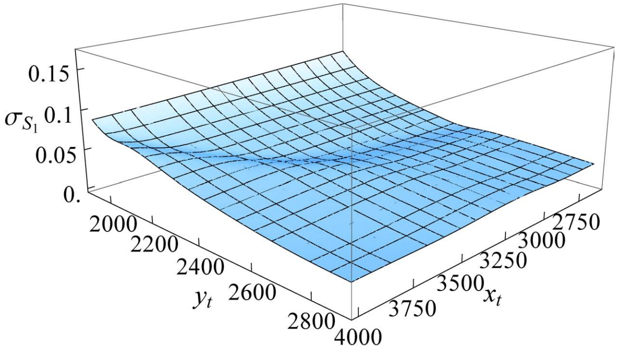
$t = 3$	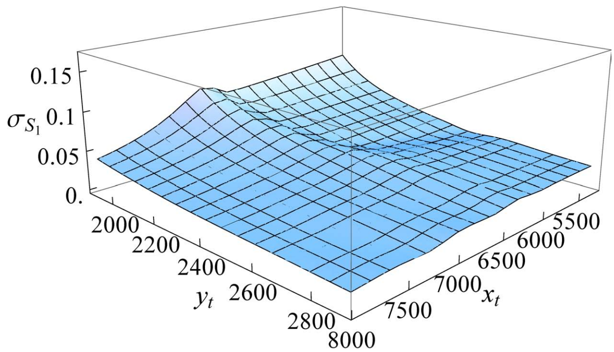
$t = 4.9$	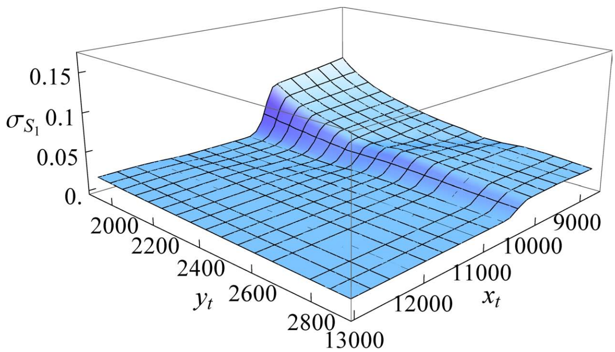

Figure 3.2 (continued).

a smoothing effect. This is desired by policy makers because stable prices increase the confidence to the trading system and tend to trigger early investment into carbon-friendly technologies.[82]

We exemplarily apply our model to calculate theoretical permit prices for the beginning of 2011, i.e., $t = 3$, based on economy-wide cumulative realized emissions x_3 and the prevailing business-as-usual emission rate y_3. Realized emissions are officially published by the EU Commission every year[83] and were 2,060, 1,873, and 1,932 million tons for the years 2008, 2009, and 2010. As the sum of these figures we obtain cumulative realized emissions of $x_3 = 5{,}865$. It is more challenging to infer the prevailing business-as-usual emission rate y_3 of the economy since the best data available is the amount of realized emissions $x_{2,3}$ during 2010, which is composed of economy-wide business-as-usual emissions and short-term shocks reduced by abatement in line with (3.4), i.e.,[84]

$$x_{2,3} = \int_2^3 (y_s + n_s - \xi_s)ds = 1{,}932. \tag{3.25}$$

We first adjust for the abatement realized by the economy in 2010, $\int_2^3 \xi_s ds$. Unfortunately there is little fundamental data available, and most related studies quantify economy-wide abatement by an econometric analysis of emission projections and realized emissions, focussing on Phase I of the EU ETS from 2005 to 2007.[85] We thus take a simplistic approach based on the result that the prevailing permit spot price is equal to the marginal abatement costs of the economy, which means $\xi_t = S_1(t)/\gamma$, $\gamma \in \{\gamma_1, \gamma_2\}$ according to (3.19) with the quadratic abatement cost function (3.20). Therefore the average permit price in 2010, 14.34 Euros,[86] divided by γ provides an estimate of economy-wide abatement $\int_2^3 \xi_s ds$, which results to 143.4 million tons in 2010 for the low and 71.7 million tons for the high abatement cost scenario. Given (3.25), the resulting estimate for $\int_2^3 (y_s + n_s)ds$ is 2,075.4 for the low and 2,003.7 for the high abatement cost scenario. We finally infer the prevailing business-as-usual emission rate

[82] It is widely known from the real options literature (e.g., Pindyck 1988) that price uncertainty increases the value of the *option to delay* investment, while stable prices lead to early investment.

[83] Chapter 5 provides further information on the publication of realized emissions by the EU Commission.

[84] In accordance with the other economy-wide variables previously defined, it is $n_t = \sum_{i \in I} n_t^i$.

[85] See Laing et al. (2013) for an overview of related studies, especially Table 1. As an example, Ellerman and Buchner (2008) come to the conclusion that abatement in 2005 and 2006 was "probably between 50 and 100 million" tons of carbon dioxide per year.

[86] Spot market prices of emission permits traded within the EU ETS are provided by BlueNext.

y_3 by matching the first moments according to the conditions

$$\int_2^3 (y_s + n_s)ds = \mathbb{E}_2 \left\{ \int_2^3 (y_s + n_s)ds \right\} \quad \text{and} \quad y_3 = \mathbb{E}_2 \{y_3\}, \tag{3.26}$$

which yields[87]

$$y_3 = \int_2^3 (y_s + n_s)ds + \frac{1}{2}\mu_y. \tag{3.27}$$

Accordingly we have after rounding $y_3 = 2{,}076$ for the low and $y_3 = 2{,}004$ for the high abatement cost scenario. The inferred business-as-usual emission rate y_3 is in both abatement cost scenarios below the average allocation of 2,080 permits per year in Phase II. These low emission levels are a consequence of the economic downturn caused by the recent financial crisis, and lead to a large surplus of emission permits in the current EU ETS.

Based on the economy-wide realized emissions x_3 and the prevailing emission rate y_3 we calculate theoretical permit prices within our calibrated model. The low emission levels naturally translate to prices that are at the lower end of the possible price range illustrated by Figure 3.1. In particular, we obtain a permit price of 26.90 (45.41) Euros in the four-period setting with low (high) abatement costs, and 12.81 (14.25) Euros in the two-period setting with low (high) abatement costs. Comparing these model prices to spot market prices of emission permits in 2011, which were on average 13.02 Euros, suggests that considering the EU ETS as a system of four periods leads to an overpricing of emission permit prices, while the prices resulting from a two-period setting are reasonably close to market prices. This observation might be interpreted as evidence that market participants in the EU ETS price the compliance periods after 2020 only to a very minor degree, such that they basically incorporate only two compliance periods (Phase II and Phase III) into emission permit prices. It is not unlikely that a two-period setting is indeed best suited to approximate the current situation of the EU ETS for at least two reasons. First, compliance periods starting in the remote future (in 2021 or later) are generally associated with high political uncertainty. This political uncertainty is fueled by the large permit surplus in the EU ETS and corresponding low permit

[87] Note that for the dynamics of y_t given by (3.21) and the definition of n_t, we have

$$\mathbb{E}_2 \left\{ \int_2^3 (y_s + n_s)ds \right\} + \frac{1}{2}\mu_y = \int_2^3 (y_2 + \mu_y(s-2))ds + \frac{1}{2}\mu_y = y_2 + \mu_y = \mathbb{E}_2 \{y_3\}.$$

prices, raising doubts on the effectiveness of the EU ETS as an environmental policy instrument. In an extreme scenario, the EU ETS could completely lose political support by 2020 and would not be continued, such that all emission permits would become worthless. Second, one possibility to tackle the prevailing permit surplus in the EU ETS on the long run is to restrict banking at the end of Phase III to a certain extent, since it is often criticized that unlimited banking accumulates an over-allocation over compliance periods (see Grubb 2012). In this case, however, many permits would become worthless at the end of Phase III as well, such that following periods after 2020 do not lead to a value component in today's permits. Overall, our calibrated model suggests that complete political certainty about the conditions outlined by the EU Commission until 2036 would lead to an additional value component of 14.09 (31.16) Euros in today's emission permit prices in the low (high) abatement cost scenario, which is currently incorporated only to a small extent due to the reasons mentioned.

3.4.2. Futures Price Curve

We further illustrate the permit futures price curve for different emissions scenarios within our calibrated two-period setting with low abatement costs. At $t = 3$, we fix a medium emissions scenario at realized emissions of $x_3 = 6{,}900$ and a prevailing business-as-usual emission rate of $y_3 = 2{,}442$. For both x_3 and y_3, the low (high) emissions scenario is 15% below (above) these values, such that the low/low scenario exactly corresponds to the state $x_3 = 5{,}865$, $y_3 = 2{,}076$ of the EU ETS documented in the last section. Table 3.2 summarizes the emissions scenarios considered.

Table 3.2.: Emissions scenarios at $t = 3$ in terms of economy-wide cumulative emissions x_3 and the prevailing business-as-usual emission rate y_3. A scenario of medium emissions is fixed at $x_3 = 6{,}900$ and $y_3 = 2{,}442$, and the low (high) emissions scenario is 15% below (above) these values.

Scenario ($t = 3$)	Cumulative Emissions x_3	Prevailing Emission Rate y_3
low/low	5,865	2,076
low/high	5,865	2,808
medium/medium	6,900	2,442
high/low	7,935	2,076
high/high	7,935	2,808

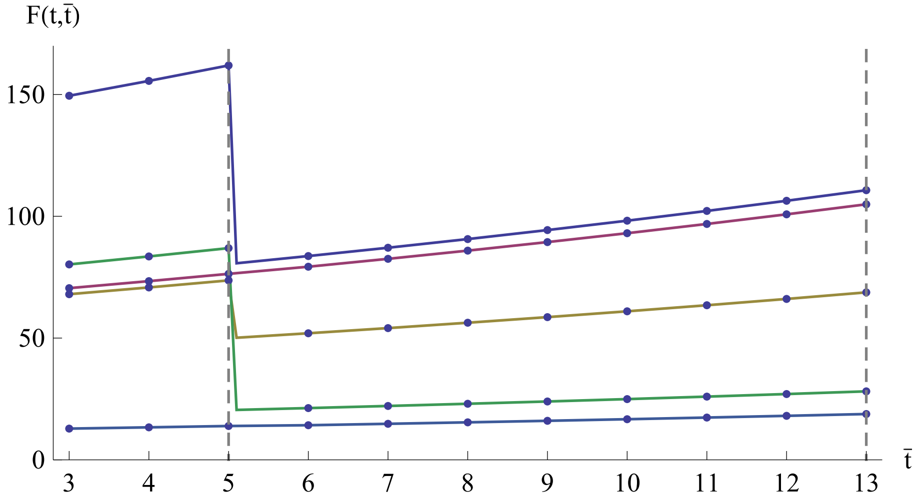

Figure 3.3.: Futures price curves (futures prices $F(t,\bar{t})$ dependent on maturity $\bar{t}$) at $t = 3$ within a two-period EU ETS setting. We consider different scenarios of realized cumulative emissions x_3 and the prevailing business-as-usual emission rate y_3 as stated in Table 3.2: — is the scenario of high realized emissions and a high prevailing emission rate (high/high), — is the low/high scenario, — is medium/medium, — is high/low, and — is the low/low scenario. The dashed vertical lines mark the end of the first and of the second compliance period. Parameter values are chosen according to Table 3.1.

Figure 3.3 depicts futures price curves for the different scenarios as calculated from our model.[88] As stated by Proposition 4, futures are in contango within a compliance period, in line with the standard cost-of-carry relationship. To the contrary, the end of the compliance period leads to backwardation for inter-period futures. The plots illustrate that this backwardation is strongest for high realized emissions. In such a scenario, the probability of permit shortage at the end of the ongoing compliance period is high, and the current emission permits can be used to avoid penalty payments. This is not possible, however, with a futures contract delivering a permit for the next compliance period, inducing the backwardation. As opposed to this, inter-period futures are only

[88] The price of futures maturing in period $k \in \{1, 2\}$ is calculated based on the price of period-k permits and the cost-of-carry relationship within compliance periods, see (3.14). Since Proposition 7 yields a PDE solution only for permit spot prices, we calculate the price of period-2 permits by Monte-Carlo simulation based on (3.8). For this and all other Monte-Carlo simulations documented in this thesis, we discretize processes to 260 trading days per year and simulate 10,000 price paths.

marginally backwardated when emissions are very low and there is an expected surplus of permits for the ongoing compliance period. In this case, almost the whole value of an emission permit is attributable to the following compliance periods. While the probability of penalties to accrue for the ongoing period is almost zero, it is much greater for the following compliance periods due to tightened allocations and the uncertainty driving the emissions process. Such a scenario is comparable to the situation of the EU ETS in the last years of Phase II. Our model predicts that in this case the whole futures price curve is almost in contango, since an additional Phase II permit will be banked and converted to a Phase III permit with a very high probability.

3.4.3. Characteristics of Volatility Smiles

Besides futures contracts, the most important exchange-traded derivatives in the context of emission trading systems are European options, written on emission permit futures with the same maturity date.[89] As nonlinear derivatives, option prices depend on the whole probability distribution of permit prices. Our aim is to characterize the volatility smile shapes of European carbon options within our equilibrium model. Since carbon options are written on a strip of European binary call options according to Proposition 2, the pricing problem is structurally similar to compound options first studied by Geske (1979). As revealed in Section 3.4.1, local volatilities of emission permits are generally negatively related to prices, suggesting a downward-sloping volatility smile in this market. The shape of the smile is, however, not immediately implied by local volatilities since it is also affected by the time-dependent volatility behavior until the option's expiry.

In our risk-neutral setting the price of a European call option with strike K and maturity $\bar{t}$ written on emission permit futures with the same maturity is given by

$$C(t,\bar{t},K) = e^{-r(\bar{t}-t)}\mathbb{E}_t\left\{\left(F(\bar{t},\bar{t}) - K\right)^+\right\}. \tag{3.28}$$

We calculate call option prices for several emission level scenarios within the chosen setting of two compliance periods and low abatement costs by simulating the probability distributions of permit prices. The related Black (1976) implied volatility at strike

[89] We abstract from the fact that there are usually a few days between the option's expiry and the maturity date of the futures contract.

K is denoted by $IV(K)$ and we write IV_{ATM} for $IV(F(t,\bar{t}))$. To capture the shape of volatility smiles, we follow Ederington and Guan (2013): We calculate implied volatilities for nine strikes above and nine strikes below $F(t,\bar{t})$, given by

$$K_j := F(t,\bar{t})(1 + \frac{1}{10} j IV_{ATM} \sqrt{\bar{t} - t}) \tag{3.29}$$

with $j \in \{-9, \ldots, 9\}$. The range of strike prices relevant for market participants depends on the underlying's volatility until the option's expiry date, which is accounted for by this choice. Then we standardize implied volatilities according to $SIV_j = \frac{IV(K_j)}{IV_{ATM}}$. By regressing SIV_j on $\frac{j}{100}$ for $j \in \{-9, \ldots, 0\}$, we obtain the slope of the smile for strikes below $F(t,\bar{t})$, denoted by LS. Doing the same for $j \in \{0, \ldots, 9\}$, we get HS, the slope of the smile for strikes above $F(t,\bar{t})$. Based on this procedure, we obtain two figures LS and HS describing the slope of the volatility smile. If LS is negative and HS positive, implied volatilities decrease in the strike price for strikes below $F(t,\bar{t})$, and increase for strikes above $F(t,\bar{t})$, a pattern which we call smile-shaped. If both LS and HS are negative, implied volatilities are generally decreasing in the strike price and the smile is downward-sloping. The other two combinations for LS and HS are interpreted analogously.

The results for different scenarios and time parameters are stated by Table 3.3. It is eye-catching that the volatility smile is downward-sloping for the vast majority of emissions scenarios. In fact, both LS and HS are negative for 136 of the 150 scenarios. Further, the downward-slope of the volatility smile is strongest for scenarios of very low emissions. These results accord to the negative relation of emission permit prices and volatilities and reveal how this behavior translates to option prices. Still, other shapes are also possible, since the single binary options can add up to various shapes of the price probability distributions, depending on time, emission levels, and maturity. In fact, this makes all kinds of volatility smiles possible, be it smile-shaped, upward-sloping, downward-sloping, or even hump-shaped. Figure 3.4 gives an example for each kind of possible volatility smile shape and shows the related log price probability distribution for a corresponding scenario.

Note that the volatility smile shapes in our study are induced by the characteristics of permit price distributions under the real measure. As for traditional energy commodities, it can be assumed that market participants perceive high permit prices as bad states (see Geman 2005). Therefore the inclusion of risk premia might reduce the downward-slope of the smile predicted by the distribution of underlying permit prices in our model.

Table 3.3.: Slope of volatility smiles, represented by LS and HS for strike prices below and above the underlying emission permit futures price $F(t, \bar{t})$. Given cumulative emissions x_t and the prevailing business-as-usual emission rate y_t at time t, the price of a European call option with maturity $\bar{t}$ written on futures with the same maturity is calculated by Monte-Carlo simulation according to (3.28).

		y_t									
		2,000		2,200		2,400		2,600		2,800	
	x_t	LS	HS	LS	HS	LS	HS	LS	HS	LS	HS
$t = 0.5, \bar{t} = 1$	1,000	−0.78	−0.76	−0.36	−0.31	−0.19	−0.12	−0.08	−0.14	−0.06	−0.04
	1,100	−0.68	−0.64	−0.24	−0.27	−0.04	−0.16	−0.30	−0.37	−0.18	−0.11
	1,200	−0.76	−0.62	−0.39	−0.31	−0.20	−0.34	−0.01	−0.05	−0.18	−0.03
	1,300	−0.77	−0.64	−0.31	−0.23	−0.15	−0.32	−0.03	−0.06	−0.06	−0.13
	1,400	−0.70	−0.64	−0.38	−0.32	−0.11	−0.03	−0.25	−0.14	−0.00	−0.15
$t = 0.5, \bar{t} = 3$	1,000	−2.06	−1.42	−0.94	−0.72	−0.47	−0.51	−0.38	−0.18	−0.06	−0.17
	1,100	−2.05	−1.39	−0.83	−0.76	−0.52	−0.53	−0.44	−0.55	−0.27	−0.25
	1,200	−1.94	−1.27	−0.76	−0.84	−0.48	−0.52	0.01	0.13	−0.27	−0.15
	1,300	−1.84	−1.30	−0.86	−0.69	−0.44	−0.34	−0.31	−0.26	−0.21	−0.22
	1,400	−1.75	−1.22	−0.71	−0.63	−0.52	−0.19	−0.29	−0.36	−0.15	−0.23
$t = 0.5, \bar{t} = 4.9$	1,000	−3.17	−1.81	−1.23	−0.91	−0.63	−0.70	−0.60	−0.37	−0.07	0.52
	1,100	−2.95	−1.73	−1.05	−0.88	−0.78	−0.70	−0.61	−0.37	−0.30	−0.72
	1,200	−2.82	−1.78	−1.14	−0.87	−0.72	−0.51	−0.75	−0.14	−0.66	−1.38
	1,300	−2.66	−1.64	−1.03	−0.82	−0.87	−0.45	0.24	−0.11	−0.98	−1.12
	1,400	−2.52	−1.58	−1.00	−0.74	−0.85	−0.79	−0.52	−0.55	−0.84	−0.64

Table 3.3 (continued).

		y_t									
		2,000		2,200		2,400		2,600		2,800	
	x_t	LS	HS	LS	HS	LS	HS	LS	HS	LS	HS
$t = 2.5, \bar{t} = 3$	5,000	−0.79	−0.67	−0.46	−0.28	−0.19	−0.23	−0.21	−0.07	−0.25	−0.37
	5,500	−0.61	−0.51	−0.32	−0.27	−0.19	−0.27	−0.04	−0.10	−0.18	−0.30
	6,000	−0.39	−0.33	−0.30	−0.27	−0.13	−0.04	−0.15	−0.17	−0.26	−0.21
	6,500	−0.29	−0.25	−0.19	−0.20	−0.16	−0.23	−0.06	−0.06	0.03	−0.02
	7,000	−0.13	0.01	−0.03	−0.11	−0.10	−0.19	−0.15	−0.04	−0.10	−0.15
$t = 2.5, \bar{t} = 4.9$	5,000	−2.14	−1.42	−0.89	−0.70	−0.46	−0.60	−0.71	−0.47	−0.22	−0.43
	5,500	−1.50	−1.11	−0.61	−0.62	−0.43	−0.36	−0.41	−0.33	0.36	0.50
	6,000	−0.79	−0.64	−0.57	−0.57	−0.23	−0.31	−0.18	−0.25	−0.73	−0.61
	6,500	−0.36	−0.36	−0.29	−0.28	−0.19	−0.28	0.12	0.24	−0.29	−0.73
	7,000	−0.45	−0.32	−0.24	−0.21	−0.09	−0.13	−0.24	−0.13	−0.48	−0.54
$t = 4.5, \bar{t} = 4.9$	9,000	−0.74	−0.61	−0.36	−0.13	−0.21	−0.15	−0.10	−0.08	−0.04	−0.02
	9,900	−0.09	−0.04	−0.10	−0.06	0.04	−0.11	−0.05	−0.24	−0.04	−0.13
	10,800	−0.01	−0.02	0.01	−0.14	−0.10	−0.13	−0.09	−0.07	−0.57	−1.46
	11,700	−0.05	0.02	−0.15	−0.07	−0.04	−0.09	−0.15	−0.11	3.44	1.23
	12,600	0.05	0.05	0.03	−0.07	−0.04	−0.09	−0.69	−0.76	3.93	0.38

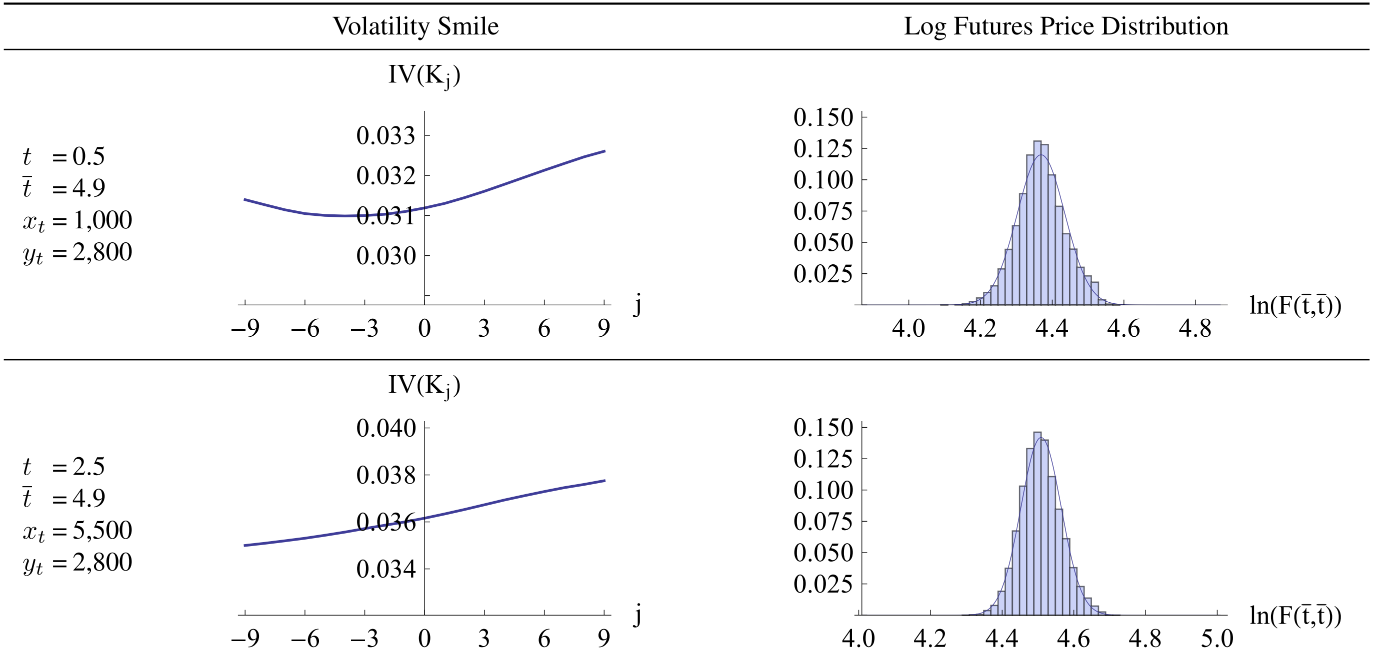

Figure 3.4.: Implied volatility smiles of European futures options (left-hand side) and related histograms of log permit futures prices (right-hand side) within a two-period EU ETS setting. The plots illustrate the possibility of a smile-shaped, upward-sloping, downward-sloping, or hump-shaped volatility smile depending on the constellation of the time parameters t and $\bar{t}$ and the emission levels x_t and y_t. Volatility smiles show implied volatilities $IV(K_j)$ dependent on strike prices K_j according to (3.29), i.e., $j = 0$ stands for an at-the-money option and $j < 0$ ($j > 0$) for strike prices below (above) the futures price $F(t, \bar{t})$. Histograms present probabilities of log permit futures prices $\ln(F(\bar{t}, \bar{t}))$. The blue line represents the normal density function with the same mean and variance. Parameter values are chosen according to Table 3.1.

	Volatility Smile	Log Futures Price Distribution
$t = 2.5$, $\bar{t} = 3$, $x_t = 5{,}500$, $y_t = 2{,}000$	see image 1	see image 2
$t = 0.5$, $\bar{t} = 4.9$, $x_t = 1{,}300$, $y_t = 2{,}600$	see image 3	see image 4

$t = 2.5$
$\bar{t} = 3$
$x_t = 5{,}500$
$y_t = 2{,}000$

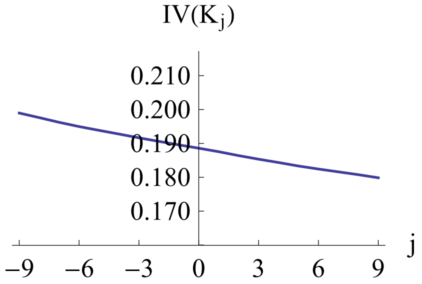

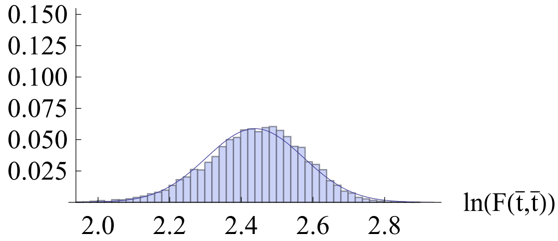

$t = 0.5$
$\bar{t} = 4.9$
$x_t = 1{,}300$
$y_t = 2{,}600$

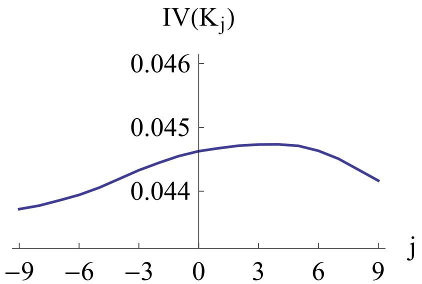

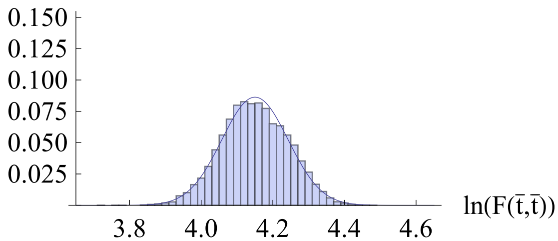

Figure 3.4 (continued).

4. Reduced-Form Models: Calibration and Option Pricing

4.1. Introduction

As shown in the previous chapter, the design of an emission trading system induces specific features of the permit price dynamics. This gives rise to the natural questions whether these features are represented in observed futures and option prices, and how market models should be specified to capture them appropriately. Reduced-form market models for emission permits are intended to account for these particularities without having the complexity of full equilibrium models. Starting from Proposition 2 of the last chapter, we obtain a reduced-form model framework by following the approach of Carmona and Hinz (2011) to specify the dynamics of economy-wide cumulative emissions directly under the risk-neutral measure. Within this framework, we evaluate a battery of different model variants with respect to their historical fit to futures prices as well as their in- and out-of-sample option pricing performance.

Most of the empirical literature on emission permits focuses on the calibration of standard models like geometric Brownian motion, jump-diffusion, mean-reverting, regime-switching, or GARCH models to European emission permit spot, futures, or option prices (see Wagner 2007; Paolella and Taschini 2008; Benz and Trück 2009; Daskalakis et al. 2009; Frey 2010). Carmona and Hinz (2011) are the first to propose reduced-form models that account for the specific properties of emission permits and are still feasible for calibration to futures or option prices. They exemplarily calibrate a model for one single compliance period to market prices from 2007 to 2009, on the one hand to futures with maturity in 2012, on the other hand to options. The authors further propose a market model accounting for two compliance periods and derive related option pricing formulae, but refrain from a calibration of the two-period model. Grüll and Taschini

(2009) evaluate the historical model fit of the Carmona and Hinz (2011) one-period model and another reduced-form model derived from the Chesney and Taschini (2012) framework based on historical futures prices from Phase I and Phase II. As benchmark models they use a geometric Brownian motion and a normal-inverse Gaussian (NIG) process. Still, there is no paper until now assessing the performance of different reduced-form specifications within a unified model framework, neither regarding historical fit to futures prices nor with respect to option pricing. Especially, none of the existing studies reports on the historical or implicit calibration of reduced-form models that account for more than one compliance period. Consequently there is no evidence yet on how reduced-form models should be specified in order to fit futures and option prices observed in the market in an appropriate way.

In the next section, we deduce our reduced-form model framework for emission permits as a generic extension of the Carmona and Hinz (2011) model. We specify the dynamics of the single price components and reduce the specification problem to the parametrization of the emissions' volatility by showing that all emissions processes in a certain class lead to the same class of futures price dynamics. For option pricing we rely on the approach of Carmona and Hinz (2011) and generalize it to our framework. Section 4.3 presents the futures and option data for our empirical analysis. In Section 4.4, we develop a general estimation approach based on the unscented Kalman filter. We calibrate a battery of different model specifications to historical futures prices and evaluate their empirical performance. Section 4.5 investigates the in- and out-of-sample option pricing performance of our model variants based on implicit calibration.

4.2. Reduced-Form Models for Emission Permits

4.2.1. Model Framework

Our goal is to deduce a framework of reduced-form models for emission permit prices that can be calibrated to market data and is feasible for option pricing. Instead of modeling permit spot prices, we model the dynamics of intra-period permit futures directly, first because these are the most liquid contracts traded in the context of emission trading systems, and second because options are usually written on futures and not on the permits themselves. Our starting point is Proposition 2 of the last chapter, which characterizes the prices of emission permits traded within an emission trading system with compliance periods $[0, T_1], [T_1, T_2], \ldots, [T_{n-1}, T_n]$. As the first step, we write the price of futures on period-1 emission permits with maturity $\bar{t} \in [0, T_1)$ at time $t \in [0, \bar{t}]$ under the risk-neutral measure $\mathbb{Q}$. Since all agents are modeled with risk-neutral preferences in Chapter 3, the transition from the real to the risk-neutral measure is trivial.[90] Together with the cost-of-carry relationship for intra-period futures, (3.14), we directly obtain

$$F(t, \bar{t}) = \sum_{j=1}^{n} e^{-r(T_j - \bar{t})} \mathbb{Q}_t \left\{ x_{T_j} > q_j \right\} p_j. \tag{4.1}$$

While this approach models all compliance periods of the emissions trading system explicitly, the results of Chapter 3 suggest that the binary character of emission permit prices is less apparent when the end of the compliance period is in the remote future. Therefore it appears natural to consider alternative models that account only for the first $m \leq n$ compliance periods explicitly and model the remaining value by a price component R_t that does not account for the binary character of emission permit prices and follows a standard process for futures price dynamics. Futures prices are then given by

$$F(t, \bar{t}) = \sum_{j=1}^{m} e^{-r(T_j - \bar{t})} \mathbb{Q}_t \left\{ x_{T_j} > q_j \right\} p_j + R_t. \tag{4.2}$$

Note that for $m = n$ and $R_t = 0$ we exactly obtain the original model (4.1).

4.2.2. Dynamics of Price Components

In the context of Chapter 3, the cumulative emissions x_{T_k} at the end of compliance period k depend on the dynamics of the economy-wide emissions process given by (3.9) and (3.10), particularly on the endogenous optimal abatement strategy. Since this dependency makes it difficult to calibrate the full equilibrium model to market data, we take a simplified approach: For each compliance period k, we consider the time-t expected cumulative emissions up to the end of the period, T_k, that is $x_{T_k|t} = \mathbb{E}_t \left\{ x_{T_k} \right\}$. Obviously, we have $x_{T_k|T_k} = x_{T_k}$ for all $k = 1, \ldots, m$, such that (4.2) holds when replacing x_{T_k} by $x_{T_k|T_k}$.

[90] In Section 4.4 we make the reverse transition from the risk-neutral to the real measure and depart from the assumption of risk-neutral agents by introducing risk premia explicitly.

According to the reduced-form approach of Carmona and Hinz (2011), we model the dynamics of $x_{T_k|t}$, $k = 1, \ldots, m$, directly under the risk-neutral measure, in form of exogenous Itô processes

$$dx_{T_k|t} = \mu_k(t, x_{T_k|t})dt + \sigma_k(t, x_{T_k|t})dW_t^k. \tag{4.3}$$

With (4.3), the dynamics of the *risk-neutral shortage probabilities* $A_{k,t} := \mathbb{Q}_t \{x_{T_k} > q_k\}$ for the single compliance periods $k = 1, \ldots, m$ can be derived.

As a simple example, choose an arithmetic Brownian motion

$$dx_{T_k|t} = \mu_k(t)dt + \sigma_k(t)dW_t^k \tag{4.4}$$

with time-dependent drift $\mu_k(t)$ and volatility $\sigma_k(t)$. Given $x_{T_k|t}$, x_{T_k} is normally distributed with mean $x_{T_k|t} + \int_t^{T_k} \mu_k(s)ds$ and variance $\int_t^{T_k} \sigma_k^2(s)ds$, so that we have

$$A_{k,t} = \Phi\left(\frac{x_{T_k|t} + \int_t^{T_k} \mu_k(s)ds - q_k}{\sqrt{\int_t^{T_k} \sigma_k^2(s)ds}}\right), \tag{4.5}$$

where Φ is the cumulative standard normal distribution function. By Itô's Lemma, we obtain the dynamics of $A_{k,t}$ as

$$\begin{aligned}
dA_{k,t} &= \frac{\partial A_{k,t}}{\partial x_{T_k|t}}\sigma_k(t)dW_t^k \\
&= \Phi'\left(\frac{x_{T_k|t} + \int_t^{T_k} \mu_k(s)ds - q_k}{\sqrt{\int_t^{T_k} \sigma_k^2(s)ds}}\right)\frac{1}{\sqrt{\int_t^{T_k} \sigma_k^2(s)ds}}\sigma_k(t)dW_t^k \\
&= \Phi'\left(\Phi^{-1}(A_{k,t})\right)\frac{\sigma_k(t)}{\sqrt{\int_t^{T_k} \sigma_k^2(s)ds}}dW_t^k \\
&= \Phi'\left(\Phi^{-1}(A_{k,t})\right)\sqrt{z_k(t)}dW_t^k,
\end{aligned} \tag{4.6}$$

where Φ' is the first derivative of Φ and $z_k(t) = \frac{\sigma_k^2(t)}{\int_t^{T_k} \sigma_k^2(s)ds}$. Note that the drift of $A_{k,t}$ results to zero since we have $\mathbb{Q}_t \{A_{k,\tau}\} = \mathbb{Q}_t \{\mathbb{Q}_\tau \{x_{T_k} > q_k\}\} = \mathbb{Q}_t \{x_{T_k} > q_k\} = A_{k,t}$ for all $\tau > t$ due to the law of iterated expectations, which implies the martingale property. The volatility of the risk-neutral shortage probabilities A_k is determined by the ratio of the emissions processes' instantaneous volatility and its future volatility until the end of the compliance period T_k.

It is nearby to argue that an arithmetic Brownian motion is an inappropriate choice for the dynamics of expected cumulative emissions because it can attain negative values, and a geometric Brownian motion is more favorable. Another proposal could be to choose a mean-reverting process for (logarithmic) expected cumulative emissions to represent the mechanism that high emission levels lead to higher prices that trigger more abatement measures, leading to decreasing emissions then. Surprisingly, we can show in Appendix B.1 that all according choices for the emissions processes lead to the same class of dynamics for A_k as (4.6).

If an additional price component $R_t \neq 0$ is incorporated, we take the modeling approach

$$R_t = e^{-r(\max\{\bar{t},T_m\}-\bar{t})} A_{m+1,t}, \tag{4.7}$$

distinguishing between the two cases $m = 0$ and $m \geq 1$. For $m \geq 1$, $A_{m+1,t}$ describes the expected value of an emission permit directly after T_m, the end of the last compliance period explicitly modeled, conditional on time-t information. For $m = 0$, when none of the compliance periods is modeled explicitly, we have $F(t, \bar{t}) = R_t = A_{m+1,t}$ such that A_{m+1} captures the entire futures price. In contrast to the particular form (4.6) for the shortage probabilities $A_1, \ldots, A_m$, we are rather free in the choice of the dynamics of A_{m+1}, but at least we require that all price components are non-negative and permit futures prices are martingales under the risk-neutral measure. Since the prices of the shortage probabilities are non-negative martingales per definition, it is left to demand that A_{m+1} is a non-negative martingale as well. In this thesis we focus on a component following a geometric Brownian motion

$$dA_{m+1,t} = \sigma_R A_{m+1,t} dW_t^{m+1}, \tag{4.8}$$

which is one of the simplest models fulfilling the required properties and an often-used standard model for futures price dynamics since the seminal work of Black (1976).

Altogether, the price dynamics of emission permit futures according to (4.2) derives from the dynamics of $A_1, \ldots, A_{m+1}$ given by (4.6) and (4.8) and the correlation matrix of the Wiener processes $W^1, \ldots, W^{m+1}$, which we denote as $(\rho_{k_1 k_2})_{k_1,k_2=1,\ldots,m+1}$. Note that for the case $m = 2$ and without additional price component, i.e., $R_t = 0$, we exactly obtain the two-period market model proposed by Carmona and Hinz (2011), such that our framework can be seen as a generic extension of this approach.

4.2.3. Option Pricing

We generalize the option pricing formulae derived by Carmona and Hinz (2011) to our framework of models with an arbitrary number of binary price components and eventually an additional component following a geometric Brownian motion. Using the transformation $\lambda_k = \Phi^{-1}(A_k)$, $k = 1, \ldots, m$, and $\lambda_{m+1} = \ln A_{m+1}$, the futures price given by (4.2) can be written as[91]

$$F(t, \bar{t}) = \sum_{j=1}^{m} e^{-r(T_j - \bar{t})} \Phi(\lambda_{j,t}) p_j + e^{-r(\max\{\bar{t}, T_m\} - \bar{t})} e^{\lambda_{m+1,t}}. \tag{4.9}$$

The price of a European call option with strike price K and maturity τ written on the futures contract F is then

$$\begin{aligned} C(t, \tau, K) &= e^{-r(\tau - t)} \mathbb{E}_t^{\mathbb{Q}} \left\{ (F(\tau, \bar{t}) - K)^+ \right\} \\ &= e^{-r(\tau - t)} \mathbb{E}_t^{\mathbb{Q}} \left\{ \left(\sum_{j=1}^{m} e^{-r(T_j - \bar{t})} \Phi(\lambda_{j,\tau}) p_j + e^{-r(\max\{\bar{t}, T_m\} - \bar{t})} e^{\lambda_{m+1,\tau}} - K \right)^+ \right\}. \end{aligned} \tag{4.10}$$

We obtain the dynamics of $\lambda_1, \ldots, \lambda_{m+1}$, from (4.6) by applying Itô's Lemma, which yields

$$\begin{aligned} d\lambda_{k,t} &= \frac{1}{2} \lambda_{k,t} z_k(t) dt + \sqrt{z_k(t)} dW_t^k, \quad k = 1, \ldots, m, \\ d\lambda_{m+1,t} &= -\frac{1}{2} \sigma_R^2 dt + \sigma_R dW_t^{m+1}. \end{aligned} \tag{4.11}$$

Given $\lambda_{k,t}$, we can write $\lambda_{k,\tau}$ with $\tau > t$ in explicit form according to Karatzas and Shreve (1991), pp. 360–361. In particular, the explicit form for $\lambda_{k,\tau}$, $k = 1, \ldots, m$, is given by

$$\lambda_{k,\tau} = e^{\frac{1}{2} \int_t^\tau z_k(s) ds} \lambda_{k,t} + \int_t^\tau e^{\frac{1}{2} \int_s^\tau z_k(u) du} \sqrt{z_k(s)} dW_s^k, \tag{4.12}$$

[91] For $R_t = 0$, simply drop the last term $e^{-r(\max\{\bar{t}, T_m\} - \bar{t})} e^{\lambda_{m+1,t}}$ in (4.9) and all subsequent equations.

and for $\lambda_{m+1,\tau}$ we have the well-known form

$$\lambda_{m+1,\tau} = \lambda_{m+1,t} - \frac{1}{2}\sigma_R^2(\tau - t) + \int_t^\tau \sigma_R dW_s^{m+1}. \tag{4.13}$$

Therefore, $(\lambda_{1,\tau}, \dots, \lambda_{m+1,\tau})$ is normally distributed and we can write (4.10) as

$$\begin{aligned} C(t,\tau,K) = e^{-r(\tau-t)} \int_{\mathbb{R}^{m+1}} \Bigg(\sum_{j=1}^{m} e^{-r(T_j-\bar{t})} \Phi(x_j) p_j \\ + e^{-r(\max\{\bar{t},T_m\}-\bar{t})} e^{x_{m+1}} - K \Bigg)^+ \\ \cdot \varphi(\mu_{t,\tau}, \nu_{t,\tau}; x_1, x_2, \dots, x_{m+1})(dx_1, dx_2, \dots, dx_{m+1}), \end{aligned} \tag{4.14}$$

where $\varphi(\mu_{t,\tau}, \nu_{t,\tau}; .)$ is the density of a $m+1$-variate normal distribution with mean $\mu_{t,\tau} = (\mu_{t,\tau}^k)_{k=1,\dots,m+1}$ and covariance matrix $\nu_{t,\tau} = (\nu_{t,\tau}^{k_1,k_2})_{k_1,k_2=1,\dots,m+1}$ given by

$$\mu_{t,\tau}^k = \mathbb{E}_t^{\mathbb{Q}}\{\lambda_{k,\tau}\} = \lambda_{k,t} e^{\frac{1}{2}\int_t^\tau z_k(s)ds}, \quad k = 1, \dots, m, \tag{4.15}$$

$$\mu_{t,\tau}^{m+1} = \mathbb{E}_t^{\mathbb{Q}}\{\lambda_{m+1,\tau}\} = \lambda_{m+1,t} - \frac{1}{2}\sigma_R^2(\tau - t), \tag{4.16}$$

and

$$\begin{aligned} \nu_{t,\tau}^{k_1,k_2} &= \mathrm{Cov}_t^{\mathbb{Q}}\{\lambda_{k_1,\tau}, \lambda_{k_2,\tau}\} \\ &= \int_t^\tau e^{\frac{1}{2}\int_s^\tau (z_{k_1}(u)+z_{k_2}(u))du} \sqrt{z_{k_1}(s)}\sqrt{z_{k_2}(s)} \rho_{k_1 k_2} ds, \quad k_1, k_2 = 1, \dots, m, \end{aligned} \tag{4.17}$$

$$\begin{aligned} \nu_{t,\tau}^{k,m+1} &= \mathrm{Cov}_t^{\mathbb{Q}}\{\lambda_{k,\tau}, \lambda_{m+1,\tau}\} \\ &= \int_t^\tau e^{\frac{1}{2}\int_s^\tau z_k(u)du} \sqrt{z_k(s)} \sigma_R \rho_{km+1} ds, \quad k = 1, \dots, m, \end{aligned} \tag{4.18}$$

$$\nu_{t,\tau}^{m+1,m+1} = \mathrm{Var}_t^{\mathbb{Q}}\{\lambda_{m+1,\tau}\} = \sigma_R^2(\tau - t). \tag{4.19}$$

All integrals can be evaluated efficiently by numerical integration. As Appendix B.2 shows, one can reduce the computational effort in some cases by evaluating the integrals in a particular order. The price of a European put option with the same strike price and maturity follows directly from the put-call parity.

4.2.4. Model Specification

We specify different model variants within our framework in order to evaluate their empirical performance. Particularly we are interested in the aspect of multiple compliance periods, the specification of an additional price component for compliance periods that are not explicitly modeled, and the choice of the emissions process. As seen in Section 4.2.2, the last point reduces to the choice of the emissions' volatility parametrization.

A geometric Brownian motion (GBM) is the simplest model variant within our framework, modeling no compliance period explicitly and taking the whole price as an "additional" component. Representing classical standard models for futures price dynamics at the same time, it perfectly serves as a benchmark model for assessing reduced-form models that account for at least one compliance period explicitly.[92] In this sense, the simplest non-degenerate reduced-form model we analyze is a model having one explicitly modeled compliance period as the single price component. Furthermore, we evaluate models with one explicit compliance period plus an additional price component, and specifications with two explicitly modeled compliance periods.

According to (4.6), the exact parametrization z_k of the single price components results from the volatility functions σ_k of the emissions processes (4.3). However, it is more convenient to specify z_k directly, and Carmona and Hinz (2011) show that for every continuous function $z_k\colon (0,T) \to \mathbb{R}^+$ satisfying

$$\lim_{t \to T_k} \int_0^t z_k(s)ds = \infty, \tag{4.20}$$

there exists a continuous function $\sigma_k\colon (0,T_k) \to \mathbb{R}^+$ that fulfills $\frac{\sigma_k^2(t)}{\int_t^{T_k} \sigma_k^2(s)ds} = z_k(t)$. These authors consider the parametrizations $z_k^{CH}(t) = \frac{\beta_k}{T_k - t}$ with $\beta_k > 0$ and $z_k^{CH\alpha}(t) = \frac{\beta_k}{(T_k-t)^{\alpha_k}}$, which fulfills condition (4.20) for $\beta_k > 0$ and $\alpha_k \geq 1$. They note, however, that an unconstrained estimation of $z_k^{CH\alpha}$ to empirical data tends to yield an α_k that is smaller than 1. We thus propose a different two-parameter specification $z_k^{CSCH}(t) =$

[92] Unlike Grüll and Taschini (2009) and others, we exclude more sophisticated standard models, e.g., NIG processes, from our analysis, since our focus is on the performance of reduced-form models within a pure Itô framework. We leave it open for future research to consider a reduced-form model framework for emission permit prices based on general Lévy processes.

Table 4.1.: Specification of reduced-form model variants. GBM is a geometric Brownian motion, having no explicitly modeled compliance period, but an additional component within our framework. For the names of the other variants, the number followed by "P" stands for the number of compliance periods explicitly modeled, "CH" or "CSCH" stands for the specific parametrization of z_k, and "R" specifies the existence of an additional price component.

	Price Components	Compliance Periods	Add. Component	z_k
GBM	1	0	X	–
1PCH	1	1	–	CH
1PCSCH	1	1	–	CSCH
1PCHR	2	1	X	CH
1PCSCHR	2	1	X	CSCH
2PCH	2	2	–	CH
2PCSCH	2	2	–	CSCH

$\frac{\beta_k}{\frac{T_k}{2}\left(\left(1+\frac{T_k-t}{T_k}\right)^{\alpha_k}-\left(1-\frac{T_k-t}{T_k}\right)^{\alpha_k}\right)}$.[93] This parametrization also fulfills (4.20) for $\alpha_k \geq 1$, it is equal to z_k^{CH} for $\alpha_k = 1$, and the empirical estimates for α_k tend to be larger than 1 for this specification, see Section 4.4 and Section 4.5. Therefore we choose the parametrizations z_k^{CH} and z_k^{CSCH} for our analysis.

Overall, the combination of the different model features yields seven different model variants, which are summarized by Table 4.1.

4.3. Data

Our empirical analysis builds on futures and option data traded in the context of the EU ETS. We use daily prices of EUA futures and European options written on these futures traded from January 1, 2008 to June 30, 2012 provided by the European Climate Exchange (ECX). All prices are determined under the ECX settlement procedure that takes place every day from 4:50 to 5:00 p.m. local time. As outlined in Section 2.3.2, we always consider the December futures contract next to maturity and roll over to the next contract on the last day of October. In the same way, we only consider options expiring in the next December until the last trading day of October, and then

[93] The motivation for this parametrization is purely technical and does not have an intuitive economic interpretation. We label this parametrization by "CSCH" due to its affinity to the hyperbolic cosecant.

Table 4.2.: Average prices, standard deviations, and number of observations for different moneyness and maturity categories of our option sample. The cleaned sample comprises 1,457 option prices traded from 2008 to 2012 on the ECX.

		Calls Days to Maturity			Puts Days to Maturity		
Moneyness		<160	160-280	>280	<160	160-280	>280
deep OTM	Avg. Price	1.34	0.94	0.39	0.94	0.71	0.26
	StdDev. Price	0.33	0.44	0.25	0.34	0.25	0.11
	Obs.	35	72	33	46	50	28
OTM	Avg. Price	1.65	1.38	0.71	1.59	1.19	0.73
	StdDev. Price	0.41	0.48	0.27	0.50	0.44	0.28
	Obs.	138	223	132	124	174	137
ITM	Avg. Price	2.07	1.91	1.28	2.50	1.81	1.14
	StdDev. Price	0.31	0.54	0.26	0.74	0.49	0.34
	Obs.	44	73	33	43	33	30
deep ITM	Avg. Price	–	3.84	–	3.66	–	2.00
	StdDev. Price	–	0.16	–	0.45	–	0.04
	Obs.	0	5	0	2	0	2

switch over to options expiring in December of the next year. Moreover, we only include settlement prices of options traded at least once on the same day either via screen trading or the exchange-for-physical/exchange-for-swaps facilities of the ECX. We apply the standard cleaning criteria for option data (see Bakshi et al. 1997; Trolle and Schwartz 2009), that is we exclude options traded at prices smaller than 0.06 Euros as well as observations of call or put prices violating the no-arbitrage condition $C(t,\tau,K) \geq e^{-r(\tau-t)}(F(t,\bar{t}) - K)$ or $P(t,\tau,K) \geq e^{-r(\tau-t)}(K - F(t,\bar{t}))$. We further follow the literature (see Dumas et al. 1998; Trolle and Schwartz 2009) and restrict our analysis to options with moneynesses within a certain range, in our case between 0.8 and 1.2, since options that are very deep out-of-the-money (OTM) or in-the-money (ITM) are typically subject to large pricing biases.

After this procedure, our sample contains 1,457 observations which are categorized with respect to moneyness and time to maturity in Table 4.2. Moneyness categories are defined as is Section 2.3.2, i.e., a call (put) option is OTM for a moneyness between 1 and 1.15 (0.85 and 1), deep OTM if its moneyness is larger (smaller) than 1.15

(0.85), ITM if the moneyness is between 0.85 and 1 (1 and 1.15), and deep ITM if the moneyness is smaller (larger) than 0.85 (1.15). We differentiate between maturities longer than 280 days, maturities between 160 and 280 days, and maturities shorter than 160 days. Our cleaned sample consists to almost equal parts of calls (about 54%) and put options (about 46%). Moreover, the price observations of our sample are well distributed over maturity categories, whereas the medium maturity category accounts for more observations than either the short and long maturities. In line with the overall transaction volumes considered in Section 2.3.2, the number of OTM options in our sample largely overweighs the number of ITM options. In contrast, deep OTM options are less represented in our cleaned sample than in the full data set due to our sample selection procedure. The selection of options with expiry in the directly following December only, the exclusion of options traded at small prices, and finally the selected range of moneynesses are all to the disadvantage of very deep OTM options.

The term structure of risk-free interest rates is obtained using EURIBOR rates for maturities up to one year and EuroSwap rates for longer maturities. For a given maturity, we linearly interpolate the two interest rates whose maturities straddle it.

4.4. Calibration to Historical Data

To calibrate reduced-form models to historical permit futures prices, we need to specify the dynamics under the real measure. Assuming constant market prices of risk $h_1, \ldots, h_m, h_R$ the processes $\widetilde{W}_t^k = W_t^k - h_k t$, $k = 1, \ldots, m$, and $\widetilde{W}_t^{m+1} = W_t^{m+1} - h_R t$ are Brownian motions under the real measure and the dynamics of the shortage probabilities and the additional price component follow from (4.6) and (4.8) as

$$\begin{aligned} dA_{k,t} &= \Phi'\left(\Phi^{-1}(A_{k,t})\right) h_k \sqrt{z_k(t)} dt \\ &\qquad + \Phi'\left(\Phi^{-1}(A_{k,t})\right) \sqrt{z_k(t)} d\widetilde{W}_t^k, \quad k = 1, \ldots, m, \\ dA_{m+1,t} &= \sigma_R h_R A_{m+1,t} dt + \sigma_R A_{m+1,t} d\widetilde{W}_t^{m+1}. \end{aligned} \tag{4.21}$$

If the single A_k are all observable in the market, parameters can simply be estimated by maximum likelihood according to Carmona and Hinz (2011). This would be given if futures contracts with maturities in all compliance periods considered were traded with sufficient liquidity. However, it is rather the case that only futures contracts of the ongoing compliance period are sufficiently liquid, so that only the futures price F of current emission permits can be observed. Thus we require an approach that decomposes the aggregate emission permit price into its single value components according to (4.2).

4.4.1. Methodology

We estimate the reduced-form model variants by quasi-maximum likelihood in conjunction with the unscented Kalman filter. We work again with the transformation $\lambda_k = \Phi^{-1}(A_k)$, $k = 1, \dots, m$, and $\lambda_{m+1} = \ln A_{m+1}$, and apply Itô's Lemma to obtain the resulting dynamics from (4.21) as

$$\begin{aligned} d\lambda_{k,t} &= (h_k\sqrt{z_k(t)} + \frac{1}{2}\lambda_{k,t}z_k(t))dt + \sqrt{z_k(t)}d\widetilde{W}_t^k, \quad k = 1, \dots, m, \\ d\lambda_{m+1,t} &= (\sigma_R h_R - \frac{1}{2}\sigma_R^2)dt + \sigma_R d\widetilde{W}_t^{m+1}, \end{aligned} \tag{4.22}$$

and the futures price is given by (4.9). The Kalman filter allows to extract the paths of the latent state variables $\lambda_1, \dots, \lambda_{m+1}$ from a time series of observed futures prices $F(t, \bar{t})$ according to the given system of equations. Based on the dynamics (4.22) of the state variables with fixed parameter values $(h_1, \beta_1, \alpha_1, \dots, h_m, \beta_m, \alpha_m, h_R, \sigma_R)$ and their relation to the futures price (4.9), variations of the futures price F can be statistically attributed to variations of the single state variables. If, for example, futures prices F fluctuate exactly according to a geometric Brownian motion with parameters h_R and σ_R, these movements are most likely caused by the last price component in (4.9), while fluctuations of the other state variables would lead to futures price variations that are not completely in line with a geometric Brownian motion. By retransforming the estimated paths of the state variables $\lambda_1, \dots, \lambda_{m+1}$ to the risk-neutral shortage probabilities $A_k = \Phi(\lambda_k)$, $k = 1, \dots, m$, and the component $A_{m+1} = e^{\lambda_{m+1}}$, we obtain a statistical decomposition of the observed futures prices F into the single price components $e^{-r(T_k - \bar{t})}A_k p_k$, $k = 1, \dots, m$, which are attributable to the m compliance periods explicitly modeled, and the additional price component R according to (4.2).

Technically, we cast our model given by equations (4.9) and (4.22) into the state-space form, which consists of a measurement and a transition equation. The transition equation describes the dynamics of the latent variables $\lambda_1, \dots, \lambda_{m+1}$ in discrete time. It is obtained by discretizing (4.22) as

$$\begin{pmatrix} \lambda_{1,t+1} \\ \vdots \\ \lambda_{m+1,t+1} \end{pmatrix} = G_t + H_t \begin{pmatrix} \lambda_{1,t} \\ \vdots \\ \lambda_{m+1,t} \end{pmatrix} + w_t \tag{4.23}$$

with

$$G_t = \begin{pmatrix} h_1\sqrt{z_1(t)} \\ \vdots \\ h_m\sqrt{z_m(t)} \\ \sigma_R h_R - \frac{1}{2}\sigma_R^2 \end{pmatrix} \quad \text{and} \quad H_t = \begin{pmatrix} 1+\frac{1}{2}z_1(t) & 0 & \dots & 0 \\ 0 & \ddots & \ddots & \vdots \\ \vdots & \ddots & 1+\frac{1}{2}z_m(t) & 0 \\ 0 & \dots & 0 & 1 \end{pmatrix} \tag{4.24}$$

and independently distributed error terms $w_t \sim \mathcal{N}(0, \Omega_t)$ with covariance matrix

$$\Omega_t = \begin{pmatrix} z_1(t) & \dots & \rho_{1m}\sqrt{z_1(t)z_m(t)} & \rho_{1m+1}\sqrt{z_1(t)}\sigma_R \\ \vdots & \ddots & \vdots & \vdots \\ \rho_{1m}\sqrt{z_1(t)z_n(t)} & \dots & z_m(t) & \rho_{mm+1}\sqrt{z_m(t)}\sigma_R \\ \rho_{1m+1}\sqrt{z_1(t)}\sigma_R & \dots & \rho_{mm+1}\sqrt{z_m(t)}\sigma_R & \sigma_R^2 \end{pmatrix}. \tag{4.25}$$

The measurement equation defines the relationship between the values of the latent state variables $\lambda_1, \dots, \lambda_{m+1}$ and permit futures prices F observed in the market. It follows from (4.9) as

$$F(t,\bar{t}) = \sum_{j=1}^{m} e^{-r(T_j-\bar{t})}\Phi(\lambda_{j,t})p_j + e^{-r(\max\{\bar{t},T_m\}-\bar{t})}e^{\lambda_{m+1,t}} + u_t, \tag{4.26}$$

where $u_t \sim \mathcal{N}(0, \psi)$ represents an independent and identically distributed error term. The error u_t accounts for the fact that market prices can only be observed up to a certain accuracy due to bid-ask spreads and minimum tick sizes. We set the variance ψ to 0.01 according to a minimum tick size of 0.01 Euros in the European carbon market.

While the standard Kalman (1960) filter is based on transition and measurement equations that are linear in the state variables, the measurement equation (4.26) is highly nonlinear in our case by the occurrence of cumulative normal distributions and the exponential function. We therefore use the square-root unscented Kalman filter developed by van der Merwe and Wan (2001), an algorithm that handles the nonlinearities in a robust and computationally efficient way. Especially, the unscented Kalman filter identifies the latent states much more accurately than a pure linearization technique (known as the extended Kalman filter), as pointed out by Christoffersen et al. (2012). Since the implementation of the unscented Kalman filter is rather generic once the state-space form is given, we refer to van der Merwe and Wan (2001) and Appendix B of Carr and Wu (2010) for details.[94] The Kalman filter also enables us to compute the log-likelihood function for the given set of parameters $(h_1, \beta_1, \alpha_1, \ldots, h_m, \beta_m, \alpha_m, h_R, \sigma_R)$. We estimate the parameters by numerically maximizing the likelihood with respect to the model parameters using the Nelder-Mead algorithm.[95]

4.4.2. Results

Table 4.3 shows parameter estimates and standard errors for the different model variants, as well as the log-likelihood and the value of the AIC. The parameter estimates for a GBM reveal that EUA prices fluctuate by approximately 37.6% per year, and the drift coefficient is negative according to a considerable decline of EUA prices for the period of investigation. This negative price drift is also reflected by the h_1 parameter of reduced-form models for one compliance period, 1PCH and 1PCSCH. For the models with two price components it is eye-catching that the first component has a highly negative drift, while the h_2 or h_R parameter of the second component is positive. This corresponds to the behavior of the single price components, filtered as part of our estimation procedure (see Figure 4.1). Consistently across all model variants with two price components, we observe that the first price component of EUA futures, which is attributable to Phase II of the EU ETS, collapsed in 2008 and 2009. This is in line with anecdotal evidence from the market, saying that the main part of the EUA price traded in the second half of Phase II is attributable to the following compliance period from 2013 to 2020. Due the economic downturn in consequence of the financial crisis,

[94] The only non-generic point is the initialization procedure. Since the transition equation is non-stationary in all of its components, we initialize the unscented Kalman filter by using diffuse priors (see Harvey 1989, pp. 121-122). In particular, we employ the approach of Rosenberg (1973) to treat the initial state as fixed and unknown, and infer it by maximum likelihood estimation (see Durbin and Koopman 2001, pp. 117-188).

[95] For the model parametrization z_k^{CH}, the parameters $\alpha_1, \ldots, \alpha_m$ are set to 1 and not included into the numerical optimization.

Table 4.3.: Historical parameter estimates and standard errors (in parentheses) for the different model variants defined in Section 4.2.4. All models are calibrated to EUA futures prices from January 1, 2008 to June 30, 2012 provided by the ECX. We report the maximized value of the log-likelihood function (LLF) as well as the value of the Akaike information criterion (AIC). If k is the number of model parameters and d the number of non-stationary state variables, the AIC is defined as $AIC = 2(k + d) - 2LLF$ (see Harvey 1989, p. 270).

	h_1	β_1	α_1	h_2	β_2	α_2	h_R	σ_R	ρ	LLF	AIC
GBM	—	—	—	—	—	—	−0.458	0.376	—	568.27	−1130.53
							(0.465)	(0.009)			
1PCH	−0.603	0.182	—	—	—	—	—	—	—	469.68	−933.35
	(0.468)	(0.009)									
1PCSCH	−0.603	0.259	1.465	—	—	—	—	—	—	475.22	−942.45
	(0.473)	(0.029)	(0.150)								
1PCHR	−5.610	0.401	—	—	—	—	0.216	0.327	0.518	574.44	−1134.87
	(0.582)	(0.044)					(0.498)	(0.011)	(0.061)		
1PCSCHR	−5.707	545.740	12.181	—	—	—	0.131	0.327	0.597	579.27	−1142.55
	(0.588)	(1060.231)	(3.036)				(0.527)	(0.010)	(0.063)		
2PCH	−5.587	0.394	—	0.191	0.444	—	—	—	0.419	575.88	−1137.76
	(0.555)	(0.043)		(0.498)	(0.025)				(0.081)		
2PCSCH	−5.629	384.770	11.466	0.335	9.375	6.008	—	—	0.477	584.19	−1150.38
	(0.564)	(654.742)	(2.631)	(0.533)	(6.449)	(1.191)			(0.069)		

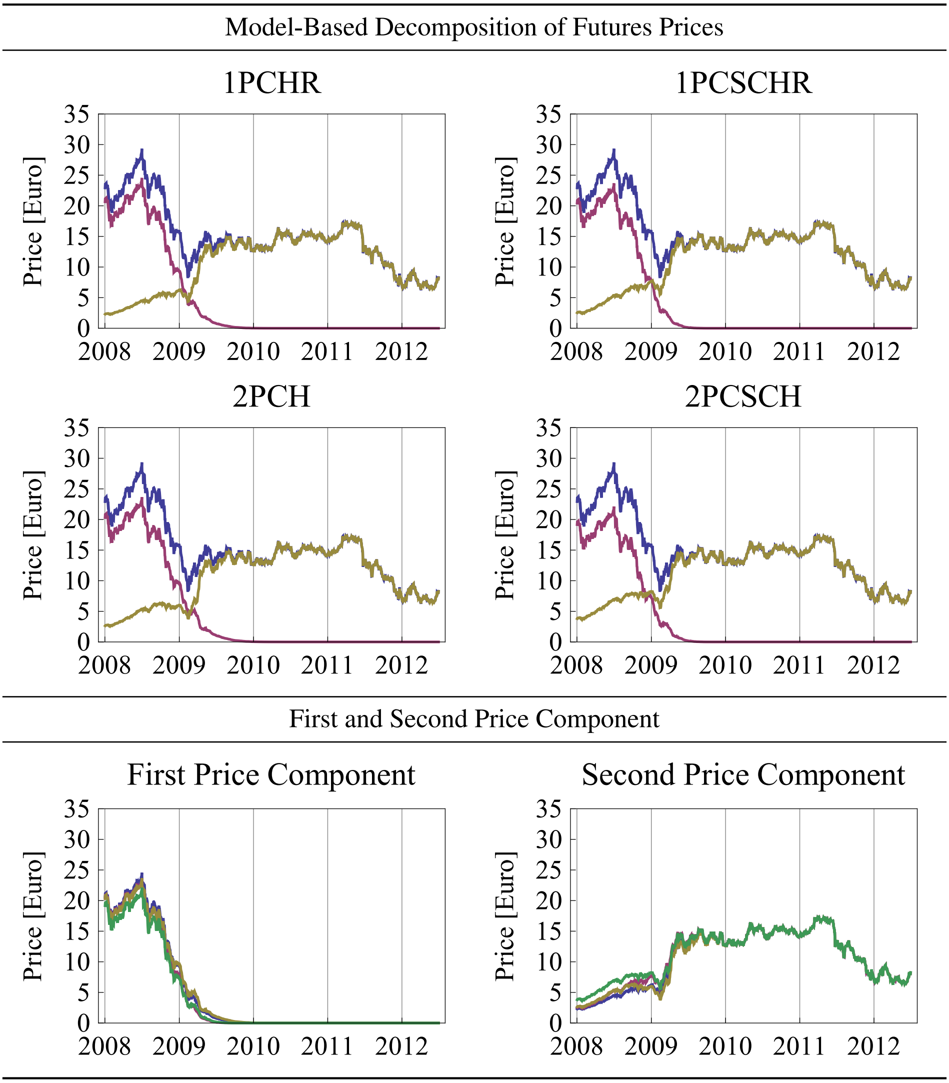

Figure 4.1.: Paths of single price components according to (4.2) as estimated by historical calibration to EUA futures prices. The upper panel shows the observed futures price (—) decomposed into the first (—) and second (—) price component as filtered by our estimation procedure. The lower panel presents the first and second price component for the 1PCHR (—), 1PCSCHR (—), 2PCH (—) and 2PCSCH (—) model.

expected cumulative emissions for Phase II were low and a permit shortage in 2012 was highly unlikely. For Phase III, however, tighter allocations and the volatility of emissions lead to a significant probability of penalty payments to accrue, and a value component clearly larger than zero. The relatively low standard error for the drift parameter of the first price component in two-period models confirms that this collapse can be precisely identified by the statistical estimation procedure. To the contrary, we observe large standard errors for the drift parameter of the second price component and also for the models with only one price component, suggesting that a drift cannot clearly be established in these cases.

The volatility parameters of these models can also be interpreted in light of the behavior of the single price components. Since the σ_R of the 1P(CS)CHR model[96] describes the second price component, which behaves much less turbulent than the first one, the parameter estimates are smaller than the σ_R for the GBM, which captures the volatility of the whole prices. Similarly, the parameter β_1 of the 1PCHR and 2PCH model, representing the volatility of the first price component, is clearly larger than the β_1 of the whole prices as estimated in context of the 1PCH model. The volatility parameter for a one-parameter volatility function can be estimated with high precision, as indicated by low corresponding standard errors across all model variants GBM, 1PCH, 1PCHR, and 2PCH. In contrast, standard errors are extremely large for the β_k parameters of two-parameter volatility functions in case of models with two price components, 1PCSCHR and 2PCSCH. This observation suggests that in these cases the volatility function can be described almost equally well by other combinations of α_k and β_k and the likelihood function is very flat in the direction of these parameters.

Finally, the correlation ρ of the risk factors driving the two price components is consistently between 0.4 and 0.6 for all model variants, with low standard errors. Especially for the 2P(CS)CH model, where the risk factors stand for the stochastic dynamics of expected cumulative emissions for the two compliance periods, it makes intuitive sense that the Wiener processes are not uncorrelated, but also not perfectly correlated: On the one hand, the emissions until the end of the first compliance period are obviously part of the cumulative emissions until the end of the second one, but on the other hand, the expected emissions within the second compliance period are also driven by other, longer-term factors.

[96] We abbreviate by writing "(CS)CH" when a statement holds for both the CH and the CSCH parametrization.

We compare the historical fit of the estimated models by the log-likelihood of the Kalman filter estimation and the AIC. The AIC adjusts the log-likelihood value by penalizing the number of free model parameters and latent variables and allows for comparisons between non-nested models. It is eye-catching that all model specifications with two price components show a better historical fit than a GBM, which is the benchmark model within our framework, while the market models for one compliance period, 1PCH and 1PCSCH, perform worse. The flaw of these one-period market models is that they capture the binary behavior of the first price component, but neglect the value coming from the following compliance periods. Since the historical EUA prices do not show a clear tendency to converge to zero or the penalty in 2012, these models show a bad fit to historical data. In contrast, a GBM does not represent any of the binary price properties, but can in principle attain all prices at the end of the compliance period in 2012. Market models with two price components incorporate both the binary price properties as well as the value component of the next compliance period. These models provide additional degrees of freedom compared to the simpler specifications, but they also impose more structure on the EUA futures prices. The fact that they perform better than the models with only one price component even in terms of the AIC, which corrects for the number of parameters and latent variables, shows that this structure is very well represented by empirical data and should not be neglected when specifying market models for emission permit prices. Among the variants with two price components, models explicitly accounting for two compliance periods show a better fit than models with one compliance period plus an additional component, but especially for the simple parametrizations 1PCHR and 2PCH the difference is very small. Using a specification with two parameters improves the performance, measured by the AIC, in all cases.

As a last plausibility check, we consider the volatility $\sigma_1(t)$ of the expected cumulative emissions $x_{T_1|t}$ according to (4.4), which is determined by the form of $z_1(t)$ and the parameter values β_1 and α_1. Economic intuition suggests that the volatility of $x_{T_1|t}$ decreases towards the end of the compliance period when the major part of the cumulative emissions is known already. Figure 4.2 shows that this argument clearly favors the two-period models with two volatility parameters β_k and α_k, which follow this behavior for the parameters estimated. Contrary, the one-period models or the simpler models with $\alpha_k = 1$ imply that the volatility of expected cumulative emissions increases towards infinity at the end of the compliance period.

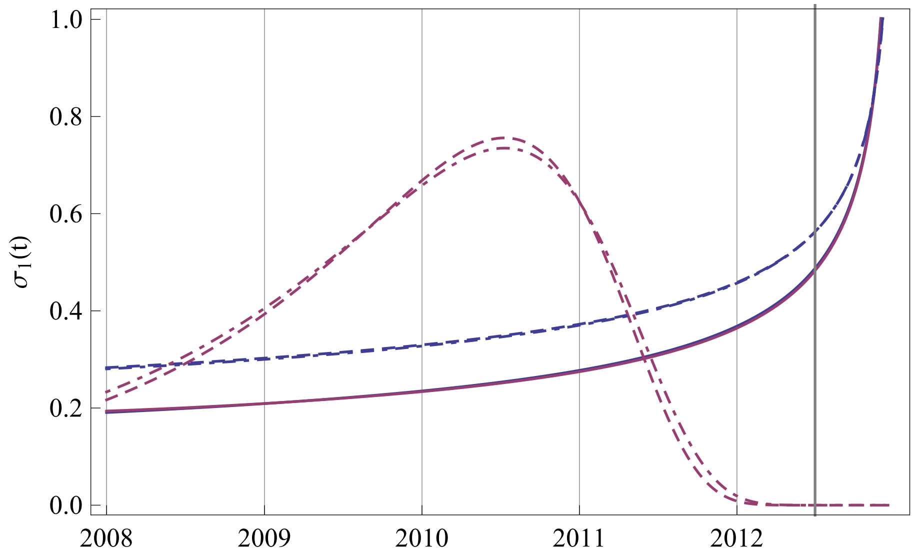

Figure 4.2.: Volatility functions $\sigma_1(t)$ of expected cumulative emissions $x_{T_1|t}$ according to (4.4) for the models 1PCH (solid), 1PCHR (dashed), and 2PCH (dot-dashed) plotted in blue and the corresponding models with additional volatility parameter α_1 plotted in purple. $\sigma_1(t)$ is the p.a. volatility of $x_{T_1|t}$ given by $\sigma_1(t) = \sqrt{z_1(t)e^{-\int_0^t z_1(s)ds}}$ (see Carmona and Hinz 2011). The solid vertical line marks the end of our sample period on June 30, 2012. Parameters are chosen according to the historical estimates in Table 4.3.

Altogether, our results reveal that appropriately specified market models for emission permits outperform standard models for futures price dynamics — as represented by a geometric Brownian motion within our framework — with respect to the historical fit. While models consisting of one binary price component standing for a single compliance period perform very poorly, an additional price component, be it in form of another explicitly modeled compliance period or an unspecific component evolving according to a geometric Brownian motion, leads to a large improvement of the performance. Furthermore, reduced-form models with two volatility parameters β_k and α_k explain historical EUA futures prices better than the simple parametrization with $\alpha_k = 1$. For the models with two price components, the additional parameter α_k also leads to an expected cumulative emissions' volatility function that is in line with the economic intuition.

4.5. Option Pricing

We evaluate the option pricing performance of the different model variants for the sample of option prices described in Section 4.3. To get a first impression of the structural properties of EUA option prices, we plot the average volatility smiles for the years 2009 to 2012, see Figure 4.3. It is eye-catching that the smile is flat in 2009, while there actually exists a smile for 2010 and later. The flat smile in 2009 is completely in line with the observation of Carmona and Hinz (2011) that within their sample period, until the end of September 2009, "traders [...] priced EUA options using Black 76 formula". Such a flat smile is, however, very unusual for any kind of option market, and existed most probably because traders used very simplified valuation methods during this early stage of the Phase II EUA option market. As the other plots show, the option market departed from a flat smile in the following years to a downward-sloping smile, and the downward-slope increased more and more from 2010 to 2012. This observation particularly confirms our model prediction of a downward-sloping smile from Section 3.4.3 and suggests that the market has learnt about the distributional properties of emission permit prices as induced by the design of the system, which are represented by option prices.

4.5.1. Parameter Estimation

To calibrate the reduced-form model specifications to observed option prices, we minimize the pricing errors between empirical prices and model-based theoretical prices according to (4.10) with respect to the parameter values $(\beta_1, \alpha_1, \ldots, \beta_m, \alpha_m, \sigma_R)$. Option prices also depend on the state variables $\lambda_1, \ldots, \lambda_{m+1}$, which we assume to follow the paths estimated from historical futures prices in Section 4.4. By this approach we proceed on the assumption that the states of the latent variables can be very well extracted from historical futures price data, and the additional information about the state variables contained in option prices is relatively small. Overall, our estimation approach is a two-stage procedure that achieves computational feasibility by inferring information about the state variables from historical futures prices, before re-estimating the model parameters using option data.[97] We re-calibrate the models for each month

[97] Similar two-stage procedures are frequently applied for other model classes, especially multi-factor stochastic volatility models, see for example Broadie et al. (2007).

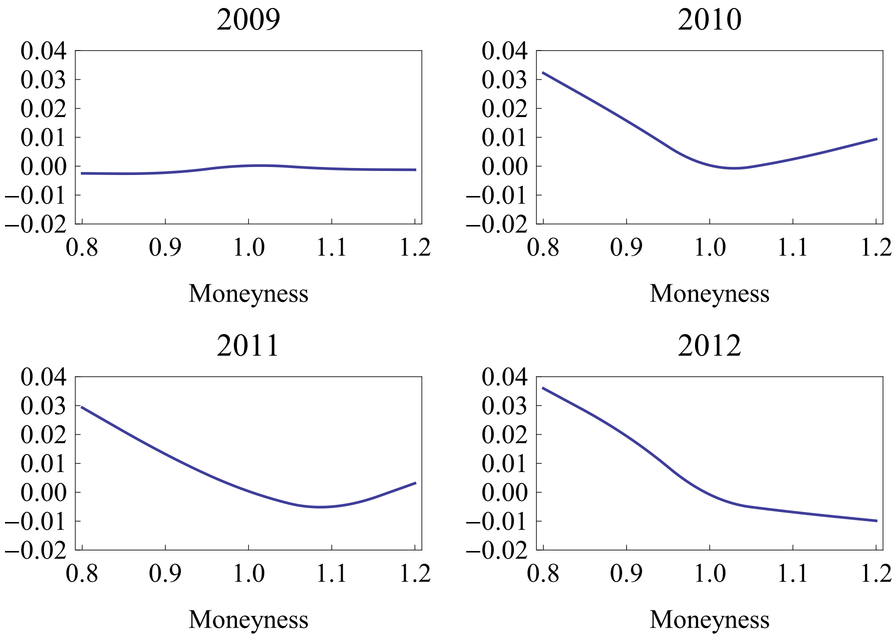

Figure 4.3.: Average volatility smile of EUA options for each year from 2009 to 2012. Smiles are calculated as the average difference between the Black (1976) implied volatility for the particular moneyness and the at-the-money implied volatility.

of our option data set. For that, we minimize aggregate pricing errors between theoretical and empirical option prices as measured by the relative root-mean-squared error (RRMSE). The RRMSE makes the estimates as robust as possible with respect to different performance measures (see Christoffersen and Jacobs 2004). We use numerical minimization based on the Nelder-Mead algorithm, setting the historical parameter estimates from Section 4.4 as starting values.

Table 4.4 shows the results of the implicit estimation. Since we get different implied parameter estimates for each month of our sample according to the re-calibration procedure, we report both the mean and the standard deviation of the implied estimates over all months of our sample. Comparing to the historical parameter estimates in Table 4.3, we observe that the implied and historical estimates for the correlation parameter ρ are reasonably close to each other, especially for the models 1PCHR and 2PCH, while the

Table 4.4.: Mean and standard deviation (in parentheses) of parameter estimates from monthly re-calibration to option prices of the different model variants defined in Section 4.2.4. Parameters are estimated by minimization of the RRMSE between empirical and model-based theoretical option prices.

	β_1	α_1	β_2	α_2	σ_R	ρ
GBM	—	—	—	—	0.459	—
					(0.119)	
1PCH	0.175	—	—	—	—	—
	(0.157)					
1PCSCH	0.274	1.346	—	—	—	—
	(0.330)	(0.375)				
1PCHR	1.268	—	—	—	0.445	0.502
	(0.489)				(0.127)	(0.052)
1PCSCHR	204.365	5.920	—	—	0.468	0.800
	(178.272)	(3.186)			(0.133)	(0.101)
2PCH	0.844	—	0.786	—	—	0.449
	(0.514)		(0.343)			(0.104)
2PCSCH	114.021	5.137	3.679	3.075	—	0.607
	(116.077)	(2.888)	(2.791)	(1.375)		(0.263)

volatility parameters deviate more strongly from the historical estimates. For the models with a one-parameter volatility function, i.e., GBM, 1PCH, 1PCHR, and 2PCH, the implied volatility parameters are almost consistently higher than the historical ones, with exception of the β_1 parameter in the 1PCH model. This pattern is typical also for several other markets and is usually explained by stochastic volatility that is compensated by a variance risk premium (see, e.g., Carr and Wu 2009; Trolle and Schwartz 2010). It would be a natural extension of our model framework to introduce a stochastic volatility factor to account for this observation. The large deviation of the implicitly estimated parameters of two-parameter volatility functions from the historical ones are in line with the large standard error and the resulting imprecision of the estimation discussed before, and is also reflected by a large standard deviation of the implied parameter estimates across the single months of our sample.

4.5.2. Pricing Performance

Based on the implied parameter estimates for each month of our data set, we evaluate the in- and out-of-sample option pricing performance of the different model variants. For the in-sample evaluation, we compare empirical prices of each month to theoretical prices calculated with the corresponding parameter estimates for that month. This comparison primarily reveals whether the underlying model is able to capture the cross-sectional properties (i.e., the volatility smile) of empirical option prices properly. For the out-of-sample analysis, theoretical option prices are calculated based on the parameter estimates for the previous month. In addition to cross-sectional properties, this analysis also stresses the time-series properties of option prices and points out if they are correctly represented by the model variant under consideration. We measure the deviations of theoretical from empirical option prices for both the in- and out-of-sample evaluation by means of different performance measures, which are summarized in Table 4.5, calculated over each year of our sample. Comparing the option pricing performance of the different model variants, we mainly refer to the RRMSE measure and use the other measures to check for robustness.

We start with the results for the years 2009 and 2010 reported in Table 4.6. In 2009, the best in-sample fit to option prices is achieved by a Black (1976) model driven by a GBM, which is not particularly surprising in light of the flat volatility smile during that year. The outstanding performance of the Black (1976) model is, however, not completely supported out-of-sample where the 1PCHR fits option prices better than a GBM, suggesting that it captures the time series properties more properly. For 2010, our results do not provide any clear picture which model has the best option pricing performance. In-sample all models are very close to each other, and out-of-sample all specifications apart from the 1P(CS)CH model show a similar performance. We remark, however, that the results for this earlier part of the sample must be treated with caution. Due to the early stage of the Phase II EUA option market, market participants used very simple models for option pricing rather than accounting for the particularities of the emission trading system and their precise implications, which explains the remarkably flat volatility smile in 2009. Given the overwhelming evidence from other option markets, we believe that a totally flat volatility smile is highly unlikely to be a permanent condition for emission permit options. That none of the model variants is clearly favored over the others in 2010 might indicate that the market switched to

Table 4.5.: Measures for the option pricing performance based on a set of N observed option prices P_i^{obs} and corresponding theoretical prices P_i^{th}, $i = 1, \ldots, N$.

Measure	Formula
Root-mean-squared error (RMSE)	$\sqrt{\frac{1}{N}\sum_{i=1}^{N}\left(P_i^{th} - P_i^{obs}\right)^2}$
Relative root-mean-squared error (RRMSE)	$\sqrt{\frac{1}{N}\sum_{i=1}^{N}\left(\frac{P_i^{th} - P_i^{obs}}{P_i^{obs}}\right)^2}$
Mean absolute error (MAE)	$\frac{1}{N}\sum_{i=1}^{N}\left\lvert P_i^{th} - P_i^{obs}\right\rvert$
Mean absolute percentage error (MAPE)	$\frac{1}{N}\sum_{i=1}^{N}\left\lvert\frac{P_i^{th} - P_i^{obs}}{P_i^{obs}}\right\rvert$
Minimum pricing error (Min)	$\min_{i=1,\ldots,N} P_i^{th} - P_i^{obs}$
Maximum pricing error (Max)	$\max_{i=1,\ldots,N} P_i^{th} - P_i^{obs}$
Percentage of positive pricing errors (PPPE)	$\frac{1}{N}\sum_{i=1}^{N} 1_{\{P_i^{th} - P_i^{obs} \geq 0\}}$

a different regime where traders depart from using the Black (1976) model for EUA option pricing. The results for the later years of Phase II promise more insights into this hypothesis.

Table 4.7 summarizes the in- and out-of-sample performances for the years 2011 and 2012. The evolution of the volatility smile over the years (see Figure 4.3) suggests that traders have adopted more sophisticated approaches for option pricing, and the state of the EUA option market towards the end of Phase II is more likely to be representative for current and future emissions markets in general. Our evaluation results reveal that the best in-sample fit to option prices is achieved by the 1P(CS)CH and 2P(CS)CH models. The 1P(CS)CH model assumes that the underlying permit price consists only of one price component with binary payoff, and also in the 2P(CS)CH model prices are mainly driven by one — the second — binary price component, due to the collapse of the first component in 2009. The good in-sample performance of these models indicates that they capture the volatility smile in emission permit option markets much better than the 1P(CS)CHR or the Black (1976) model. In fact, the difference of the 1P(CS)CHR model and the Black (1976) model is also small in 2011 and 2012, likewise because of the collapse of the first price component. Although both the 1P(CS)CH and the 2P(CS)CH model are (mainly) driven by one binary component in 2011 and 2012, they differ in the crucial fact that the binary payoff occurs already in 2012 for the former one, but only in 2020 for the latter. Therefore the "pull effect" to either zero or the amount of the penalty is much stronger for the 1P(CS)CH model, and this dynamics directly translates to the resulting option prices. This difference is brought to light by the out-of-sample analysis, where the 2P(CS)CH model consistently outperforms the 1P(CS)CH model. Particularly in 2011, the 1P(CS)CH model shows by far the worst out-of-sample performance of all models, highlighting that it is not able to capture the time-series properties of EUA option prices in an appropriate way.

Overall, we find that in the later years of Phase II the best option pricing performance is achieved by the 2P(CS)CH model, which explicitly accounts for two compliance periods of an emission trading system and the resulting binary option characteristics. This result confirms that the market indeed developed from a regime where traders naively used the most simple option pricing approach in this young market to a more mature state. The results for the year 2010, which do not clearly favor one model over the others, represent this transition. Finally, we ask if the two-parameter versions of reduced-form permit price models yield a superior option pricing performance compared to the one-parameter model variants. Our results show that the additional parameter slightly improves the in-sample fit in many cases, but the out-of-sample performance often even worsens, indicating that the additional degree of freedom rather leads to over-fitting than to an enhancement of explanatory power.

In summary, our findings reveal that the design of an emission trading scheme and its implications for the dynamics of permit prices are precisely reflected by option prices. Therefore, models tailored to account for the specific properties of emission permit prices perform best in option pricing.

Table 4.6.: In- and out-of-sample option pricing performance in 2009 and 2010 for the different model variants defined in Section 4.2.4. For the in-sample evaluation, we compare empirical prices of each month to theoretical prices calculated with the corresponding implied parameter estimates for that month. For the out-of-sample analysis, theoretical option prices are calculated based on the parameter estimates for the previous month. We report different performance measures as listed in Table 4.5.

	RMSE	RRMSE	MAE	MAPE	Min	Max	PPPE
			In-Sample				
2009							
GBM	0.08	5.47%	0.06	3.92%	−0.28	0.20	48.14%
1PCH	0.11	6.55%	0.08	4.79%	−0.34	0.20	40.00%
1PCSCH	0.08	5.79%	0.07	4.25%	−0.23	0.25	45.42%
1PCHR	0.12	6.97%	0.09	5.18%	−0.52	0.42	46.78%
1PCSCHR	0.12	6.99%	0.09	5.11%	−0.53	0.53	45.08%
2PCH	0.13	8.12%	0.10	5.96%	−0.65	0.51	45.76%
2PCSCH	0.15	8.08%	0.10	6.08%	−0.54	0.69	43.39%
2010							
GBM	0.08	9.45%	0.06	7.07%	−0.31	0.19	57.51%
1PCH	0.09	9.25%	0.06	6.99%	−0.34	0.21	56.22%
1PCSCH	0.09	9.25%	0.06	6.99%	−0.34	0.21	56.44%
1PCHR	0.08	9.47%	0.06	7.09%	−0.31	0.20	57.30%
1PCSCHR	0.08	9.48%	0.06	7.10%	−0.31	0.20	57.73%
2PCH	0.09	9.13%	0.07	6.96%	−0.35	0.21	56.01%
2PCSCH	0.09	9.13%	0.07	6.96%	−0.35	0.22	56.01%
			Out-of-Sample				
2009							
GBM	0.17	10.06%	0.14	8.16%	−0.37	0.38	63.05%
1PCH	0.22	11.89%	0.14	8.17%	−0.39	0.68	52.54%
1PCSCH	0.22	11.91%	0.15	8.45%	−0.39	0.67	63.39%
1PCHR	0.16	9.83%	0.13	7.63%	−0.72	0.38	47.80%
1PCSCHR	0.20	11.06%	0.15	8.41%	−0.60	0.73	57.29%
2PCH	0.21	12.34%	0.15	9.34%	−0.77	0.45	48.81%
2PCSCH	0.36	17.74%	0.24	12.87%	−1.06	0.49	29.15%
2010							
GBM	0.18	17.93%	0.14	14.13%	−0.43	0.38	71.24%
1PCH	0.20	19.28%	0.16	15.67%	−0.47	0.50	74.89%
1PCSCH	0.20	19.27%	0.16	15.66%	−0.48	0.50	74.68%
1PCHR	0.18	17.91%	0.14	14.12%	−0.43	0.39	71.24%
1PCSCHR	0.18	17.94%	0.14	14.14%	−0.43	0.39	71.24%
2PCH	0.19	18.05%	0.14	14.23%	−0.48	0.41	71.24%
2PCSCH	0.19	18.15%	0.15	14.31%	−0.48	0.41	71.03%

Table 4.7.: In- and out-of-sample option pricing performance in 2011 and 2012 for the different model variants defined in Section 4.2.4. For the in-sample evaluation, we compare empirical prices of each month to theoretical prices calculated with the corresponding implied parameter estimates for that month. For the out-of-sample analysis, theoretical option prices are calculated based on the parameter estimates for the previous month. We report different performance measures as listed in Table 4.5.

	RMSE	RRMSE	MAE	MAPE	Min	Max	PPPE
			In-Sample				
2011							
GBM	0.13	13.44%	0.09	9.69%	−0.46	0.30	53.49%
1PCH	0.12	11.70%	0.08	8.45%	−0.38	0.29	53.68%
1PCSCH	0.12	11.71%	0.08	8.45%	−0.38	0.29	53.68%
1PCHR	0.13	13.54%	0.09	9.77%	−0.47	0.30	53.29%
1PCSCHR	0.13	13.54%	0.09	9.78%	−0.47	0.30	53.29%
2PCH	0.12	12.14%	0.09	8.83%	−0.42	0.29	52.52%
2PCSCH	0.12	12.07%	0.09	8.75%	−0.39	0.29	52.33%
2012							
GBM	0.07	5.80%	0.05	4.54%	−0.18	0.16	50.00%
1PCH	0.05	4.41%	0.04	3.22%	−0.12	0.15	49.38%
1PCSCH	0.05	4.41%	0.04	3.23%	−0.12	0.15	49.38%
1PCHR	0.07	6.00%	0.06	4.70%	−0.18	0.17	51.25%
1PCSCHR	0.07	6.00%	0.06	4.70%	−0.18	0.17	50.62%
2PCH	0.05	4.54%	0.04	3.41%	−0.12	0.17	50.00%
2PCSCH	0.05	4.42%	0.04	3.31%	−0.13	0.17	48.75%
			Out-of-Sample				
2011							
GBM	0.17	18.71%	0.14	15.19%	−0.73	0.35	39.53%
1PCH	0.39	32.58%	0.20	18.57%	−0.49	1.87	44.57%
1PCSCH	0.39	32.57%	0.20	18.57%	−0.49	1.87	44.57%
1PCHR	0.17	18.79%	0.14	15.25%	−0.77	0.35	39.53%
1PCSCHR	0.17	18.78%	0.14	15.26%	−0.78	0.35	39.53%
2PCH	0.16	16.28%	0.13	13.34%	−0.66	0.41	38.37%
2PCSCH	0.16	16.61%	0.13	13.43%	−0.62	0.46	38.37%
2012							
GBM	0.14	11.12%	0.12	9.48%	−0.28	0.21	48.12%
1PCH	0.13	11.09%	0.11	9.33%	−0.18	0.28	59.38%
1PCSCH	0.13	11.09%	0.11	9.33%	−0.18	0.28	58.75%
1PCHR	0.14	11.22%	0.12	9.50%	−0.28	0.22	47.50%
1PCSCHR	0.14	11.20%	0.12	9.47%	−0.28	0.22	47.50%
2PCH	0.11	9.37%	0.10	8.04%	−0.22	0.24	49.38%
2PCSCH	0.11	9.33%	0.10	8.05%	−0.22	0.24	49.38%

5. Impact of the Yearly Emissions Announcement

5.1. Introduction

While the previous two chapters deal with the structural price features of emission permits and related derivatives, this chapter is dedicated to the short-term dynamics of the emission permit market. Departing from the assumption that the state of realized emissions and the prevailing emission rate is perfectly observable for the market, we ask whether there is a significant market reaction to news events relating to the past or future emissions of the economy. In particular, we consider the impact of the yearly emissions announcement event on the European carbon market. As described in Section 2.3.1, the European Commission collects data on yearly realized emissions from the regulated companies and releases aggregate figures in early April every year. In the notation of Chapter 3, this event obviously conveys information about economy-wide realized emissions x_t, and it may also give an indication for the prevailing emission rate y_t.

The potential impact of the yearly emissions announcement became clear in Phase I of the EU ETS, when the first release of realized emissions data in April 2006 indicated that economy-wide emissions for 2005 were far below the number of permits allocated to the market. As a consequence, permits lost about two thirds of their value at extremely high trading volumes, as Figure 5.1 depicts. However, the circumstances of the emissions announcement in 2006 can be considered as very special. First, it was the first event of that kind for the European emissions market at all, which was still in a rather immature state at that time. Second, preliminary information on realized emissions was accidentally released early on the European Commission's website, although the official announcement date was scheduled for May 15. On April 25, emissions data of the Czech Republic and the Netherlands became public, both indicating that emissions

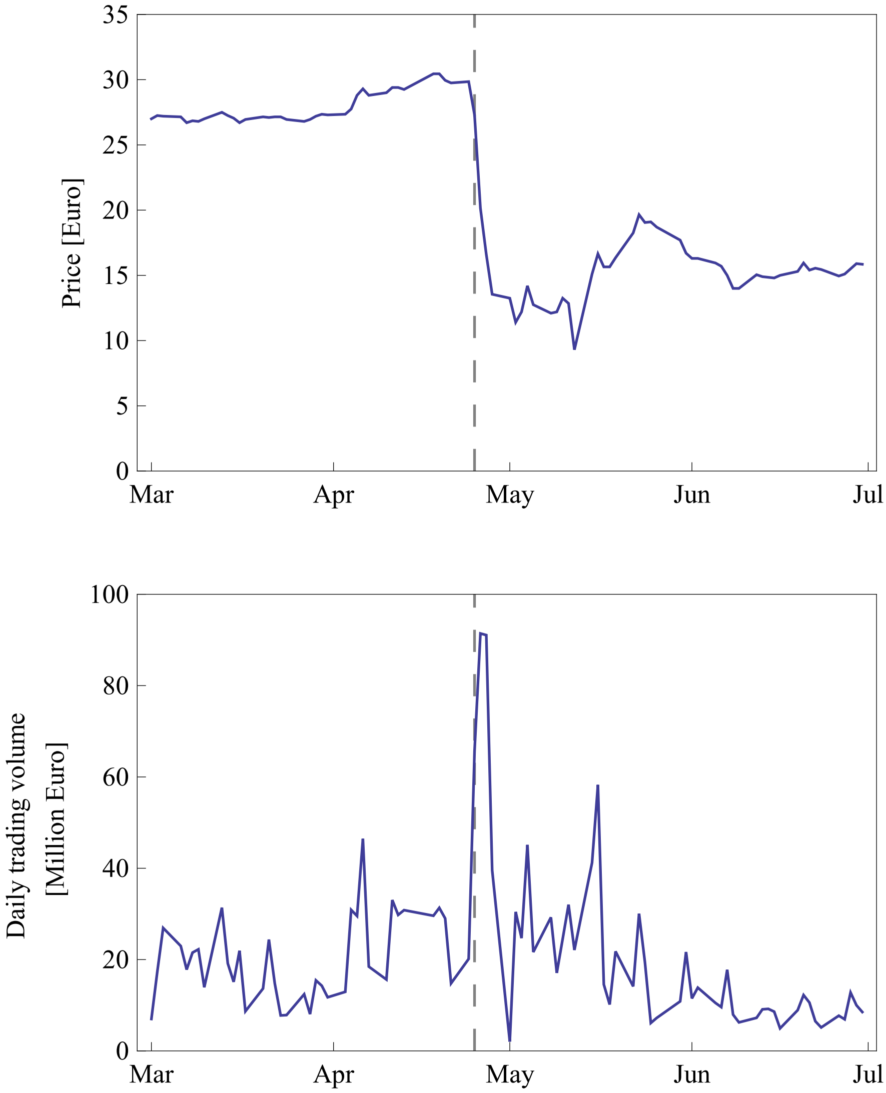

Figure 5.1.: Daily prices and trading volumes of EUA futures maturing in December 2006 from March 1 to June 30, 2006. Prices are settlement prices quoted in Euros provided by the ECX. Trading volumes are also expressed in Euros by multiplying the daily number of traded contracts by the contract size of 1,000 EUAs per contract and the daily settlement price. The dashed vertical line marks April 25, 2006, the date when first parts of the realized emissions data for 2005 were published.

were considerably below the quotas. Further information for the other participating states was released on the following days. In this sense, the emissions announcement in 2006 can be rather considered as an unscheduled event. Altogether, it is far from clear whether the dramatic impact of the event in 2006 can be generalized to a mature emissions market and properly scheduled emissions announcements.

The existing literature on the impact of the emissions announcement on the permit market is sparse. Chevallier et al. (2009) analyze changes in investors' risk aversion around the announcement event in 2007. Grüll and Kiesel (2012) investigate the general permit price sensitivity and consider the price collapse caused by the release in 2006 as one example of extreme price movements. Mansanet-Bataller and Pardo (2009) analyze the impact of decisions on National Allocation Plans (NAPs) on permit prices and control for the influence of the 2006 and 2007 emissions announcements, but do not discuss the impact of these events in particular. Conrad et al. (2012) also focus on NAP events. On classical commodity markets, a series of papers (Linn and Zhu 2004; Ates and Wang 2007; Mu 2007; Gregoire and Boucher 2008; Le 2008; Bjursell et al. 2010) analyzes the impact of structurally similar events, like the natural gas storage report or the petroleum status report,[98] finding a significant impact of these events on volatilities of natural gas and crude oil prices.

We investigate the effects of the yearly emissions announcement on the European carbon market for an event sample from 2007 to 2012. For that, we analyze market data on prices, volumes, intraday volatilities, and option-implied volatilities of EUA futures, as described in the next section. Section 5.2 further describes the details of the emissions announcement events in our sample. Section 5.3 outlines our analysis and presents the results.

[98] These events convey information about the economy-wide inventory of commodities like crude oil and natural gas. Similarly, information about the economy-wide holdings of unused emission permits is published by the yearly emissions announcement.

5.2. Data

5.2.1. Prices and Volumes

We use daily settlement prices and trading volumes of EUA futures from January 1, 2007 to June 30, 2012 for our analysis. In addition to the time period studied in Chapter 4, our sample also covers the year 2007 in this chapter in order to investigate the impact of the announcement event in 2007 on EUA futures as well. We take December 2008 futures as the relevant contracts in 2007[99] and consider always the December futures next to maturity during Phase II, with roll-over on the last day of October according to Section 2.3.2. We calculate log returns $R_t = \ln(F_t/F_{t-1})$ of the futures prices F_t[100] and delete observations on the day after the roll-over from our time series. Similarly, we consider total traded volumes in the active December contract according to our roll-over strategy, including screen trading as well as the exchange-for-physical facilities of the ECX. We express volumes in monetary value by multiplying the daily number of traded contracts by the contract size of 1,000 EUAs per contract and the daily settlement price, and denote this time series by $VOLUME_t$.

Figure 5.2 illustrates our price and volume data and highlights the dates of the emissions announcement events.

5.2.2. Realized and Implied Volatilities

We measure intraday volatility using high-frequency price data and calculate implied volatilities based on European options written on EUA futures. For intraday volatilities, we subdivide each trading day t into 120 intraday 5-minute intervals from 7:00 a.m. to 5:00 p.m. local time enumerated by $i = 1, \ldots, N$ and denote the 5-minute log returns by $R_{t,i}$. Then,

$$RV_t = 252 \sum_{i=1}^{N} R_{t,i}^2 \tag{5.1}$$

[99] We do not consider December 2007 futures since the underlying Phase I EUAs had already lost most of their value in 2007 due to the large permit over-supply and became completely worthless during that year.

[100] We deviate from the notation $F(t, \bar{t})$ for futures prices in this chapter and denote the price of the active futures contract by F_t since the maturity $\bar{t}$ is of no particular relevance for our analysis once the time series is constructed.

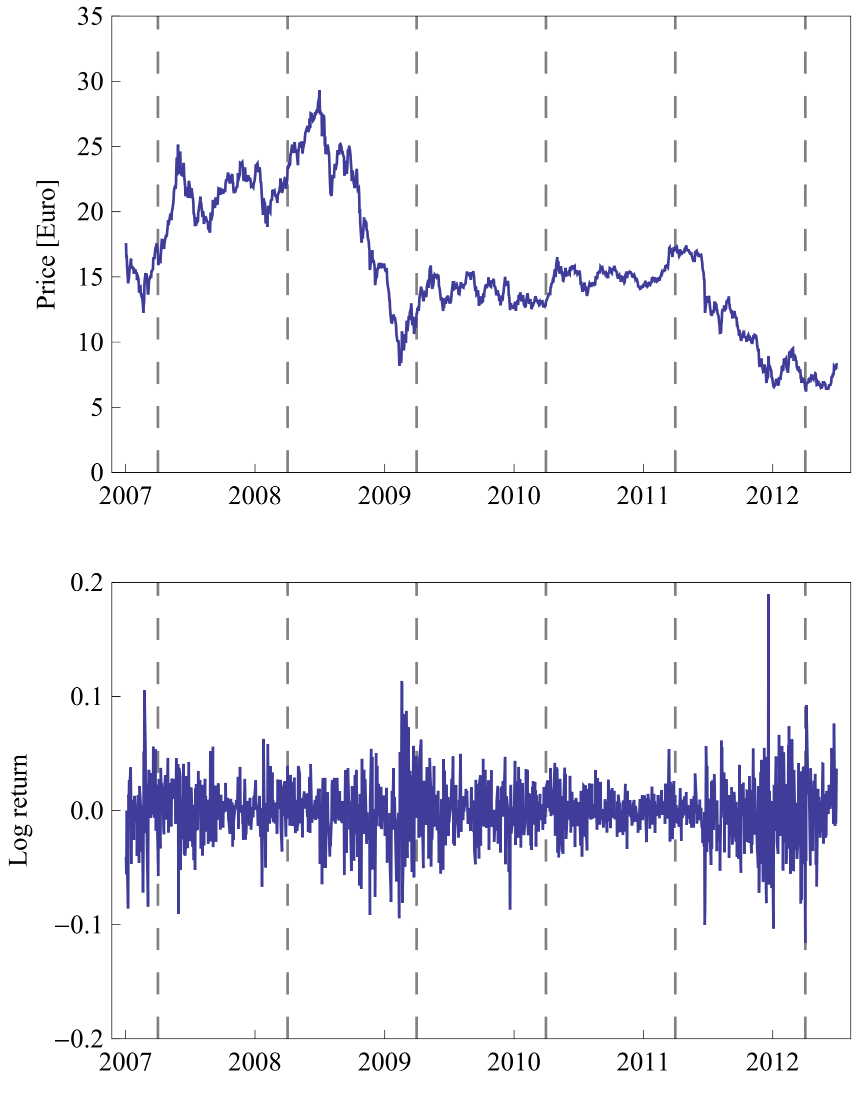

Figure 5.2.: Daily EUA futures prices and trading volumes quoted in Euros as well as corresponding log changes from January 1, 2007 to June 30, 2012. Data is provided by the ECX. The dashed vertical lines mark the release days of the yearly emissions announcement.

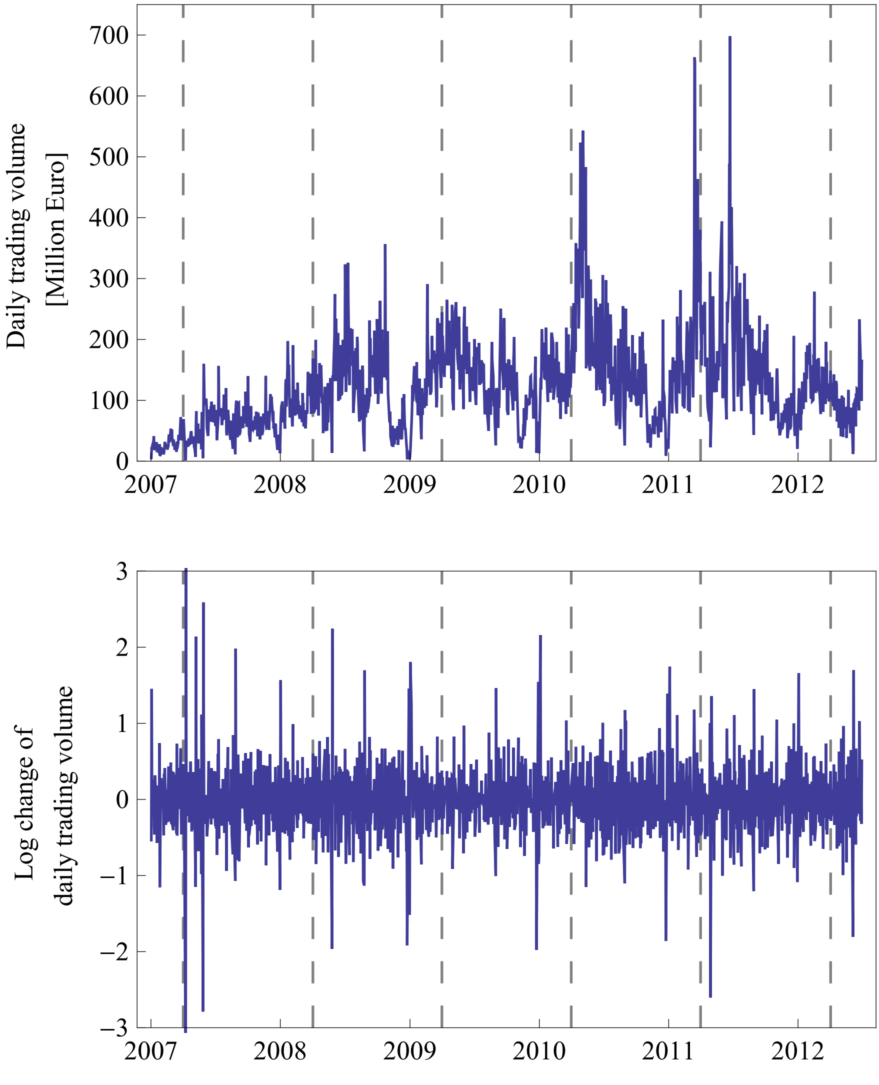

Figure 5.2 (continued).

provides a model-free measure of the intraday variance RV_t realized at day t, annualized by multiplying by a number of 252 business days per year, and $RSD_t = \sqrt{RV_t}$ is the corresponding realized standard deviation.[101] As Andersen et al. (2001) point out, this measure reflects the true volatility of returns much more accurately than measures based on lower frequencies. We use 5-minute intraday price data of EUA futures from the Thomson Reuters DataScope Tickhistory archive.[102]

For implied volatilities we build on the model-free approach developed by Carr and Madan (1998), Demeterfi et al. (1999), and Britten-Jones and Neuberger (2000), among others. Accordingly, the annualized implied variance $IV(t, \tau)$ from t to τ can be calculated based on a continuum of out-of-the-money (OTM) call and put options with maturity τ and strikes $K \in [F_t, \infty)$ ($K \in [0, F_t]$), where F_t is the underlying futures price. Let $C(t, \tau, K)$ ($P(t, \tau, K)$) be the price of a call (put) option on EUA futures with expiry date τ and strike K, and $b(t, \tau)$ is the price of a zero bond maturing at τ. Then, under no-arbitrage, the implied variance is

$$IV(t,\tau) = \frac{2}{b(t,\tau)(\tau - t)} \left(\int_0^{F_t} \frac{P(t,\tau,K)}{K^2} dK + \int_{F_t}^{\infty} \frac{C(t,\tau,K)}{K^2} dK \right), \quad (5.2)$$

and we denote the time series of implied volatilities $ISD(t, \tau) = \sqrt{IV(t, \tau)}$ constructed according to our roll-over strategy by ISD_t. Daily settlement prices of EUA futures options are provided by the ECX. To generate the continuum of option prices required by the model-free approach (5.2), we linearly interpolate between the Black (1976) implied volatilities of all available options. In contrast to Chapter 4, we make use of all available settlement prices regardless of the moneyness and whether the option is traded on that particular day. The underlying rationale is that interpolating between all settlement prices provides at least as much information about the model-free implied volatility as interpolating only between traded options. Still, we clean the data like in Chapter 4 by excluding options with prices smaller than 0.06 Euros as well as quotations violating no-arbitrage bounds. For each day within our sample period there remain settlement prices of at least 5 OTM calls and 6 OTM puts, with 25 OTM calls and 18 OTM puts on average. Zero bond prices $b(t, \tau)$ are inferred from the term structure of risk-free interest rates as represented by EURIBOR rates for maturities up to

[101] Since we measure intraday volatility, close-to-open returns are not included into the sum.

[102] We thank SIRCA for providing access to the Thomson Reuters DataScope Tickhistory archive, `http://www.sirca.org.au`.

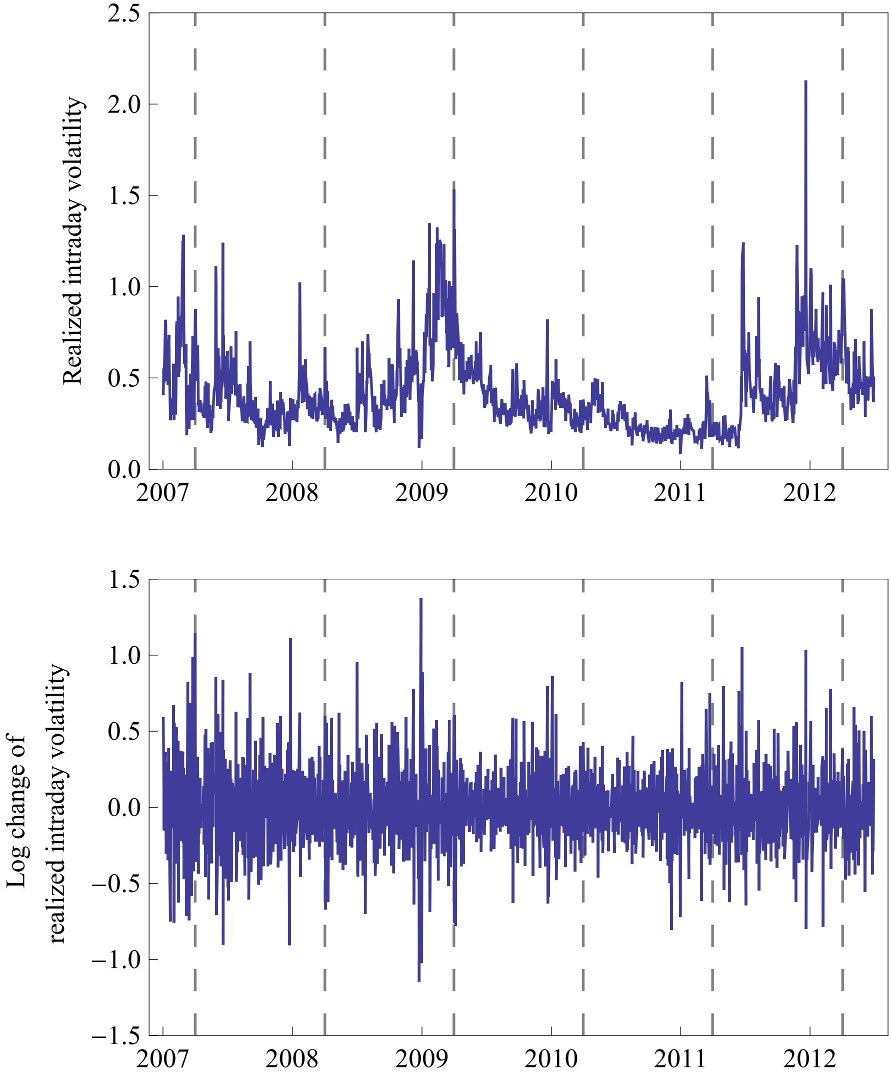

Figure 5.3.: Daily realized intraday volatilities and option-implied volatilities of EUA futures as well as corresponding log changes from January 1, 2007 to June 30, 2012. Realized intraday volatilities are computed using the model-free high-frequency approach (5.1) based on 5-minute price data provided by the Thomson Reuters DataScope Tickhistory archive. Implied volatilities are inferred according to the model-free approach (5.2) from settlement prices of EUA futures options quoted by the ECX. The dashed vertical lines mark the release days of the yearly emissions announcement.

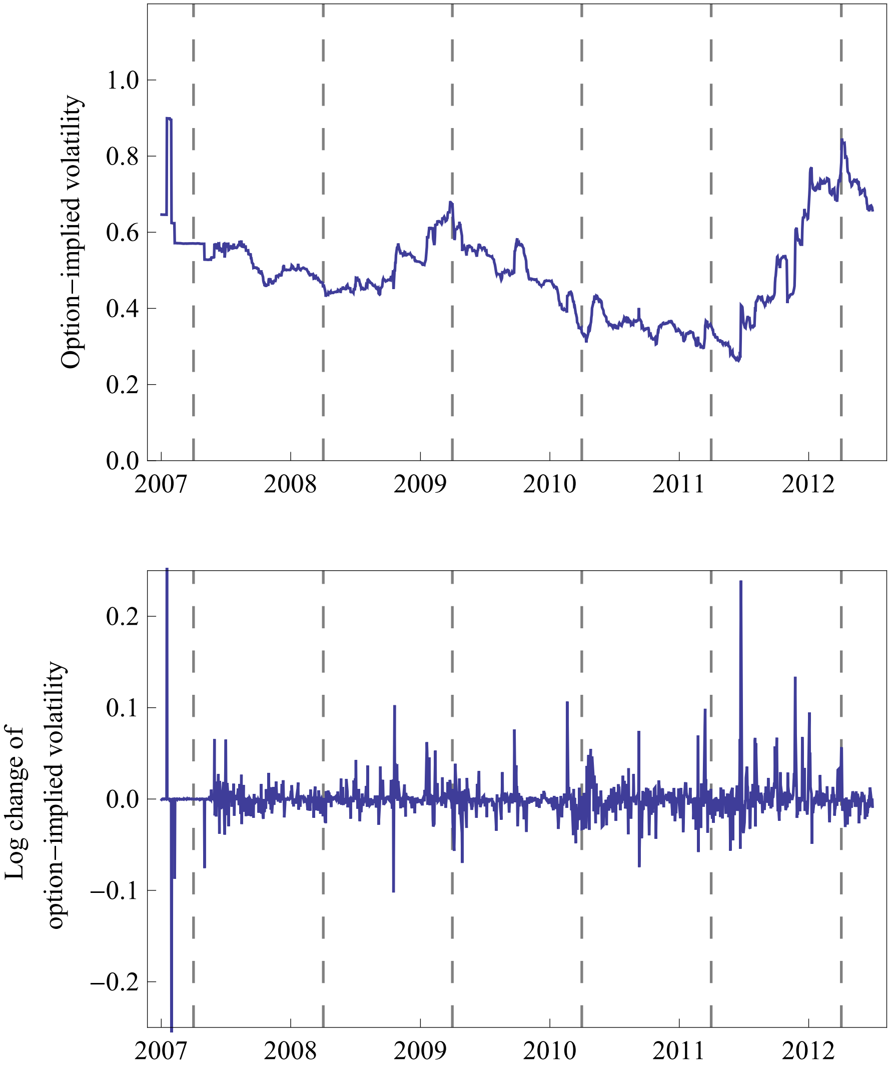

Figure 5.3 (continued).

one year and EuroSwap rates for longer maturities. For a given maturity, we linearly interpolate the two interest rates whose maturities straddle it.

Figure 5.3 shows realized intraday and option-implied volatilities. Although realized intraday volatilities fluctuate much stronger than the longer-term implied volatilities, a certain comovement is observable. Both time series reach high levels in the first quarter of 2009, from which they steadily decrease until 2011 before rising again quickly. This comovement represents the interdependence between implied and actual volatility: Implied volatility predicts future volatility and incorporates information about volatility realized in the past (see Christensen and Prabhala 1998).

5.2.3. Emissions Announcement Events

The event sample for our analysis consists of the yearly emissions announcements from 2007 to 2012. We do not include the 2006 event due to the special circumstances described before. Table 5.1 gives an overview of the event set and the released figures.[103] As evidence of the surprise caused by the single emissions announcements, we infer prior market expectations from a poll carried out by Reuters for the years 2009, 2010, and 2011, and from Reuters market reports for the other events.[104] Although this surprise data is not extensive enough to incorporate it into a quantitative analysis, it allows to sharpen the conclusions from our empirical results.

After the dramatically large permit surplus for 2005 was announced in 2006, traders consistently expected a similarly high over-allocation for the following years. Accordingly, it was no surprise that emissions in 2006 were about 125 million tons below the quotas. The market was similarly long of permits in 2007 (102 million tons), but this time traders were surprised since this figure meant a slight increase of emissions compared to the previous year, “contrary to an expected drop”, as reported by Reuters. Note that these two events were of negligible importance for emission permit prices of Phase I because a large over-supply was known in 2006 already, and emissions of 2007

[103] We refer to data from the first official press release after an emissions announcement. In 2007 and 2008, this data includes emissions from Austria, Belgium, Cyprus, the Czech Republic, Denmark, Estonia, Finland, France, Germany, Greece, Hungary, Ireland, Italy, Latvia, Lithuania, Luxembourg, the Netherlands, Poland, Portugal, the Slovak Republic, Slovenia, Spain, Sweden, and the United Kingdom. In 2009, Malta and Romania are added, and in 2010, Bulgaria, Liechtenstein, and Norway are included as well.

[104] The Reuters poll summarizing market participants’ expectations for the European carbon market was launched in mid-2008. As of mid-2011, forecasts on economy-wide emissions are not covered by the poll any more and only price estimates are reported.

Table 5.1.: Emissions announcement events from 2007 to 2012 and released figures. On the event date, the European Commission publishes aggregate figures on emissions realized in the previous year on its website. We refer to data from the first official press release after the announcement date (European Commission 2007, 2008a, 2009, 2010b, 2011b, 2012b). Realized emissions are reported in million tons of carbon dioxide and opposed to the number of permits allocated for that year (in millions). The difference between both figures is the resulting permit surplus/shortage for a particular year.

Event Date	Compliance Year	Compliance Period	Permits Allocated	Realized Emissions	Permits long/short
Apr 2, 2007	2006	2005-2007	2,152	2,027	125
Apr 2, 2008	2007	2005-2007	2,152	2,050	102
Apr 1, 2009	2008	2008-2012	1,909	2,060	-151
Apr 1, 2010	2009	2008-2012	1,967	1,873	94
Apr 1, 2011	2010	2008-2012	1,994	1,932	62
Apr 2, 2012	2011	2008-2012	2,017	1,899	118

were announced when Phase I was already over. In contrast, the released figures were of interest as an indication about future emissions in Phase II. In 2008, the first year of Phase II, it occurred for the first time that realized emissions exceeded the quotas. The market was short by about 151 million tons, which was at the upper end, but still within the expectations of market participants ranging from 100 million tons long (Citigroup) to 180 million tons short (IDEAcarbon). This changed again in the following years due to the financial crisis and the subsequent economic downturn. Adjusting their forecasts, traders expected the market to be over-supplied by at least 190 million tons (Deutsche Bank) and at most 60 million tons (Nomisma Energia) in 2009. The actual figures of 94 million tons, released on April 1, 2010, were within this range of expectations. Emission levels slightly recovered in 2010 and the permit surplus of 62 million tons was again at the upper end of prior projections, ranging from 50 million tons long (Nomisma Energia) to 190 million tons long (MF Global). A further continuation of the economic recovery was expected for 2011. However, the realized emissions, released on April 2, 2012, “dropped below expectations” as reported by Reuters and were 118 million tons below the quota.

By visual inspection of the price, volume, and volatility time series (see Figure 5.2 and Figure 5.3) around the event dates, it is not possible to get a clear impression of the effects caused by the emissions announcement events. Only for intraday volatility, a peak at the event day in 2007, 2008, and 2009 is observable, but given the large fluctuation it is questionable if there is any statistical significance. We define dummy variables for the event periods to investigate the general impact of the yearly emissions announcement in the next section. D_0 is 1 on the actual day of an emissions announcement, and 0 otherwise. In the same way, D_{-1} and D_{+1} indicate the day directly before and after an announcement, and $D_{[-4,-2]}$ and $D_{[+2,+4]}$ stand for the time window from four to two days prior and subsequent to an announcement.

5.3. Empirical Analysis

5.3.1. Price Impact

The unanticipated price impact of the yearly emissions announcement can be measured by the magnitude of abnormal performance around the release date. A significant abnormal return on the event date would indicate that the release of realized emissions conveys unanticipated information to the market. Further, abnormal returns on the subsequent days would suggest an inefficient market that does not incorporate new information within the same day, while abnormal returns on pre-event days could arise due to information leakage. We consider abnormal returns based on a mean-adjusted return model, i.e., the abnormal return $AR_t = R_t - \widehat{R}$ on day t is defined as the difference between the actual return R_t and the mean return $\widehat{R}$ over the sample period.[105] Following Ederington and Lee (1996), we perform a dummy regression for absolute abnormal returns $AAR_t = |AR_t|$ over the whole sample period with event dummies as defined in Section 5.2.3. The results are reported in the first line of Table 5.2. Indeed, we observe a significant price impact of the emissions announcement event. Absolute abnormal returns on days of the realized emissions release are on average about three times as high as on normal trading days, according to an increase by 0.022 compared to the normal level of 0.011.[106] Furthermore, our results yield no evidence of any in-

[105] For alternative normal return models we refer to the overview papers by MacKinlay (1997) and Binder (1998).

[106] Note that the intercept term of the dummy regression multiplied by $\sqrt{\pi/2}$ can also be interpreted as the general volatility of daily returns, while $\sqrt{\pi/2}$ times the coefficient of the event dummy is an estimate for the additional volatility on event days, see Ederington and Lee (1993). Accordingly, we observe an overall volatility of 4.14% on event days compared to a volatility of 1.38% without the event window.

formation leakages or market inefficiencies, so that in general the price reaction only affects the event day return.

The price impact of an individual event might deviate from this averaged result due to a particularly small or large surprise effect of the information released. In addition, the direction of an abnormal return depends on the realized emissions being below or above market expectations. The magnitude and direction of abnormal returns AR_t for the single events of our sample is illustrated in Figure 5.4. Significant abnormal returns on the event day can be observed for the years 2008 and 2012, suggesting a particularly large surprise effect as opposed to the other years. This is in line with market reports from Reuters as described in Section 5.2.3, stating that in 2008 increased emissions were released “contrary to an expected drop”, and the realized emissions announced at the 2012 event “dropped below expectations”. Accordingly, the abnormal return has a positive sign for the event day in 2008, and is significantly negative for the 2012 release date. For the other events, no significant abnormal returns are observable, which is in accordance with realized emissions being within the range of analysts’ expectations. Overall, the analysis of the single events confirms the general result that the announcement of previous year’s emissions has a price impact, the magnitude of which naturally depends on the surprise effect caused by the information released.

5.3.2. Trading Volume

The impact of a news event is generally not only reflected by the size of abnormal returns, but also by the trading activity on the release day. Trading volume rises when important information is released to the market, and the increase is the stronger the larger the surprise effect of the new information is (see, e.g., Bamber 1986).[107] To investigate the influence of the emissions announcement on trading volumes in emission permit futures, we follow Ajinkya and Jain (1989) and Mai and Tchemeni (1996) and consider logarithmic volumes in monetary value $\ln(VOLUME_t)$. The event dummy regression for log volumes yields the results reported in the second line of Table 5.2. As for abnormal returns, we find a significant effect of the emissions announcement on

Section 5.3.3 provides a detailed analysis of event-induced volatility based on realized intraday volatilities.

[107] Absolute price changes and volumes are positively correlated in general, not only in the context of news releases. This relationship is found empirically (see Karpoff 1987 for a survey) and predicted by theoretical models (Holthausen and Verrecchia 1990; Harris and Raviv 1993; Blume et al. 1994).

Table 5.2.: Impact of the emissions announcement measured by absolute abnormal returns, trading volumes, realized intraday volatilities, and changes in option-implied volatilities. The dummy regression

$$Z_t = \alpha + \sum_i \beta_i D_{i,t} + \sum_{j=2007}^{2011} \gamma_j Y_{j,t} + \sum_{k=1}^{L} \delta_k Z_{t-k} + \varepsilon_t$$

is estimated for $Z = AAR$, $\ln(VOLUME)$, $\ln(RSD)$, $\Delta\ln(ISD)$, with event period dummies D_i as defined in Section 5.2.3. We include year dummies Y_j to control for year fixed effects, and lags of the dependent variable to account for serial correlation. Selecting the lag length L with respect to the Akaike information criterion yields 6 lags for absolute abnormal returns, 5 lags for trading volumes, 5 lags for realized intraday volatilities, and 1 lag for changes in option-implied volatilities. For each dummy regression, we report the estimated intercept and event dummy coefficients in the first line. Standard errors (in parentheses) are computed according to the Newey and West (1987, 1994) procedure to correct for auto-correlated or heteroskedastic error terms. *, **, and *** stand for significance at the 10, 5, and 1 percent level.

		Event Period Dummies				
	Intercept	[-4;-2]	-1	0	+1	[+2;+4]
AAR	0.011***	−0.004	−0.002	0.022*	−0.002	0.000
	(0.002)	(0.003)	(0.005)	(0.013)	(0.008)	(0.003)
ln(VOLUME)	3.250***	−0.078*	0.012	0.253**	0.040	−0.195
	(0.552)	(0.040)	(0.096)	(0.100)	(0.137)	(0.192)
ln(RSD)	−0.068***	−0.087***	−0.049	0.515***	0.049	−0.022
	(0.019)	(0.019)	(0.092)	(0.121)	(0.117)	(0.045)
Δln(ISD)	0.000	−0.001	−0.003	0.005	−0.005	−0.010*
	(0.002)	(0.002)	(0.004)	(0.011)	(0.011)	(0.005)

trading volumes. On the event day, trading volume increases about 29% according to a coefficient value of 0.253. In contrast to this extremely high trading activity on the release day itself, the market is rather calm on the preceding days. Trading volumes are significantly lower than normal in the window from 4 to 2 days prior to the event date. Such behavior is known as the "calm before the storm" effect (Jones et al. 1998): Trading is quiet when the market awaits a large information shock due to a scheduled public news release.[108] A view on the trading volumes around the single events (see Figure 5.4) confirms that trading activity is higher than normal on the release day in all cases, whereas the effect is statistically significant only for 2007, 2008, and 2009. Particularly in 2008, the increased volume corresponds to an abnormal return on the event day, in line with the claim that "it takes volume to make prices move" (Karpoff 1987). This direct relationship is, however, not that clearly pronounced for the other events of our sample.

5.3.3. Volatilities

We further investigate the impact of the yearly emissions announcement on actual intraday volatilities as well as on option-implied volatilities. In light of our results for abnormal returns and trading volumes, we can expect increased volatilities on realized emissions release days.[109] Indeed, the event dummy regression results for logarithmic intraday volatilities $\ln(RSD_t)$ (see Table 5.2) show that market volatility is significantly higher than normal on days of the emissions announcement. A coefficient of 0.515 stands for an intraday volatility on the event day that is 67% above regular levels. In addition to that, we also observe a "calm before the storm" effect for volatilities, indicated by significantly lower figures from 4 to 2 days prior to the release. Considering the single events in particular (see Figure 5.5), we consistently observe higher intraday volatilities on the announcement day in all cases, with statistical significance in 2008, 2009, and 2012. Especially in 2008 and 2012, intraday volatility does not directly revert to normal on the following day, but persists at an increased level. This shows that an

[108] For example, French et al. (1989) find empirical evidence of this effect for agricultural futures markets.

[109] Such an effect is well established in the literature for many different markets and announcement types. Especially for energy markets, a series of papers (Linn and Zhu 2004; Ates and Wang 2007; Mu 2007; Gregoire and Boucher 2008; Le 2008; Bjursell et al. 2010) reports on increased volatilities of natural gas and crude oil futures around the release of the weekly natural gas storage report and the petroleum status report.

announcement with significant price impact may cause nervous trading that lasts even one day after the release.

The behavior of actual volatilities around the event date should be reflected by adjustments of option-implied volatilities. As Ederington and Lee (1996) argue, two effects are responsible for changes in implied volatilities around news announcements: First, the expected volatility for any day t is obviously included in the implied volatility on day $t-1$, but not at the end of day t anymore. That means that if the volatility on event day t is expected to be higher than the average volatility until the options' maturity, then the implied volatility should decrease from $t-1$ to t due to the dropping out of the highly volatile day. Second, the release of unexpected information could possibly cause a revision of the expected future volatility. This may affect implied volatilities in either direction. However, only the first effect is likely to persist when multiple events are considered, because under rational expectations of market participants revisions in either direction are equally likely and should cancel out on average. We consider log changes of implied volatility $\Delta \ln(ISD_t) = \ln(ISD_t/ISD_{t-1})$ and report results of the event dummy regression in the last line of Table 5.2. Implied volatilities decrease significantly within the interval from 2 to 4 days after the event. As argued above, this behavior cannot be explained by revisions of expectations about future volatility, since it applies on average over all events of our sample. The decline is consequently attributable to the volatilities expected for the preceding days, which are no longer included in the option-implied volatilities. This indicates that the market expects increased volatilities on and around the event day. A possible reason for the implied volatilities not to decrease earlier than 2 days after the announcement can be either that the market expects also higher-than-normal volatilities on the days after the event or that the EUA option market is not completely efficient and reacts with a certain delay.

Although the behavior of implied volatilities around an individual event can be driven by both of the effects mentioned, Figure 5.5 suggests for the events from 2007 to 2011 that significant decreases in implied volatility directly correspond to significantly higher-than-normal realized volatilities around the event. Particularly, the decline of implied volatilities in 2008 and 2009 subsequent to the emissions announcement is in line with the thesis that the market expected high volatilities around the event for these years. As seen before, these expectations were fulfilled and volatilities were high indeed. To the contrary, there is no significant change in implied volatilities in 2007, 2010, and 2011, and realized volatilities are also not significantly increased in these cases. A different pattern is observable for the 2012 event: Implied volatilities significantly increase on the event day as well as on the two following days, hinting that the information released on April 2, 2012 leads to higher expected permit price volatilities until the end of 2012. A possible reason is the political uncertainty due to the discussion on a political intervention in the European carbon market that is stimulated by the unexpectedly high over-supply of emission permits.[110] However, the plot of implied volatilities in Figure 5.3 suggests that parts of this uncertainty prevailed only on the short run and declined in the following weeks.

[110] We discuss potential measures of the EU Commission addressing the large permit surplus in the EU ETS in the conclusion and outlook of this thesis (Chapter 6).

Abnormal Returns

2007

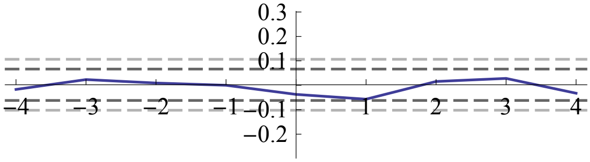

2008

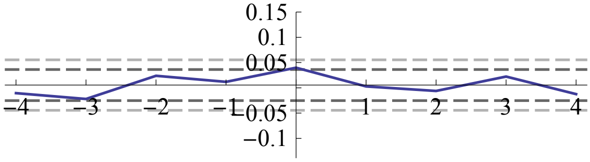

2009

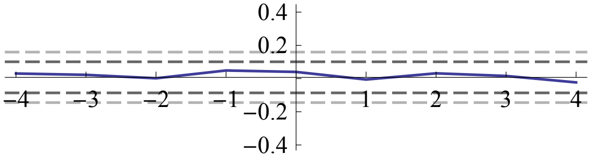

2010

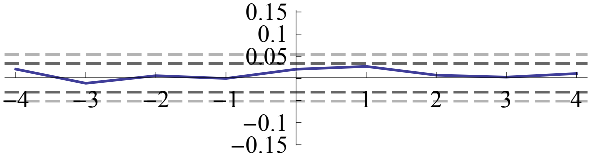

2011

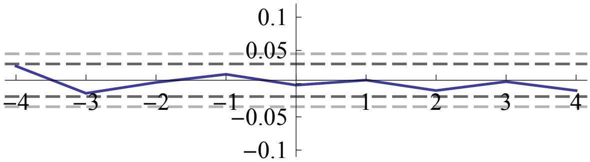

2012

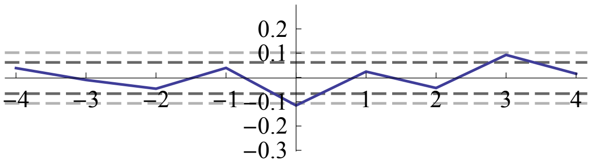

Figure 5.4.: Behavior of daily abnormal returns and log trading volumes around the emissions announcement events from 2007 to 2012. Abnormal returns are calculated based on a mean-adjusted return model as described in Section 5.3.1. Time 0 on the x-axis is the release date of the figures on previous year's emissions. The x-axis intersects with the y-axis at the value of the mean abnormal return (or log trading volume, respectively) estimated within a window from 40 to 11 days prior to the event date. The dashed horizontal lines represent bounds of significance to the 10% and 1% level for the standard two-tailed t-test according to Brown and Warner (1980, 1985), based on the variance estimated over the same window.

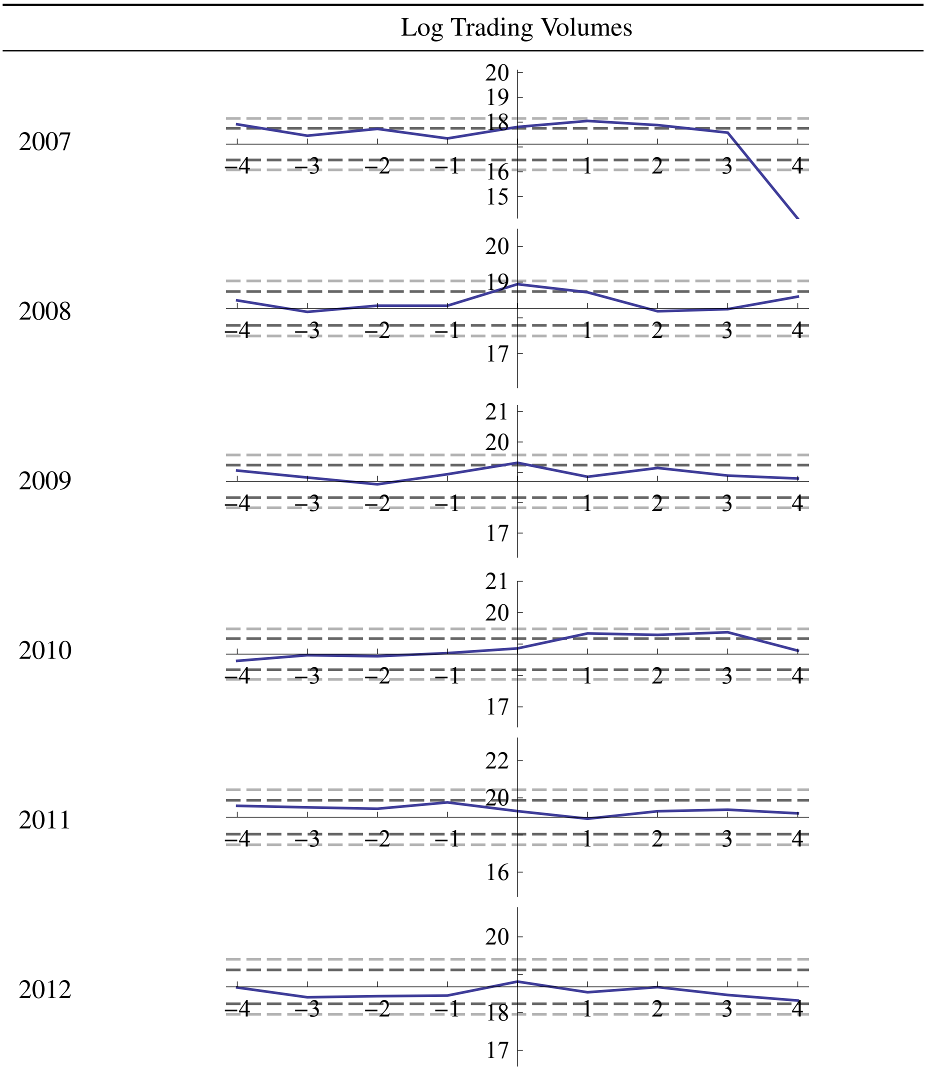

Figure 5.4 (continued).

Log Intraday Volatilities

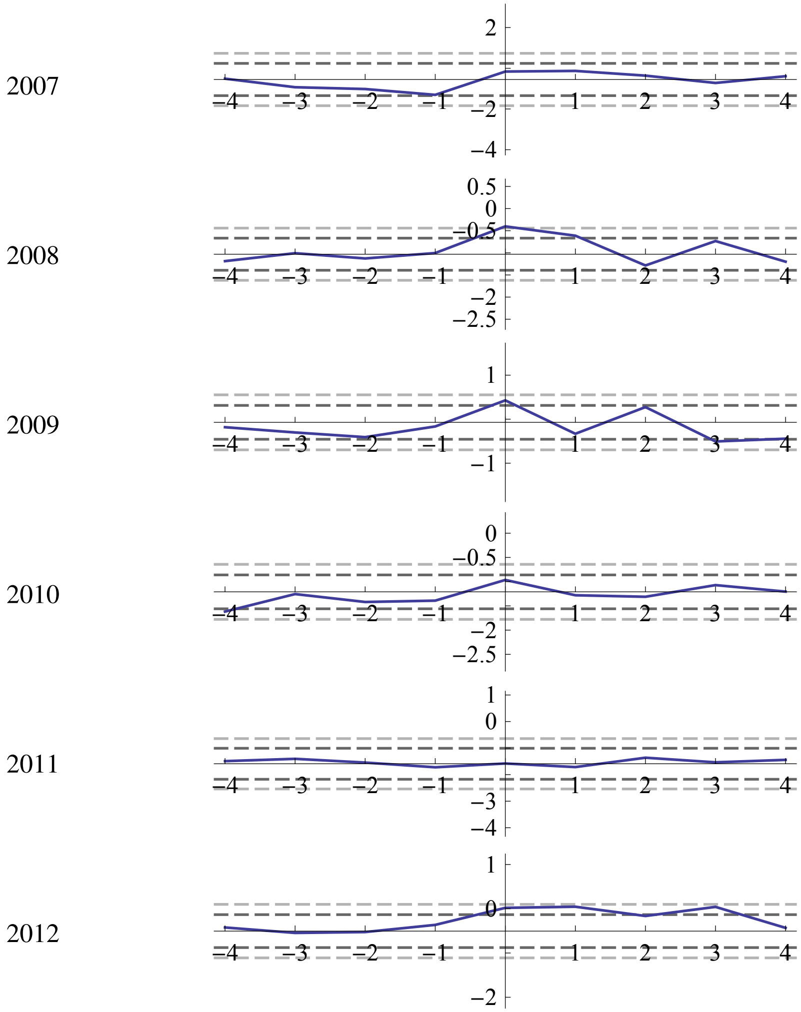

Figure 5.5.: Behavior of log realized intraday volatilities and log changes of implied volatilities around the emissions announcement events from 2007 to 2012. Realized intraday volatilities and option-implied volatilities are calculated in a model-free fashion as described in Section 5.2.2. Time 0 on the x-axis is the release date of the figures on previous year's emissions. The x-axis intersects with the y-axis at the value of the mean log intraday volatility (or log change of implied volatilities, respectively) estimated within a window from 40 to 11 days prior to the event date. The dashed horizontal lines represent bounds of significance to the 10% and 1% level for the standard two-tailed t-test according to Brown and Warner (1980, 1985), based on the variance estimated over the same window.

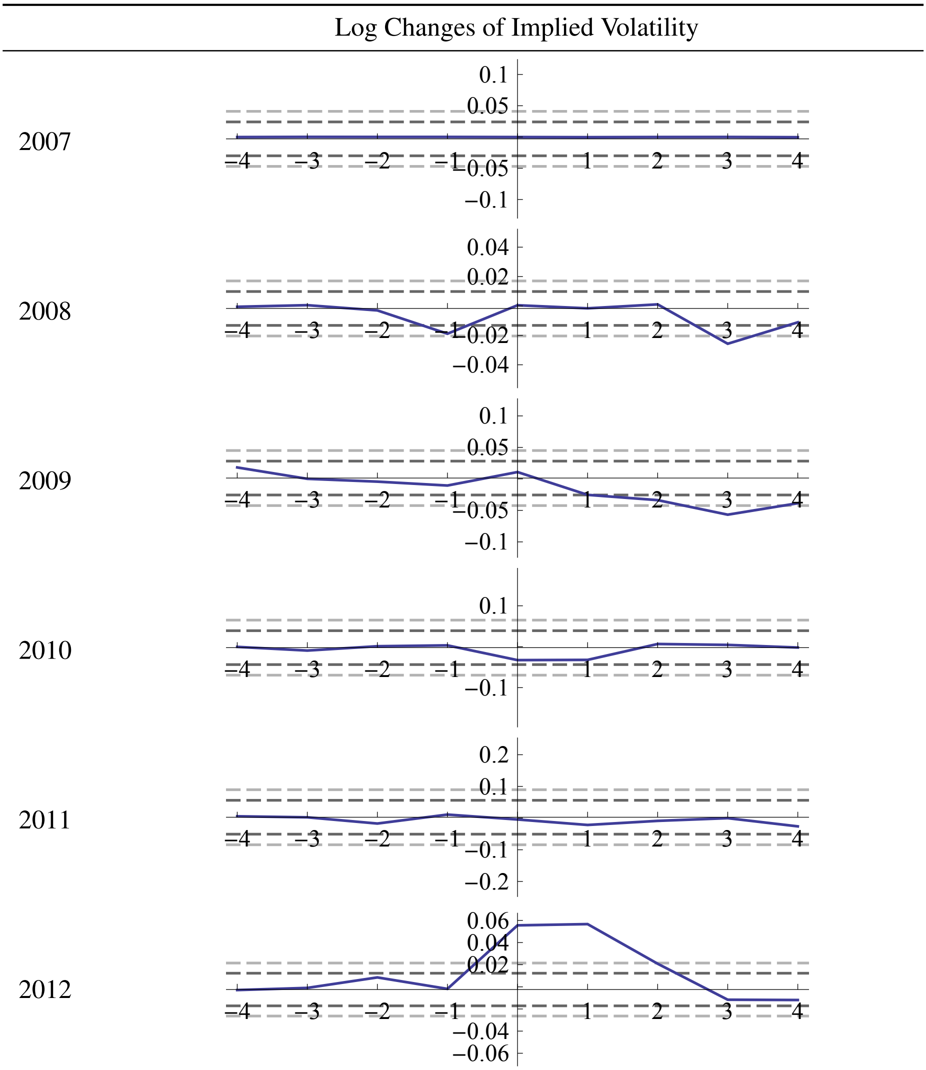

Figure 5.5 (continued).

6. Conclusion and Outlook

In this thesis we study the stochastic behavior of emission permit prices and its implications for related derivatives from a theoretical and empirical perspective.

Chapter 3 develops a stochastic equilibrium model for emissions markets that accounts for all important design features of today's state-of-the-art emission trading systems. We show that an emission permit can be characterized as a strip of binary options written on economy-wide emissions, which induces several properties of the permit price dynamics. Our model further predicts that the term structure of permit futures prices is in contango within the compliance periods of an emission trading system, while it exhibits backwardation across compliance periods. Emission permits thus combine characteristics of both consumption and investment assets. As a consequence, standard instantaneous convenience yield models prove to be inappropriate for pricing inter-period futures since they do not account for this hybrid character and lead to an inconsistent pricing of futures with different maturities. Calibrating our model to a setting in line with the EU ETS provides further insights into the specific features of permit prices and volatilities in the world's most significant emissions market and allows us to derive important implications for option pricing. Overall, this chapter reveals how the design of today's emission trading systems translates to characteristic properties of emission permit prices and related derivatives from a theoretical perspective. Our results suggest that models accounting for the specific design features of the system are better suited for modeling the price dynamics of emission permits and pricing derivatives in this market.

In Chapter 4 we derive reduced-form models for emission permit prices that account for these features and are still feasible for calibration to futures or option prices. Based on our equilibrium model, we obtain a framework that generically extends the Carmona and Hinz (2011) two-period market model. We evaluate a battery of different model variants within our framework regarding their fit to historical futures prices and their in- and out-of-sample option pricing performance. A model explicitly accounting for two compliance periods of an emission trading system and the resulting binary option characteristics shows the best fit to historical futures prices in the European emissions market and also overall the best option pricing performance. It particularly outperforms standard models — as represented by a Black (1976) model within our framework — and models incorporating only one compliance period of the cap-and-trade system. These results confirm our theoretical predictions and show that the particular design of an emission trading scheme and the induced permit price behavior is precisely reflected by empirical price data.

Chapter 5 investigates the short-term impact of news events on the emission permit market. We analyze the effects related to the annual announcement of realized emissions on the European market for carbon permits. Our findings show that the emissions announcement generally leads to significant absolute abnormal returns on the event day, which are accompanied by increased trading volumes and high intraday volatilities. To the contrary, trading is particularly calm before the event, as suggested by significantly lower trading volumes and volatilities. Moreover, evidence from the option market shows that the high event-day volatility is expected by the market and incorporated in option prices. Our findings reveal the short-term dynamics of emissions markets and substantiate that the European carbon market anticipates important news events and reacts efficiently to new information released.

Current developments of the global emissions market provide interesting starting points for future research on the stochastic behavior of emission permit prices. In this thesis we consider the design features of an emission trading system as well as details on the amount of allocated permits and other important parameters as publicly known and fixed from the beginning. Recent lessons from existing emission trading systems show, however, that changes of the economic environment may prompt a readjustment of the system to new circumstances. A salient example is the prevailing permit surplus in the EU ETS as a consequence of the financial crisis and the subsequent economic downturn, which has driven emission permit prices to levels below 10 Euros. According to the European Commission, the system was not over-allocated ex-ante and "it was expected that the ETS phase 2 cap would be ambitious. But the crisis unfolding as of 2008 has radically altered the picture [...]".[111] One could argue that there is no need to read-

[111] See the report of the European Commission (2012c).

just the system since a prevailing permit surplus just means that the reduction goals are reached with high probability, which is naturally reflected by low prices. On the other hand, the lacking demand for emission permits may lead to a collapse of the market for an indefinite time. Further, current media reports on the EU ETS show that persistent low prices on emissions markets are often interpreted as market failure by the public, undermining the general support for emission trading systems. Finally, it is questionable if the goal "to promote reductions of greenhouse gas emissions"[112] through the EU ETS can still be maintained when prices are too low to provide incentives for abatement or long-term investments. For these reasons the European Commission considers adjusting the overall allocation of permits for the ongoing Phase III, either by taking a number of permits out of the system or by strengthening the reduction goals. As an additional short-term measure, it is proposed to *set-aside* the allocation of 900 million permits from the first years (2013 to 2015) of Phase III and to bring them back into the system at the end of Phase III (2019 and 2020), to increase the scarcity of available emission permits temporarily. Another example for a readjustment of an emission trading system is the RGGI system, which has undergone an extensive review in 2012. As a result, the member states agreed on a reduction of the cap by 45%.[113] Current market reports reveal that this decision has led to a revitalization of the heavily over-allocated scheme. Although the history of emissions trading is still short, these examples suggest that adjustments of caps and other design features are the rule rather than the exception. It appears as a relevant topic for future research to introduce the regulator's flexibility of readjusting the system — be it an explicit design feature as proposed by Newell et al. (2005) or implicitly given by the regulator's authority — into our model framework and analyze the consequences for the agents' strategies and for equilibrium permit prices.

Another tendency in the global development of emissions markets is that political negotiations to establish price-based environmental policies with a large (geographical) scope are often delayed or fail. The first commitment period of the Kyoto Protocol ended in 2012, and a succeeding policy will not be adopted before 2015. The United States failed to establish a US-wide emissions trading system since the American Clean Energy and Security Act of 2009 was denied approval by the Senate. To the contrary, the supporting entities often implement emissions trading on a smaller, regional level first, and subsequently elaborate plans to connect these systems to other initiatives in

[112] See Article 1 of Directive 2003/87/EC.
[113] See the official announcement of the Regional Greenhouse Gas Initiative (2013).

order to increase where-flexibility for emission abatements. Examples are the cap-and-trade systems in the states of California and Quebec, which are both in operation since 2013 and will be linked by the beginning of 2014. On a larger scale, Australia and the European Commission have agreed on linking their systems bilaterally by 2018,[114] while EUAs can be imported into the Australian scheme already from 2015 on. Political insiders also report that California is in talks both with the European Union and Australia to link the CA ETS with their systems. In a similar way, it is not unlikely that China's domestic emissions trading systems launched in several cities and regions pave the way for a larger, maybe nation-wide, system. On the long run, political leaders of China and Australia already envision an "Asia-Pacific carbon market" with possible members California, Australia, New Zealand, Japan, Korea, and China.[115] These developments suggest that emission trading systems of the future are interlinked with each other in various ways, with significant consequences on the price mechanism in emissions markets. Related effects are considered by Carmona and Fehr (2011) and Barrieu and Fehr (2011) for the link of the EU ETS to the Clean Development Mechanism as part of the Kyoto Protocol. Grüll and Taschini (2012) study the price mechanism for different types of links in a static framework. It seems as a promising direction for future research to extend the equilibrium model for emissions markets developed in this thesis to a framework of multiple interlinked emission trading systems to study the price dynamics of the different emission permits and their correlation structure within a stochastic dynamic framework. The announced linkages of existing emission trading systems will provide empirical data to test resulting hypotheses.

[114] See IP/12/916 of the European Commission (2012a).

[115] The Australian Minister of Climate Change and Energy Efficiency, Greg Combet, outlined his vision of an "Asia-Pacific carbon market" in his speech at the Australia China Climate Change Forum, see Combet (2013).

A. Equilibrium Price Dynamics of Emission Permits: Proofs

A.1. Optimality Conditions for Individual Companies

We characterize the optimal trading and abatement strategies (θ^i, ξ^i) of the individual companies for given permit price processes $S_1(t), \ldots, S_n(t)$. The resulting optimality conditions relate the company's marginal abatement costs and the expected penalty payments to the given permit prices. We first decompose the individual optimization problem (3.5) into a recursive system of n simpler problems, one for each compliance period of the emission trading system, including the value function V_k^i of the period k problem into the terminal condition of the period $k-1$ problem, with $V_{n+1}^i = 0$:

$$
\begin{aligned}
&V_k^i(t, x_t^i, y_t^i, Q_{k,t}^i, \ldots, Q_{n,t}^i) \\
&= \min_{(\theta_k^i, \xi_k^i)} \mathbb{E}_{T_{k-1}} \left\{ \int_t^{T_k} e^{-r(s-T_{k-1})} C^i(\xi_s^i) ds + \sum_{j=k}^{n} \int_t^{T_k} e^{-r(s-T_{k-1})} S_j(s) \theta_{j,s}^i ds \right. \\
&\left. + e^{-r(T_k - T_{k-1})} (p_k(x_{T_k}^i - Q_{k,T_k}^i)^+ + V_{k+1}^i(T_k, x_{T_k}^i, y_{T_k}^i, Q_{k+1,T_k}^i, \ldots, Q_{n,T_k}^i)) \right\},
\end{aligned}
\tag{A.1}
$$

for $t \in [T_{k-1}, T_k]$ and $k = 1, \ldots, n$, where (θ_k^i, ξ_k^i) is the restriction of (θ^i, ξ^i) to the time interval $[T_{k-1}, T_k]$ and we introduce the additional state variables $Q_{k,t}^i = \sum_{j=1}^{k} \left(e_j^i + \int_0^{\min\{t, T_j\}} \theta_{j,s}^i ds \right)$ in generalization of $Q_k^i = Q_{k,T_k}^i$. According to the dynamic programming principle (see Bertsekas 1976), an optimal solution (θ^i, ξ^i) of the original problem is also a solution of the decomposed problem (A.1), and V_1^i is identical to the value function of the original problem for $t \in [0, T_1]$. The dynamics of the state variables follow from (3.4), (3.2), and the definition of $Q^i_{k,t}$ as

$$\begin{aligned} dx^i_t &= (y^i_t - \xi^i_t)dt + \sigma^i_\varepsilon dW^i_t, \\ dy^i_t &= \mu^i_y(t)dt + \sigma^i_y(t)dZ^i_t, \\ dQ^i_{l,t} &= \sum_{j=k}^{l} \theta^i_{l,t} dt, \quad l = k, \dots, n. \end{aligned} \tag{A.2}$$

We derive optimality conditions for the trading and abatement strategy (θ^i, ξ^i) by applying the stochastic maximum principle to the problems (A.1), proceeding recursively from $k = n$ to $k = 1$.[116] A strategy (θ^i_n, ξ^i_n) for period n that *min*imizes the costs according to (A.1) *max*imizes the Hamiltonian

$$\begin{aligned} H_n(t, x^i, y^i, \theta^i, \xi^i, \rho_n) = {} & \rho_{n,x^i}(t) \cdot (y^i_t - \xi^i_t) + \rho_{n,y^i}(t) \cdot \mu^i_y(t) \\ & + \rho_{n,Q^i_n}(t) \cdot \theta^i_{n,t} - e^{-r(t-T_{n-1})}(C^i(\xi^i_t) + S_n(t)\theta^i_{n,t}). \end{aligned} \tag{A.3}$$

at every point in time $t \in [T_{n-1}, T_n]$, where $(\rho_{n,x^i}, \rho_{n,y^i}, \rho_{n,Q^i_n})$ are the adjoint processes corresponding to the state variables (x^i, y^i, Q^i_n). Differentiating (A.3) with respect to the control variables and setting the derivatives to zero yields the optimality conditions

$$\begin{aligned} \frac{\partial H_n}{\partial \xi^i} &= -\rho_{n,x^i}(t) - e^{-r(t-T_{n-1})} \frac{\partial C^i}{\partial \xi^i}(\xi^i_t) = 0, \\ \frac{\partial H_n}{\partial \theta^i_n} &= \rho_{n,Q^i_n}(t) - e^{-r(t-T_{n-1})} S_n(t) = 0. \end{aligned} \tag{A.4}$$

It remains to derive the adjoint processes ρ_{n,x^i} and ρ_{n,Q^i_n}, which are defined by the stochastic differential equations

$$\begin{aligned} d\rho_{n,x^i}(t) &= \omega_{n,x^i}(t)dW^i_t + \zeta_{n,x^i}(t)dZ^i_t, \\ d\rho_{n,Q^i_n}(t) &= \omega_{n,Q^i_n}(t)dW^i_t + \zeta_{n,Q^i_n}(t)dZ^i_t, \end{aligned} \tag{A.5}$$

[116] See Yong and Zhou (1999), Chapter 3 for a comprehensive introduction of the stochastic maximum principle for optimal control problems. For our problem, we apply the stochastic maximum principle for the case of a non-smooth terminal condition, see Chighoub et al. (2009).

with stochastic processes $(\omega_{n,x^i}, \omega_{n,Q_n^i}, \zeta_{n,x^i}, \zeta_{n,Q_n^i})$ and terminal conditions

$$\begin{aligned}\rho_{n,x^i}(T_n) &= -e^{-r(T_n-T_{n-1})}1_{\{x^i_{T_n}>Q^i_{n,T_n}\}}p_n,\\ \rho_{n,Q_n^i}(T_n) &= e^{-r(T_n-T_{n-1})}1_{\{x^i_{T_n}>Q^i_{n,T_n}\}}p_n.\end{aligned} \tag{A.6}$$

We can directly identify the solution[117]

$$\begin{aligned}\rho_{n,x^i}(t) &= -e^{-r(T_n-T_{n-1})}\mathbb{P}_t\left\{x^i_{T_n} > Q^i_{n,T_n}\right\}p_n,\\ \rho_{n,Q_n^i}(t) &= e^{-r(T_n-T_{n-1})}\mathbb{P}_t\left\{x^i_{T_n} > Q^i_{n,T_n}\right\}p_n.\end{aligned} \tag{A.7}$$

The adjoint processes can be interpreted as the shadow price of the corresponding state variable. For example, ρ_{n,Q_n^i} is the value that can be attributed to having one marginal unit of period-n permits more. Here, this is the discounted penalty weighted by the probability of penalties to accrue, which makes perfect economic sense.
Inserting the adjoint processes into (A.4) we arrive at the condition

$$\frac{\partial C^i}{\partial \xi^i}(\xi^i_t) = e^{-r(T_n-t)}\mathbb{P}_t\left\{x^i_{T_n} > Q^i_{n,T_n}\right\}p_n = S_n(t), \tag{A.8}$$

which proves Proposition 1 for $t \in [T_{n-1}, T_n]$ and $k = n$.

Before proceeding to $k = n-1$, note that negative of the adjoint process for a state variable equals the first derivative of the value function with respect to the same variable (see Clarke and Vinter 1987), that is

$$-\rho_{n,x^i}(t) = \frac{\partial V_n^i}{\partial x^i}, \qquad -\rho_{n,y^i}(t) = \frac{\partial V_n^i}{\partial y^i}, \qquad -\rho_{n,Q_n^i}(t) = \frac{\partial V_n^i}{\partial Q_n^i} \tag{A.9}$$

for $t \in [T_{n-1}, T_n)$.
Now consider the optimal control problem (A.1) for $k = n-1$. In this case the Hamiltonian is given by

$$\begin{aligned}H_{n-1}(t, x^i, y^i, \theta^i, \xi^i, \rho_{n-1}) &= \rho_{n-1,x^i}(t)\cdot(y^i_t - \xi^i_t) + \rho_{n-1,y^i}(t)\cdot\mu^i_y(t)\\ &\quad + \rho_{n-1,Q^i_{n-1}}(t)\cdot\theta^i_{n-1,t} + \rho_{n-1,Q^i_n}(t)\cdot(\theta^i_{n-1,t}+\theta^i_{n,t})\\ &\quad - e^{-r(t-T_{n-2})}(C^i(\xi^i_t) + S_{n-1}(t)\theta^i_{n-1,t} + S_n(t)\theta^i_{n,t}),\end{aligned} \tag{A.10}$$

[117] For the existence of a regular solution we refer to Carmona et al. (2013).

and as before we obtain the optimum by differentiating with respect to the control variables and setting the derivatives to zero:

$$\begin{aligned}\frac{\partial H_{n-1}}{\partial \xi^i} &= -\rho_{n-1,x^i}(t) - e^{-r(t-T_{n-2})}\frac{\partial C^i}{\partial \xi^i}(\xi_t^i) = 0,\\ \frac{\partial H_{n-1}}{\partial \theta_{n-1}^i} &= \rho_{n-1,Q_{n-1}^i}(t) + \rho_{n-1,Q_n^i}(t) - e^{-r(t-T_{n-2})}S_{n-1}(t) = 0,\\ \frac{\partial H_{n-1}}{\partial \theta_n^i} &= \rho_{n-1,Q_n^i}(t) - e^{-r(t-T_{n-2})}S_n(t) = 0.\end{aligned} \tag{A.11}$$

It is left to insert the adjoint processes $(\rho_{n-1,x^i}, \rho_{n-1,Q_{n-1}^i}, \rho_{n-1,Q_n^i})$ solving the equations

$$\begin{aligned}d\rho_{n-1,x^i}(t) &= \omega_{n-1,x^i}(t)dW_t^i + \zeta_{n-1,x^i}(t)dZ_t^i,\\ d\rho_{n-1,Q_{n-1}^i}(t) &= \omega_{n-1,Q_{n-1}^i}(t)dW_t^i + \zeta_{n-1,Q_{n-1}^i}(t)dZ_t^i,\\ d\rho_{n-1,Q_n^i}(t) &= \omega_{n-1,Q_n^i}(t)dW_t^i + \zeta_{n-1,Q_n^i}(t)dZ_t^i,\end{aligned} \tag{A.12}$$

with terminal conditions

$$\begin{aligned}\rho_{n-1,x^i}(T_{n-1}) &= -e^{-r(T_{n-1}-T_{n-2})}\big(1_{\{x_{T_{n-1}}^i > Q_{n-1,T_{n-1}}^i\}}p_{n-1}\\ &\qquad + \frac{\partial V_n^i}{\partial x^i}(T_{n-1}, x_{T_{n-1}}^i, y_{T_{n-1}}^i, Q_{n,T_{n-1}}^i)\big),\\ \rho_{n-1,Q_{n-1}^i}(T_{n-1}) &= e^{-r(T_{n-1}-T_{n-2})}1_{\{x_{T_{n-1}}^i > Q_{n-1,T_{n-1}}^i\}}p_{n-1},\\ \rho_{n-1,Q_n^i}(T_{n-1}) &= -e^{-r(T_{n-1}-T_{n-2})}\frac{\partial V_n^i}{\partial Q_n^i}(T_{n-1}, x_{T_{n-1}}^i, y_{T_{n-1}}^i, Q_{n,T_{n-1}}^i),\end{aligned} \tag{A.13}$$

After inserting the derivatives of V_n^i according to (A.7) and (A.9), we identify the solution

$$\begin{aligned}\rho_{n-1,x^i}(t) &= -\sum_{j=n-1}^{n} e^{-r(T_j-T_{n-2})}\mathbb{P}_t\left\{x_{T_j}^i > Q_{j,T_j}^i\right\}p_j,\\ \rho_{n-1,Q_{n-1}^i}(t) &= e^{-r(T_{n-1}-T_{n-2})}\mathbb{P}_t\left\{x_{T_{n-1}}^i > Q_{n-1,T_{n-1}}^i\right\}p_{n-1},\\ \rho_{n-1,Q_n^i}(t) &= e^{-r(T_n-T_{n-2})}\mathbb{P}_t\left\{x_{T_n}^i > Q_{n,T_n}^i\right\}p_n.\end{aligned} \tag{A.14}$$

Using the adjoint processes in (A.11) finally yields the optimality conditions

$$\frac{\partial C^i}{\partial \xi^i}(\xi^i_t) = \sum_{j=n-1}^{n} e^{-r(T_j-t)}\mathbb{P}_t\left\{x^i_{T_j} > Q^i_{j,T_j}\right\}p_j = S_{n-1}(t), \qquad \text{(A.15)}$$
$$e^{-r(T_n-t)}\mathbb{P}_t\left\{x^i_{T_n} > Q^i_{n,T_n}\right\}p_n = S_n(t),$$

which proves Proposition 1 for $t \in [T_{n-2}, T_{n-1}]$ and $k = n-1$. Proceeding along the same lines for $k = n-2$ to $k = 1$ completes the proof of Proposition 1.

A.2. Individual Optimality of Global Optimal Solution

We construct equilibrium permit price processes $S_1, \ldots, S_n$ through equation (3.8) by letting the individual abatement strategies ξ^i driving the economy-wide realized emissions x_t be given by the solution of the joint cost problem of the whole economy I. Then we simplify the joint cost problem to the global problem (3.18) acting on aggregate volumes.[118]

The joint cost problem is to minimize the sum of the individual companies' costs according to (3.5) by an optimal trading and abatement strategy $(\Theta, \Xi) = (\theta^i, \xi^i)_{i\in I}$ subject to the market-clearing constraint. Since costs and revenues from individual trading cancel out on aggregate under market clearing, we obtain the problem

$$\min_{(\Theta,\Xi)} \mathbb{E}_0\left\{\sum_{i\in I}\left(\int_0^{T_n} e^{-rt}C^i(\xi^i_t)dt + \sum_{j=1}^{n} e^{-rT_j}p_j(x^i_{T_j} - Q^i_j)^+\right)\right\}. \qquad \text{(A.16)}$$

Since in (A.16) the trading strategy Θ is only relevant for the penalty payments (by entering Q^i_k), we directly observe that a market-clearing trading strategy Θ optimizes (A.16) if and only if $1_{\{x^i_{T_k} > Q^i_k\}} = 1_{\{x_{T_k} > q_k\}}$ for $k = 1, \ldots, n$.[119] On the other hand,

[118] Our approach partly builds on Seifert et al. (2008) and Carmona et al. (2009). In the appendix of Seifert et al. (2008) it is shown that the global problem acting on aggregate volumes is equivalent to the sum of all companies' individual solutions, under the crucial assumption that all companies' emissions are driven by the same Wiener process. By a more general approach, Carmona et al. (2009) prove that the solution of the global problem is optimal for the individual problems also without this assumption.

[119] That means, if the number of period-k permits in the whole economy is not sufficient to cover economy-wide emissions at T_k, companies distribute the available permits in such way that none of the companies

the abatement strategy Ξ enters both the penalties (through $x^i_{T_k}$) and the abatement costs. Applying the stochastic maximum principle along the lines of Appendix A.1 yields that an optimal abatement strategy Ξ fulfills

$$\frac{\partial C^i}{\partial \xi^i}(\xi^i_t) = \sum_{j=k}^{n} e^{-r(T_j - t)} \mathbb{P}_t \left\{ x_{T_j} > q_j \right\} p_j, \quad t \in [T_{k-1}, T_k], \tag{A.17}$$

for all companies $i \in I$.

Now assume that an optimal abatement strategy of (A.16) is given by (Θ^*, Ξ^*) and choose permit price processes S^*_k, $k = 1, \ldots, n$, by

$$S^*_k(t) = \sum_{j=k}^{n} e^{-r(T_j - t)} \mathbb{P}_t \left\{ x^*_{T_j} > q_j \right\} p_j, \quad t \in [0, T_k], \tag{A.18}$$

in line with (3.8), where the asterisks indicate that economy-wide realized emissions x^*_t follow the dynamics (3.9) with abatements $\xi_t = \sum_{i \in I} \xi^i_t$ chosen according to the optimal strategy Ξ^* of the global problem (A.16).

We show that given the permit price processes (A.18), the optimal strategy (Θ^*, Ξ^*) of the joint cost problem (A.16) is also optimal for the individual problems (3.5), implying that $S^*_1, \ldots, S^*_n$ are equilibrium permit prices. For that, expand the expected value in (3.5) by adding and subtracting the term $\sum_{j=1}^{n} \int_{T_{j-1}}^{T_j} e^{-rt} S^*_j(t) \xi^i_t dt$ and split it in two parts according to

$$\begin{aligned} &\mathbb{E}_0\left\{ \int_0^{T_n} e^{-rt} C^i(\xi^i_t) dt + \sum_{j=1}^{n} \int_0^{T_j} e^{-rt} S^*_j(t) \theta^i_{j,t} dt + \sum_{j=1}^{n} e^{-rT_j} p_j (x^i_{T_j} - Q^i_j)^+ \right\} \\ &\quad = \mathbb{E}_0\left\{ \int_0^{T_n} e^{-rt} C^i(\xi^i_t) dt - \sum_{j=1}^{n} \int_{T_{j-1}}^{T_j} e^{-rt} S^*_j(t) \xi^i_t dt \right\} \\ &\qquad + \mathbb{E}_0\left\{ \sum_{j=1}^{n} \left(\int_0^{T_j} e^{-rt} S^*_j(t) \theta^i_{j,t} dt + \int_{T_{j-1}}^{T_j} e^{-rt} S^*_j(t) \xi^i_t dt + e^{-rT_j} p_j (x^i_{T_j} - Q^i_j)^+ \right) \right\}. \end{aligned} \tag{A.19}$$

individually has left-over permits. On the other hand, in case of a permit surplus companies distribute the permits in such way that none of them has to pay penalties.

We rewrite the first expectation value as

$$\mathbb{E}_0\Big\{\sum_{j=1}^{n}\int_{T_{j-1}}^{T_j} e^{-rt}(C^i(\xi_t^i) - S_j^*(t)\xi_t^i)dt\Big\} \tag{A.20}$$

by subdividing the first integral. Obviously, this term is minimized by all abatement strategies ξ^i fulfilling

$$\frac{\partial C^i}{\partial \xi^i}(\xi_t^i) = S_k^*(t), \quad t \in [T_{k-1}, T_k]. \tag{A.21}$$

Since both an individually optimal strategy and an optimal strategy of the joint cost problem fulfill this condition (see (3.6) and (A.17)), the resulting value is the same for both strategies.

To transform the second expectation value in (A.19), note that for an individually optimal strategy we have

$$\begin{aligned}
&e^{-rT_k}p_k(x_{T_k}^i - Q_k^i)^+\\
=&e^{-rT_k}p_k 1_{\{x_{T_k}^i > Q_k^i\}}(x_{T_k}^i - Q_k^i)\\
=&e^{-rT_k}(S_k^*(T_k) - S_{k+1}^*(T_k))\Big(\int_0^{T_k}(y_t^i + n_t^i - \xi_t^i)dt - \sum_{j=1}^{k}(e_j^i + \int_0^{T_j}\theta_{j,t}^i dt)\Big)
\end{aligned} \tag{A.22}$$

due to (3.7) and we further insert the definitions of $x_{T_k}^i$ and Q_k^i. Using this in the second term of (A.19), reordering sums and integrals shows that the control variables cancel out for an individually optimal strategy and the resulting value is

$$\mathbb{E}_0\Big\{\sum_{j=1}^{n} e^{-rT_j}(S_j^*(T_j) - S_{j+1}^*(T_j))(\int_0^{T_j}(y_t^i + n_t^i)dt - q_j^i)\Big\}. \tag{A.23}$$

Since the optimal strategy of the global problem also fulfills (3.7), it results in the same value. Overall, (Θ^*, Ξ^*) solves the individual optimization problems (3.5), and $S_1^*, \dots, S_n^*$ are equilibrium permit price processes.

Finally, we show that the joint cost problem (A.16) corresponds to the simplified aggregate problem (3.18). We have seen that for a solution of (A.16) it holds

$$\sum_{i\in I}(x^i_{T_k} - Q^i_k)^+ = (x_{T_k} - q_k)^+. \tag{A.24}$$

Further, define the aggregate abatement cost function C as

$$C(\xi_t) = \sum_{i\in I} C^i(t, {c^i}^{-1}(c^j(\xi^j_t))), \tag{A.25}$$

where $j \in I$ is one arbitrarily chosen single company, $c^i = \frac{\partial C^i}{\partial \xi^i}$ is the first derivative of C^i, ${c^i}^{-1}$ is its inverse function, and ξ^j_t is implicitly defined through $\xi_t = \sum_{i\in I} {c^i}^{-1}(c^j(\xi^j_t))$. C is well-defined because, first, $c^i(\xi^i_t)$ is equal for all companies $i \in I$ for a solution of (A.16) according to (A.17), and second, c^i is strictly increasing and thus invertible due to the convexity of C^i. Together with the differentiability of C_i, it follows that C is convex and differentiable with respect to ξ_t and it is

$$\sum_{i\in I} C^i(\xi^i_t) = C(\xi_t). \tag{A.26}$$

Therefore, a solution of (A.16) corresponds to a solution of the problem (3.18) acting on aggregate volumes. Inverting the process, one can also recover a solution of (A.16) from a solution of (3.18), such that altogether it is equivalent to study the problem (A.16) or (3.18). The definition of C and (A.17) also directly yields (3.19).

A.3. Derivation of Characteristic PDEs

We decompose the stochastic optimal control problem (3.18) into n simpler problems as in Appendix A.1, that is we consider the system

$$\begin{aligned} V_k(t, x_t, y_t) = \min_{\xi_k} \mathbb{E}_{T_{k-1}} \Bigg\{ & \int_t^{T_k} e^{-r(s-T_{k-1})} C(\xi_s) ds \\ & + e^{-r(T_k - T_{k-1})}(p_k(x_{T_k} - q_k)^+ + V_{k+1}(T_k, x_{T_k}, y_{T_k}))\Bigg\}, \end{aligned} \tag{A.27}$$

for $t \in [T_{k-1}, T_k]$ and $k = 1, \ldots, n$, where V_k is the value function of the period k problem, $V_{n+1} = 0$, and ξ_k is the restriction of the strategy ξ to $[T_{k-1}, T_k]$.

Each of the single optimization problems in (A.27) can be settled by the standard dynamic programming approach along the lines of Sethi and Thompson (2006).[120] The principle of optimality yields

$$V_k(t, x_t, y_t) = \min_{\xi_t} \mathbb{E}_{T_{k-1}} \left\{ e^{-r(t-T_{k-1})} C(\xi_t) dt + V_k(t + dt, x_t + dx_t, y_t + dy_t) \right\}. \tag{A.28}$$

On the other hand, by applying Itô's Lemma to $V_k(t, x_t, y_t)$ with dynamics of x_t and y_t as given in (3.9) and (3.10) we get

$$\mathbb{E}_{T_{k-1}}\{dV_k\} = \left(\frac{\partial V_k}{\partial t} + \frac{\partial V_k}{\partial x}(y_t - \xi_t) + \frac{\partial V_k}{\partial y}\mu_y(t) + \frac{1}{2}\frac{\partial^2 V_k}{\partial x^2}\sigma_\varepsilon^2 + \frac{1}{2}\frac{\partial^2 V_k}{\partial y^2}\sigma_y^2(t) \right) dt. \tag{A.29}$$

Using this in (A.28) leads to the Hamilton-Jacobi-Bellman (HJB) equation

$$\begin{aligned} 0 = \min_{\xi_t} \Bigg\{ & e^{-r(t-T_{k-1})} C(\xi_t) + \frac{\partial V_k}{\partial t} + \frac{\partial V_k}{\partial x}(y_t - \xi_t) \\ & + \frac{\partial V_k}{\partial y}\mu_y(t) + \frac{1}{2}\frac{\partial^2 V_k}{\partial x^2}\sigma_\varepsilon^2 + \frac{1}{2}\frac{\partial^2 V_k}{\partial y^2}\sigma_y^2(t) \Bigg\}. \end{aligned} \tag{A.30}$$

By differentiating the right-hand side with respect to ξ_t and setting the derivative to zero we obtain the solution

$$\xi_t = c^{-1}(e^{r(t-T_{k-1})} \frac{\partial V_k}{\partial x}), \tag{A.31}$$

where c stands for $\frac{\partial C}{\partial \xi_t}$. By inserting (A.31) into (A.30), we finally arrive at the characteristic PDE

$$\begin{aligned} \frac{\partial V_k}{\partial t} &= -e^{-r(t-T_{k-1})} C(c^{-1}(e^{r(t-T_{k-1})} \frac{\partial V_k}{\partial x})) \\ &- \frac{\partial V_k}{\partial x}(y_t - c^{-1}(e^{r(t-T_{k-1})} \frac{\partial V_k}{\partial x})) - \frac{\partial V_k}{\partial y}\mu_y(t) - \frac{1}{2}\frac{\partial^2 V_k}{\partial x^2}\sigma_\varepsilon^2 - \frac{1}{2}\frac{\partial^2 V_k}{\partial y^2}\sigma_y^2(t), \end{aligned} \tag{A.32}$$

[120] See also Seifert et al. (2008).

and the boundary condition

$$V_k(T_k, x_{T_k}, y_{T_k}) = e^{-r(T_k - T_{k-1})}(p_k(x_{T_k} - q_k)^+ + V_{k+1}(T_k, x_{T_k}, y_{T_k})) \quad \text{(A.33)}$$

follows from (A.27).

B. Reduced-Form Models: Calculations

B.1. Dynamics of Risk-Neutral Shortage Probabilities

We derive the dynamics of the risk-neutral shortage probabilities A_k in general and show that all emissions processes (4.3) satisfying a narrow-sense linear SDE after transformation by a strictly increasing function lead to the same class of dynamics given by (4.6). For notational ease we omit the k indicating the compliance period in this section.

Let $D_t(x_{T|t};.)$ be the cumulative density function of x_T given $x_{T|t}$ at time t. By definition, it follows

$$A_t = 1 - D_t(x_{T|t}; q) =: G_t(x_{T|t}). \tag{B.1}$$

Applying Itô's Lemma directly yields

$$dA_t = g_t(x_{T|t})\sigma(t, x_{T|t})dW_t = g_t(G_t^{-1}(A_t))\sigma(t, G_t^{-1}(A_t))dW_t, \tag{B.2}$$

where g_t is the first derivative of G_t. Equation (B.2) describes the general dynamics of the risk-neutral shortage probabilities.

Aiming at simple dynamics of A_t, we assume that $x_{T|t}$ can be transformed by a strictly increasing function υ in such a way that $\upsilon(x_{T|t})$ follows a linear SDE in the narrow sense, i.e.,

$$d\upsilon(x_{T|t}) = (a_1(t)\upsilon(x_{T|t}) + a_2(t))dt + b(t)dW_t, \tag{B.3}$$

where $a_1 \colon (0,T) \to \mathbb{R}$ and $a_2 \colon (0,T) \to \mathbb{R}$ are continuous, bounded functions and $b \colon (0,T) \to \mathbb{R}^+$ is continuous and square-integrable. This especially covers a geometric Brownian motion as proposed by Carmona and Hinz (2011) or the case that $\ln x_{T|t}$ follows an Ornstein-Uhlenbeck process $d \ln x_{T|t} = \kappa(\mu(t) - \ln x_{T|t})dt + \sigma(t)dW_t$. Given $x_{T|t}$, we can write $\upsilon(x_T)$ explicitly as

$$\upsilon(x_T) = e^{\int_t^T a_1(s)ds} \upsilon(x_{T|t}) + \int_t^T e^{\int_s^T a_1(u)du} a_2(s)ds + \int_t^T e^{\int_s^T a_1(u)du} b(s)dW_s, \tag{B.4}$$

see Karatzas and Shreve (1991), pp. 360–361. Particularly, $\upsilon(x_T)$ is normally distributed with mean

$$\mu_{\upsilon,T|t}(x_{T|t}) = e^{\int_t^T a_1(s)ds} \upsilon(x_{T|t}) + \int_t^T e^{\int_s^T a_1(u)du} a_2(s)ds \tag{B.5}$$

and standard deviation

$$\sigma_{\upsilon,T|t} = \sqrt{\int_t^T e^{2\int_s^T a_1(u)du} b^2(s)ds}. \tag{B.6}$$

It follows that the cumulative density function is given by

$$D_{t,T}(x_{T|t}; y) = \Phi\left(\frac{\upsilon(y) - \mu_{\upsilon,T|t}(x_{T|t})}{\sigma_{\upsilon,T|t}}\right), \tag{B.7}$$

and we obtain

$$g_{t,T}(x_{T|t}) = \Phi'\left(\frac{\upsilon(q) - \mu_{\upsilon,T|t}(x_{T|t})}{\sigma_{\upsilon,T|t}}\right) \frac{\mu'_{\upsilon,T|t}(x_{T|t})}{\sigma_{\upsilon,T|t}}. \tag{B.8}$$

Inserting into (B.2) yields

$$\begin{aligned} dA_t &= \Phi'\left(\Phi^{-1}(A_t)\right) \frac{\mu'_{\upsilon,T|t}(x_{T|t})\sigma(t, x_{T|t})}{\sigma_{\upsilon,T|t}} dW_t \\ &= \Phi'\left(\Phi^{-1}(A_t)\right) \frac{e^{\int_t^T a_1(s)ds} \upsilon'(x_{T|t})\sigma(t, x_{T|t})}{\sqrt{\int_t^T e^{2\int_s^T a_1(u)du} b^2(s)ds}} dW_t \end{aligned} \tag{B.9}$$

for the risk-neutral shortage probability. Now observe that the dynamics of $\upsilon(x_{T|t})$ is also given by

$$d\upsilon(x_{T|t}) = (\upsilon'(x_{T|t})\mu(t, x_{T|t}) + \frac{1}{2}\upsilon''(x_{T|t})\sigma^2(t, x_{T|t}))dt + \upsilon'(x_{T|t})\sigma(t, x_{T|t})dW_t, \tag{B.10}$$

applying Itô's Lemma to (4.3). Comparing this to (B.3) yields

$$\upsilon'(x_{T|t})\sigma(t, x_{T|t}) = b(t), \tag{B.11}$$

and we can write (B.9) as

$$\begin{aligned} dA_t &= \Phi'\left(\Phi^{-1}(A_t)\right) \frac{e^{\int_t^T a_1(s)ds} b(t)}{\sqrt{\int_t^T e^{2\int_s^T a_1(u)du} b^2(s)ds}} dW_t \\ &= \Phi'\left(\Phi^{-1}(A_t)\right) \frac{c(t)}{\sqrt{\int_t^T c^2(s)ds}} dW_t \end{aligned} \tag{B.12}$$

with $c(t) = e^{\int_t^T a_1(s)ds} b(t)$. Carmona and Hinz (2011) show that for every continuous function $z\colon (0,T) \to \mathbb{R}^+$ satisfying

$$\lim_{t \to T} \int_0^t z(s)ds = \infty, \tag{B.13}$$

there exists a square-integrable continuous function $c\colon (0,T) \to \mathbb{R}^+$ fulfilling $\frac{c^2(t)}{\int_t^T c^2(s)ds} = z(t)$. Therefore we can construct every continuous function z satisfying (B.13) by the choice $a_1(t) = 0$ and $b(t) = c(t)$. The other way round, $c(t) = e^{\int_t^T a_1(s)ds} b(t)$ is a square-integrable continuous and positive function by the properties of a_1 and b, and it follows that $z(t) = \frac{c^2(t)}{\int_t^T c^2(s)ds}$ is positive and continuous and satisfies (B.13), see Carmona and Hinz (2011).

Altogether, for all dynamics of $x_{T|t}$ for which a strictly increasing function υ exists such that $\upsilon(x_{T|t})$ follows a narrow-sense linear SDE (B.3), the class of possible dynamics for A_t is completely characterized by (4.6), with a continuous functions $z\colon (0,T) \to \mathbb{R}^+$ satisfying (B.13). Particularly, all possible dynamics for A_t can be obtained by choosing an arithmetic Brownian motion (4.4) for the expected cumulative emissions process $x_{T|t}$.

B.2. Evaluation of Option Pricing Formulae

To calculate theoretical option prices within our reduced-form model framework, equation (4.14) requires the numerical evaluation of an $m+1$-dimensional integral. While this is straightforward in the one-dimensional case ($m=0$), the following transformations may help to improve computational efficiency for models with more price components. We demonstrate these transformations for the case of $m=1$ and an additional component R_t as well as for $m=2$ and $R_t=0$.

In both cases, we decompose the bivariate normal distribution as proposed by Carmona and Hinz (2011) by defining

$$\mu^{2,c}(x_1) = \mu^2 + \frac{\nu^{1,2}}{\nu^{1,1}}(x_1 - \mu^1) \quad \text{and} \quad \nu^{2,2,c} = \nu^{2,2} - \frac{(\nu^{1,2})^2}{\nu^{1,1}}, \tag{B.14}$$

and we can write the integral in (4.14) as

$$\int_{\mathbb{R}}\int_{\mathbb{R}} (e^{-r(T_1-\bar{t})}\Phi(x_1)p_1 + e^{-r(T_1-\bar{t})}e^{x_2} - K)^+ \cdot \varphi(\mu^{2,c}(x_1), \nu^{2,2,c}; x_2)dx_2\varphi(\mu^1, \nu^{1,1}; x_1)dx_1 \tag{B.15}$$

for the case $m=1$ with an additional component R_t or as

$$\int_{\mathbb{R}}\int_{\mathbb{R}} (e^{-r(T_1-\bar{t})}\Phi(x_1)p_1 + e^{-r(T_2-\bar{t})}\Phi(x_2)p_2 - K)^+ \cdot \varphi(\mu^{2,c}(x_1), \nu^{2,2,c}; x_2)dx_2\varphi(\mu^1, \nu^{1,1}; x_1)dx_1 \tag{B.16}$$

for $m=2$ and $R_t=0$.

Defining $K^*(x_1) = K - e^{-r(T_1-\bar{t})}\Phi(x_1)p_1$, we note that the inner integral in (B.15) can completely be settled analytically according to

$$\begin{aligned}
&\int_{\mathbb{R}} (e^{-r(T_1-\bar{t})}e^{x_2} - K^*(x_1))^+ \cdot \varphi(\mu^{2,c}(x_1), \nu^{2,2,c}; x_2)dx_2 \\
&= \begin{cases} e^{-r(T_1-\bar{t})}\int_{\mathbb{R}} e^{x_2} \cdot \varphi(\mu^{2,c}(x_1), \nu^{2,2,c}; x_2)dx_2 - K^*(x_1), & \text{if } K^*(x_1) \le 0; \\ \int_{\mathbb{R}} (e^{-r(T_1-\bar{t})}e^{x_2} - K^*(x_1))^+ \cdot \varphi(\mu^{2,c}(x_1), \nu^{2,2,c}; x_2)dx_2, & \text{otherwise.} \end{cases}
\end{aligned}$$

$$= \begin{cases} e^{-r(T_1-\bar{t})} \cdot e^{\mu^{2,c}(x_1)+\frac{\nu^{2,2,c}}{2}} - K^*(x_1), & \text{if } K^*(x_1) \leq 0; \\ e^{-r(T_1-\bar{t})} \cdot e^{\mu^{2,c}(x_1)+\frac{\nu^{2,2,c}}{2}} \Phi(d_1) - K^*(x_1)\Phi(d_2), & \text{otherwise.} \end{cases} \tag{B.17}$$

with

$$d_1 = \frac{\mu^{2,c}(x_1) - \ln(\frac{K^*(x_1)}{e^{-r(T_1-\bar{t})}})}{\sqrt{\nu^{2,2,c}}} + \sqrt{\nu^{2,2,c}} \quad \text{and} \quad d_2 = d_1 - \sqrt{\nu^{2,2,c}}. \tag{B.18}$$

For (B.16), Carmona and Hinz (2011) show that numerical integration of the inner integral is only necessary if $0 < K^*(x_1) < e^{-r(T_2-\bar{t})}p_2$ since outside this interval we have

$$\begin{aligned} &\int_{\mathbb{R}} (e^{-r(T_2-\bar{t})}\Phi(x_2)p_2 - K^*(x_1))^+ \cdot \varphi(\mu^{2,c}(x_1), \nu^{2,2,c}; x_2)dx_2 \\ &= \begin{cases} 0 & \text{if } K^*(x_1) \geq e^{-r(T_2-\bar{t})}p_2; \\ e^{-r(T_2-\bar{t})}p_2\Phi\left(\frac{\mu^{2,c}(x_1)}{\sqrt{1+\nu^{2,2,c}}}\right) - K^*(x_1) & \text{if } K^*(x_1) \leq 0. \end{cases} \end{aligned} \tag{B.19}$$

Having a solution of the inner integral, it is straightforward again to evaluate the outer integral of (B.15) and (B.16).

Bibliography

111th United States Congress (2009). American Clean Energy and Security Act of 2009. US House of Representatives.

Ajinkya, B. B. and Jain, P. C. (1989). The behavior of daily stock market trading volume. *Journal of Accounting and Economics*, 11:331–359.

Andersen, T. G., Bollerslev, T., Diebold, F. X., and Ebens, H. (2001). The distribution of realized stock return volatility. *Journal of Financial Economics*, 61(1):43–76.

Ates, A. and Wang, G. H. K. (2007). Price dynamics in energy spot and futures markets: The role of inventory and weather. *Working Paper*.

Australian Government (2011). Clean Energy Act 2011.

Australian Government (2012). Guide to carbon price liability under the Clean Energy Act 2011.

Bakshi, G., Cao, C., and Chen, Z. (1997). Empirical performance of altemative option pricing models. *Journal of Finance*, 52(5):2003–2049.

Bamber, L. S. (1986). The information content of annual earnings releases: A trading volume approach. *Journal of Accounting Research*, 24(1):40–56.

Barone-Adesi, G., Engle, R. F., and Mancini, L. (2008). A GARCH option pricing model with filtered historical simulation. *Review of Financial Studies*, 21(3):1223–1258.

Barrieu, P. and Fehr, M. (2011). Integrated EUA and CER price modelling and application for spread option pricing. *Working Paper*.

Benz, E. A. and Trück, S. (2009). Modeling the price dynamics of CO2 emission allowances. *Energy Economics*, 31:4–15.

Bertsekas, D. P. (1976). *Dynamic Programming and Stochastic Control*. Academic Press, New York/San Francisco/London.

Betz, R., Rogge, K., and Schleich, J. (2005). *Flexible Instrument im Klimaschutz*. Umweltministerium Baden-Württemberg.

Binder, J. J. (1998). The event study methodology since 1969. *Review of Quantitative Finance and Accounting*, 11:111–137.

Bjursell, J., Gentle, J. E., and Wang, G. H. K. (2010). Inventory announcements, jump dynamics and volatility in U.S. energy futures markets. *Working Paper*.

Black, F. (1976). The pricing of commodity contracts. *Journal of Financial Economics*, 3:167–179.

Blume, L., Easley, D., and O'Hara, M. (1994). Market statistics and technical analysis: The role of volume. *Journal of Finance*, 49(1):153–181.

Boom, J.-T. and Dijkstra, B. R. (2009). Permit trading and credit trading: A comparison of cap-based and rate-based emissions trading under perfect and imperfect competition. *Environmental and Resource Economics*, 44(1):107–136.

Brennan, M. J. (1958). The supply of storage. *American Economic Review*, 48(1):50–72.

Brennan, M. J. and Schwartz, E. S. (1985). Evaluating natural resource investments. *Journal of Business*, 58(2):135–157.

Britten-Jones, M. and Neuberger, A. (2000). Option prices, implied price processes, and stochastic volatility. *Journal of Finance*, 55:839–866.

Broadie, M., Chernov, M., and Johannes, M. (2007). Model specification and risk premia: Evidence from futures options. *Journal of Finance*, 62(3):1453–1490.

Brown, S. J. and Warner, J. B. (1980). Measuring security price performance. *Journal of Financial Economics*, 8:205–258.

Brown, S. J. and Warner, J. B. (1985). Using daily returns: The case of event studies. *Journal of Financial Economics*, 14:3–31.

Burtraw, D., Evans, D., Krupnick, A., Palmer, K., and Toth, R. (2005). Economics of pollution trading for SO2 and NOx. *Annual Review of Environment and Resources*, 30:253–289.

California Environmental Protection Agency (2010). Proposed regulation to implement the California cap-and-trade program, part I, volume I.

California Environmental Protection Agency (2013). Amendments to California's cap-and-trade program.

Carlson, C., Burtraw, D., Cropper, M., and Palmer, K. L. (2000). Sulfur dioxide control by electric utilities: What are the gains from trade? *Journal of Political Economy*, 108(6):1292–1326.

Carmona, R., Delarue, F., Espinosa, G.-E., and Touzi, N. (2013). Singular forward-backward stochastic differential equations and emissions derivatives. *Annals of Applied Probability*, 23(3):1086–1128.

Carmona, R. and Fehr, M. (2011). The Clean Development Mechanism and joint price formation for allowances and CERs. In *Seminar on Stochastic Analysis, Random Fields and Applications VI*, volume 63 of *Progress in Probability*.

Carmona, R., Fehr, M., and Hinz, J. (2009). Optimal stochastic control and carbon price formation. *SIAM Journal on Control and Optimization*, 48(4):2168–2190.

Carmona, R., Fehr, M., Hinz, J., and Porchet, A. (2010). Market design for emission trading schemes. *SIAM Review*, 52(3):403–452.

Carmona, R. and Hinz, J. (2011). Risk-neutral models for emission allowance prices and option valuation. *Management Science*, 57(8):1453–1468.

Carr, P. and Madan, D. (1998). Towards a theory of volatility trading. In Jarrow, R., editor, *Risk Book on Volatility*. Risk, New York.

Carr, P. and Wu, L. (2009). Variance risk premiums. *Review of Financial Studies*, 22(3):1311–1341.

Carr, P. and Wu, L. (2010). Stock options and credit default swaps: A joint framework for valuation and estimation. *Journal of Financial Econometrics*, 8(4):409–449.

Casassus, J. and Collin-Dufresne, P. (2005). Stochastic convenience yield implied from commodity futures and interest rates. *Journal of Finance*, 60(5):2283–2331.

Cetin, U. and Verschuere, M. (2009). Pricing and hedging in carbon emissions markets. *International Journal of Theoretical and Applied Finance*, 12(7):949–967.

Chesney, M. and Taschini, L. (2012). The endogenous price dynamics of emission allowances and an application to CO2 option pricing. *Applied Mathematical Finance*, 19(5):447–475.

Chevallier, J. (2009). Modelling the convenience yield in carbon prices using daily and realized measures. *International Review of Applied Financial Issues and Economics*, 1(1):56–73.

Chevallier, J., Ielpo, F., and Mercier, L. (2009). Risk aversion and institutional information disclosure on the European carbon market: A case-study of the 2006 compliance event. *Energy Policy*, 37(1):15–28.

Chighoub, F., Djehiche, B., and Mezerdi, B. (2009). The stochastic maximum principle in optimal control of degenerate diffusions with non-smooth coefficients. *Random Operators and Stochastic Equations*, 17(1):37–54.

Christensen, B. J. and Prabhala, N. R. (1998). The relation between implied and realized volatility. *Journal of Financial Economics*, 50(2):125–150.

Christoffersen, P., Dorion, C., Jacobs, K., and Karoui, L. (2012). Nonlinear Kalman filtering in affine term structure models. *Working Paper*.

Christoffersen, P. and Jacobs, K. (2004). The importance of the loss function in option valuation. *Journal of Financial Economics*, 72(2):291–318.

Clarke, F. H. and Vinter, R. B. (1987). The relationship between the maximum principle and dynamic programming. *SIAM Journal on Control and Optimization*, 25(5):1291–1311.

Cline, W. R. (2011). *Carbon Abatement Costs and Climate Change Finance*. Peterson Institute for International Economics, Washington DC.

Coase, R. H. (1960). The problem of social cost. *Journal of Law and Economics, 3*, pages 1–44.

Combet, G. (2013). China and australia: Working together to deliver a low carbon future. Keynote Address, Australia China Climate Change Forum.

Conrad, C., Rittler, D., and Rotfuß, W. (2012). Modeling and explaining the dynamics of European Union allowance prices at high-frequency. *Energy Economics*, 34(1):316–326.

Cramton, P. and Kerr, S. (2002). Tradeable carbon permit auctions: How and why to auction not grandfather. *Energy Policy*, 30(4):333–345.

Crocker, T. (1966). *The Structuring of Atmospheric Pollution Control Systems*, volume 1 of *The Economics of Air Pollution*. Harold Wolozin, New York.

Cronshaw, M. B. and Kruse, J. (1996). Regulated firms in pollution permit markets with banking. *Journal of Regulatory Economics*, 9(2):179–189.

Dales, J. H. (1968). Pollution, property & prices. *University of Toronto Press, Toronto*.

Daskalakis, G., Ibikunle, G., and Diaz-Rainey, I. (2011). *The CO2 Trading Market in Europe: A Financial Perspective*, chapter 4, pages 51–67. Springer, Dordrecht/Heidelberg/London/New York.

Daskalakis, G., Psychoyios, D., and Markellos, R. N. (2009). Modeling CO2 emission allowance prices and derivatives: Evidence from the European trading scheme. *Journal of Banking and Finance*, 33(7):1230–1241.

Demeterfi, K., Derman, E., Kamal, M., and Zou, J. (1999). A guide to volatility and variance swaps. *Journal of Derivatives*, 6:9–32.

Dumas, B., Fleming, J., and Whaley, R. E. (1998). Implied volatility functions: Empirical tests. *Journal of Finance*, 53(6):2059–2106.

Durbin, J. and Koopman, S. J. (2001). *Time series analysis by state space methods*. Oxford statistical science series.

Ederington, L. and Guan, W. (2013). The cross-sectional relation between conditional heteroskedasticity, the implied volatility smile, and the variance risk premium. *Journal of Banking and Finance*, 37(9):3388–3400.

Ederington, L. H. and Lee, J. H. (1993). How markets process information: News releases and volatility. *Journal of Finance*, 48(4):1161–1191.

Ederington, L. H. and Lee, J. H. (1996). The creation and resolution of market uncertainty: The impact of information releases on implied volatility. *Journal of Financial and Quantitative Analysis*, 31(4):513–539.

Ellerman, A. D. and Buchner, B. K. (2008). Over-allocation or abatement? a preliminary analysis of the EU ETS based on the 2005-06 emissions data. *Environmental and Resource Economics*, 41(2):267–287.

European Commission (2007). Emissions trading: strong compliance in 2006, emissions decoupled from economic growth. IP/07/776.

European Commission (2008a). Emissions trading: 2007 verified emissions from EU ETS businesses. IP/08/787.

European Commission (2008b). EU action against climate change.

European Commission (2008c). Questions and answers on the revised EU emissions trading system. MEMO/08/796.

European Commission (2009). Emissions trading: EU ETS emissions fall 3 % in 2008. IP/09/794.

European Commission (2010a). Commission Decision of 22 october 2010 adjusting the Union-wide quantity of allowances to be issued under the Union Scheme for 2013 and repealing Decision 2010/384/EU. *Official Journal of the European Union*, L 279:34–35.

European Commission (2010b). Emissions trading: EU ETS emissions fall more than 11 % in 2009. IP/10/576.

European Commission (2010c). Emissions trading: Questions and answers on the EU ETS auctioning regulation. MEMO/10/338.

European Commission (2011a). Commission Regulation (EU) no 1193/2011 of 18 november 2011 establishing a Union registry for the trading period commencing on 1 january 2013, and subsequent trading periods, of the Union emissions trading scheme. *Official Journal of the European Union*, L 315:1–54.

European Commission (2011b). Emissions trading: EU ETS emissions increased in 2010 but remain well below pre-crisis level. IP/11/581.

European Commission (2012a). Australia and European Commission agree on pathway towards fully linking emissions trading systems. IP/12/916.

European Commission (2012b). Emissions trading: annual compliance round-up shows declining emissions in 2011. IP/12/477.

European Commission (2012c). The state of the European carbon market in 2012. Report From The Commission To The European Parliament And The Council.

European Parliament and Council (2003). Directive 2003/87/EC of the European Parliament and of the Council of 13 october 2003. *Official Journal of the European Union*, L 275:32–46.

European Parliament and Council (2004). Directive 2004/101/EC of the European Parliament and of the Council of 27 october 2004. *Official Journal of the European Union*, L 338:18–30.

European Parliament and Council (2009). Directive 2009/29/EC of the European Parliament and of the Council of 23 april 2009 amending Directive 2003/87/EC so as to improve and extend the greenhouse gas emission allowance trading scheme of the Community. *Official Journal of the European Union*, L 140:63–87.

Fankhauser, S. and Hepburn, C. (2010a). Designing carbon markets. part I: Carbon markets in time. *Energy Policy*, 38(8):4363–4370.

Fankhauser, S. and Hepburn, C. (2010b). Designing carbon markets, part II: Carbon markets in space. *Energy Policy*, 38(8):4381–4387.

Freestone, D. and Streck, C., editors (2009). *Legal Aspects of Carbon Trading*. Oxford University Press, New York.

French, K. R., Leftwich, R. H., and Uhrig, W. (1989). The effect of scheduled announcements on futures markets. *Working paper, Center for Research in Securities Prices, University of Chicago*.

Frey, R. (2010). Pricing CO2 future options – an empirical study. *Working Paper*.

Geman, H. (2005). *Commodities and Commodity Derivatives*. John Wiley and Sons, Chichester.

Geske, R. (1979). The valuation of compound options. *Journal of Financial Economics*, 7(1):63–81.

Goulder, L. H., Parry, I. W. H., and Burtraw, D. (1997). Revenue-raising versus other approaches to environmental protection: The critical significance of preexisting tax distortions. *RAND Journal of Economics*, 28(4):708–731.

Gregoire, P. and Boucher, M. (2008). Maturity effect and storage announcements: the case of natural gas. *International Journal of Business Forecasting and Marketing Intelligence*, 1(1):21–29.

Grubb, M. (2012). Strengthening the EU ETS. Climate Strategies.

Grüll, G. and Kiesel, R. (2012). Quantifying the CO2 permit price sensitivity. *Zeitschrift für Energiewirtschaft*, 36(2):101–111.

Grüll, G. and Taschini, L. (2009). A comparison of reduced-form permit price models and their empirical performances. *Working Paper*.

Grüll, G. and Taschini, L. (2011). Cap-and-trade properties under different hybrid scheme designs. *Journal of Environmental Economics and Management*, 61(1):107–118.

Grüll, G. and Taschini, L. (2012). Linking emission trading schemes: A short note. *Economics of Energy & Environmental Policy*, 1(3).

Harris, M. and Raviv, A. (1993). Differences of opinion make a horse race. *Review of Financial Studies*, 6(3):473–506.

Harstad, B. and Eskeland, G. S. (2010). Trading for the future: Signaling in permit markets. *Journal of Public Economics*, 94(9–10):749–760.

Harvey, A. C. (1989). *Forecasting, structural time series models and the Kalman filter*. Cambridge University Press.

Hepburn, C., Grubb, M., Neuhoff, K., Matthes, F., and Tse, M. (2006). Auctioning of EU ETS phase II allowances: how and why? *Climate Policy*, 6(1):137–160.

Hitzemann, S. and Uhrig-Homburg, M. (2013a). Empirical performance of reduced-form models for emission permit prices. *Working Paper*.

Hitzemann, S. and Uhrig-Homburg, M. (2013b). Equilibrium price dynamics of emission permits. *Working Paper*.

Hitzemann, S., Uhrig-Homburg, M., and Ehrhart, K.-M. (2013). Emission permits and the announcement of realized emissions: Price impact, trading volume, and volatilities. *Working Paper*.

Holthausen, R. W. and Verrecchia, R. E. (1990). The effect of informedness and consensus on price and volume behavior. *The Accounting Review*, 65(1):191–208.

Hood, C. (2010). Reviewing existing and proposed emissions trading systems. Information paper, International Energy Agency.

International Emissions Trading Association (2012). Greenhouse gas market 2012. new markets, new mechanisms, new opportunities.

Jarrow, R. A. (2010). Convenience yields. *Review of Derivatives Research*, 13(1):25–43.

Jones, C. M., Lamont, O., and Lumsdaine, R. L. (1998). Macroeconomic news and bond market volatility. *Journal of Financial Economics*, 47(3):315–337.

Kalman, R. E. (1960). A new approach to linear filtering and prediction problems. *Transactions of the ASME–Journal of Basic Engineering*, 82(Series D):35–45.

Karatzas, I. and Shreve, S. E. (1991). *Brownian Motion and Stochastic Calculus*. Springer.

Karpoff, J. M. (1987). The relation between price changes and trading volume: A survey. *Journal of Financial and Quantitative Analysis*, 22(1):109–126.

Kijima, M., Maeda, A., and Nishide, K. (2010). Equilibrium pricing of contingent claims in tradable permit markets. *Journal of Futures Markets*, 30(6):559–589.

Klepper, G. and Peterson, S. (2006). Marginal abatement cost curves in general equilibrium: The influence of world energy prices. *Resource and Energy Economics*, 28(1):1–23.

Kossoy, A. and Guigon, P. (2012). State and trends of the carbon market. The World Bank.

Laing, T., Sato, M., Grubb, M., and Comberti, C. (2013). Assessing the effectiveness of the EU Emissions Trading System. Centre for Climate Change Economics and Policy/Grantham Research Institute on Climate Change and the Environment.

Le, D. T. (2008). Volatility in the crude oil and natural gas markets: GARCH, asymmetry, seasonality and announcement effects. *Working Paper*.

Linn, S. C. and Zhu, Z. (2004). Natural gas prices and the gas storage report: Public news and volatility in energy futures markets. *Journal of Futures Markets*, 24(3):283–313.

Litzenberger, R. H. and Rabinowitz, N. (1995). Backwardation in oil futures markets: Theory and empirical evidence. *Journal of Finance*, 50(5):1517–1545.

MacKinlay, A. C. (1997). Event studies in economics and finance. *Journal of Economic Literature*, 35(1):13–39.

Mai, H. M. and Tchemeni, E. (1996). Etude d'événement par les volumes: Méthodologies et comparaison. *Working Paper*.

Mansanet-Bataller, M. and Pardo, A. (2009). Impacts of regulatory announcements on CO2 prices. *Journal of Energy Markets*, 2(2):77–109.

Mehling, M. and Haites, E. (2009). Mechanisms for linking emissions trading schemes. *Climate Policy*, 9(2):169–184.

Montgomery, W. (1972). Markets in licenses and efficient pollution control programs. *Journal of Economic Theory*, 5.

Mu, X. (2007). Weather, storage, and natural gas price dynamics: Fundamentals and volatility. *Energy Economics*, 29:46–63.

Nauclér, T. and Enkvist, P.-A. (2009). Pathways to a low-carbon economy. Version 2 of the global greenhouse gas abatement cost curve. *McKinsey & Company*.

New South Wales Government (2012). Green scheme to close when carbon tax starts. Media Release.

New Zealand Government (2008). Climate change response (emissions trading) amendment act 2008. Public Act.

New Zealand Government (2009). Climate change response (moderated emissions trading) amendment bill. Public Act.

Newell, R., Pizer, W., and Zhang, J. (2005). Managing permit markets to stabilize prices. *Environmental and Resource Economics*, 31(2):133–157.

Newey, W. K. and West, K. D. (1987). A simple, positive semi-definite, heteroskedasticity and autocorrelation consistent covariance matrix. *Econometrica*, 55(3):703–708.

Newey, W. K. and West, K. D. (1994). Automatic lag selection in covariance matrix estimation. *Review of Economic Studies*, 61(4):631–653.

Paolella, M. S. and Taschini, L. (2008). An econometric analysis of emission allowance prices. *Journal of Banking and Finance*, 32:2022–2032.

Paterson, M. (2012). Who and what are carbon markets for? politics and the development of climate policy. *Climate Policy*, 12(1):82–97.

Perdan, S. and Azapagic, A. (2011). Carbon trading: Current schemes and future developments. *Energy Policy*, 39(10):6040–6054.

Pindyck, R. S. (1988). Irreversible investment, capacity choice, and the value of the firm. *American Economic Review*, 78(5):969–985.

Regional Greenhouse Gas Initiative (2005). Memorandum of understanding.

Regional Greenhouse Gas Initiative (2013). RGGI states propose lowering regional CO2 emissions cap 45%, implementing a more flexible cost-control mechanism.

Rittler, D. (2012). Price discovery and volatility spillovers in the European Union emissions trading scheme: A high-frequency analysis. *Journal of Banking and Finance*, 36(3):774–785.

Rosenberg, B. (1973). Random coefficients models. the analysis of a cross section of time series by stochastically convergent parameter regression. *Annals of Economic and Social Measurement*, 2(4):399–428.

Routledge, B. R., Seppi, D. J., and Spatt, C. S. (2000). Equilibrium forward curves for commodities. *Journal of Finance*, 55(3):1297–1338.

Rubin, J. (1996). A model of intertemporal emission trading, banking, and borrowing. *Journal of Environmental Economics and Management*, 31:269–286.

Schennach, S. (2000). The economics of pollution permit banking in the context of title iv of the 1990 clean air act amendments. *Journal of Environmental Economics and Management*, 40(3):189–210.

Schmalensee, R., Joskow, P. L., Ellerman, A. D., Montero, J. P., and Bailey, E. M. (1998). An interim evaluation of sulfur dioxide emissions trading. *Journal of Economic Perspectives*, 12(3):53–68.

Schwartz, E. S. (1997). The stochastic behavior of commodity prices: Implications for valuation and hedging. *Journal of Finance*, 52(3):923–973.

Schwartz, E. S. and Smith, J. E. (2000). Short-term variations and long-term dynamics in commodity prices. *Management Science*, 46(7):893–911.

Seifert, J., Uhrig-Homburg, M., and Wagner, M. W. (2008). Dynamic behavior of CO2 spot prices. *Journal of Environmental Economics and Management*, 56(2):180–194.

Sethi, S. P. and Thompson, G. L. (2006). *Optimal control theory: applications to management science and economics*. Springer, New York/Berlin/Heidelberg, 2nd edition.

Stavins, R. N. (1995). Transaction costs and tradeable permits. *Journal of Environmental Economics and Management*, 29(2):133–148.

Stavins, R. N. (2011). The problem of the commons: Still unsettled after 100 years. *American Economic Review*, 101(1):81–108.

Stranlund, J. K. (2007). The regulatory choice of noncompliance in emissions trading programs. *Environmental and Resource Economics*, 38(1):99–117.

Taschini, L. (2008). Flexibility premium in marketable permits. *Working Paper*.

Taschini, L. (2009). Environmental economics and modeling marketable permits. *Asia-Pacific Financial Markets*, 17(4):325–343.

Tietenberg, T. H. (2006). *Emissions Trading: Principles in Practice*. RFF Press, Washington DC, 2nd edition.

Trolle, A. B. and Schwartz, E. S. (2009). Unspanned stochastic volatility and the pricing of commodity derivatives. *Journal of Finance*, 22(11):4423–4461.

Trolle, A. B. and Schwartz, E. S. (2010). Variance risk premia in energy commodities. *Journal of Derivatives*, 17(3):15–32.

Uhrig-Homburg, M. and Wagner, M. (2009). Futures price dynamics of CO2 emission allowances: An empirical analysis of the trial period. *Journal of Derivatives*, 17(2):73–88.

United Nations (1998). Kyoto protocol to the united nations framework convention on climate change.

van der Merwe, R. and Wan, E. A. (2001). The square-root unscented Kalman filter for state and parameter-estimation. *Working Paper*.

Wagner, M. W. (2007). *CO2-Emissionszertifikate – Preismodellierung und Derivatebewertung*. PhD thesis, University of Karlsruhe.

Weitzman, M. L. (1974). Prices vs. quantities. *Review of Economic Studies*, 41(4):477–491.

Western Regional Climate Action Initiative (2007). WCI governors' agreement.

Yong, J. and Zhou, X. Y. (1999). *Stochastic Controls: Hamiltonian Systems and HJB Equations*. Springer, New York/Berlin/Heidelberg.

Zapfel, P. (2007). A brief but lively chapter in eu climate policy: the Commission's perspective. In Ellerman, A. D., Buchner, B. K., and Carraro, C., editors, *Allocation in the European Emissions Trading Scheme*, chapter 2, pages 13–38. Cambridge University Press, New York.